ESCUELA
COLOMBIANA
DE INGENIERÍA
JULIO GARAVITO

VIGILADA MINEDUCACIÓN

Master Thesis

DEVELOPMENT OF A
HUMAN-ROBOT-ENVIRONMENT INTERFACE FOR
WALKER-ASSISTED LOCOMOTION

Sergio David Sierra Marín

Supervisor:

Prof. Dr. Carlos Andrés Cifuentes García

Co-supervisor:

Prof. Dr. Marcela Múnera

A thesis submitted in fulfillment of the requirements for the degree of

Master in Electronic Engineering

February 2020

"Research is to see what everybody

else has seen, and to think

what nobody else has thought."

Albert Szent−Gyorgyi

"Share your knowledge.

It's a way

to achieve immortality."

Dalai Lama

Acknowledgements

On the other hand, it is important to emphasize that this work would not have been possible without the support of a large group of people, relatives, and friends. First of all, I would like to thank my parents Luz Stella and Reinaldo, whose unconditional support, wisdom and love have made me the person I am. To my sister Juliana, who every day reminds me of the value of the family as a fundamental pillar of life. In particular, I would like to thank my companion and love of my life Laura, who has always believed in me, and with her love and unconditional support has taught me that we can always be better. Additionally, I would like to thank my thesis advisors, who have guided me through this arduous but pleasant process of becoming a researcher. To Carlos, who has taught me to see the positive side of life and always look for the best version in us. To Marcela, who with her character has taught me to make our voice count, and that it doesn't matter who or how we are, because each person has a great value. Finally, I want to express my immense gratitude and appreciation to my colleagues and friends in the laboratory. I have lived invaluable life experiences with them, and they have accompanied me during these years of work. I believe that each one of them

has left a great mark in my life and I am convinced that they are the best work team. Thanks to Alejandro, Felipe Molina, Carlos, Daniel, Felipe Ballén, Luis, Miguel, Diego, Margarita, Maria José, Daniel Jr., Nathalia, Orión, Andrés Aguirre, Jonathan, and Pips. I also thank my international friends, Tim, Mario J., Ricardo C., and Wander.

Por otra parte, es importante destacar que este trabajo no hubiese sido posible sin el apoyo de un gran grupo de personas, familiares y amigos. En primer lugar, me gustaría agradecer a mis papás Luz Stella y Reinaldo, ya que su apoyo incondicional, su sabiduría y amor incondicional han hecho de mí la persona que soy. A mi hermana Juliana, quien a cada día me recuerda el valor de la familia como pilar fundamental de la vida. En especial, quisiera agradecer con todo mi corazón, a mi compañera y amor de mi vida Laura, quien siempre ha creído en mí, y con su amor y apoyo incondicional me ha enseñado que siempre se puede ser mejor. Adicionalmente, me gustaría agradecer a mis directores de tesis, que me han

Abstract

In recent years, different factors have contributed to the growth of the population with disabilities, becoming an important focus of study and research worldwide. In this way, the constant work of medicine, engineering, and robotics have led to the development of different gait assistive devices. Among these devices, smart walkers have emerged intending to provide physical and cognitive assistance during the rehabilitation process. The smart walkers are often equipped with actuators and sensory modalities that provide monitoring mechanisms and individual's intention estimators for user interaction, as well as several control strategies for movement and assistance level control. Accordingly, this master's thesis presents the design, development, and implementation of a Human-Robot-Environment interface in a robotic platform that emulates a smart walker, the AGoRA Walker. This interface is made up of several modules such as a navigation and people detection system, a safety system, a motion intention detection system, and a group of autonomous and shared control strategies. The functionalities of the AGoRA Walker were validated through different experiments in healthy and pathological volunteers. Likewise, usability and performance tests of the platform were carried out, finding that the AGoRA Walker can provide an intuitive and natural interaction in different rehabilitation scenarios.

Keywords: Robotics, Smart Walkers, Human–Robot–Environment interaction; Control Strategies; Gait Rehabilitation.

List of Tables

List of Figures

Contents

Chapter 1

Introduction

The work presented in this document focuses on the development and preliminary validation of a Human-Robot-Environment interface (HREi) for gait rehabilitation in the AGoRA smart walker. The integration of two interfaces intended to provide Human-Robot Interaction (HRI) and Robot-Environment Interaction (REI) on a mobile robotic platform is described. A preliminary study aimed at validating the performance of the developed interface in healthy subjects is outlined. Similarly, a validation study, in which the clinical and biomechanical effects of the interface in elderly subjects is described. This chapter introduces the main motivations and research objectives that lead to the development of this work. Finally, the main contributions, publications and the remainder of this document are described.

1.1 Motivation

Nowadays, the development of robust and accurate gait rehabilitation technology has become an important research topic for several multidisciplinary teams of health professionals, engineers, and patients [1, 2]. Such interest has been mainly supported by worldwide statistics reporting recent growths in the incidence and prevalence of health conditions that affect the key components of human gait [3–5]. For instance, several neurological pathologies such as, cerebrovascular accidents (stroke), spinal cord injury (SCI) and cerebral palsy (CP) are com-

monly found to be strongly related to locomotion impairments, and therefore leading to total or partial loss of mobility and autonomy [6,7]. Additionally, the progressive deterioration of cognitive functions [8] and the neuromuscular system in the elderly [9] are commonly related to gait abnormalities.

In general terms, the mobility impaired population has been experiencing a major and constant growing, in such a way that over 1 billion people around the world (i.e., 15% of world's population) experience some form of disability [10,11]. In 2015, an study on global diseases reported that the prevalence of health conditions associated with severe disability described an increase of 23% compared to 2005 [12]. The same study stated that chronic and noncommunicable diseases, for which rehabilitation might be beneficial, account for nearly 74% of years lived with disability (YLDs) in the world [12].

More specifically, there are some statistical measurements that describe the impacts of the above mentioned health conditions on the global burden on disability. Firstly, stroke has been categorized as the leading cause of death and long-term disability by totaling 15 million cases every year [13,14]. Of these cases, 5 million% dies and other 5 million% remain permanently disabled [14]. It has been also reported that 90 % of stroke survivors present impairments such as, muscle weakness, chronic pain and poor balance [15,16]. Secondly, SCI worldwide reports have found an incidence of 250.000 to 500.000 cases every year, where an estimated of 20% to 30% of patients presents negative impacts in functioning and overall health, as well as, significant signs of depression [17,18]. Moreover, patients of SCI might suffer from total or partial loss of motor and sensory function, resulting in spasticity and pain syndromes [19]. Finally, regarding motor disability in childhood, CP is considered the most common cause of mobility impairments, being characterized by abnormal posture, movement and muscle tone [20]. Specifically, recent epidemiological studies have found that the prevalence of CP ranges from 1.5 to more than 4 case per 1.000 live births [21].

Furthermore, some demographic studies have found that global population is ageing, and

that such population presents a higher risk of disability [10]. Particularly, the World Health Organization WHO has found that by 2050 the proportion of the population over 60 years will nearly double from 12% to 22% [4, 22]. These studies report mobility impairments as a common condition in elderly populations and people with functioning and cognitive disabilities [1, 23, 24]. Moreover, some clinical findings suggest that coexisting health conditions, such as neurological pathologies and later life, might increase the risk factors of long-term disability and decrease individuals autonomy in activities of daily living (ADL) [1, 15].

In addition to the foregoing, the prospects for developing countries, such as Latin American countries, are often accompanied by social, economic and public health factors that generally hinder access to assistive technologies or rehabilitation solutions [4, 25]. For instance, as reported by the WHO, the 50% of people are not able to afford health care nor access to rehabilitation services [10]. Likewise, United Nations (UN) estimate that nearly 386 million of the working-age people suffer from some kind of disability and the unemployment rates among these population is as high as 80 % in some countries [26]. Moreover, in low- and middle-income countries there is a large unmet need to be addressed, regarding the workforce of physicians and rehabilitation professionals [12].

Considering this, several rehabilitation and assistance devices have been developed to retrain, empower or provide the affected or residual locomotion capacities [27]. Devices such as canes, crutches, walkers, and wheelchairs, as well as, ambulatory training devices are commonly found in assisted gait and rehabilitation scenarios [28, 29] and are intended to improve user's life quality. Concretely, mobility assistive devices are aimed at overcoming and compensating physical limitations by maintaining or improving individual's functioning and independence in both clinical and everyday scenarios [27, 28]. Regarding conventional walkers, these devices exhibit simple and affordable mechanical structures, as well as, partial body weight support and stability. However, natural balance, user's energetic costs, fall prevention and security issues are often compromised with conventional walkers [30, 31].

Moreover, several issues related to sensory and cognitive assistance, often required by people with physical limitations, are not completely addressed by conventional devices [32–34]. Accordingly, in order to outstrip such problems, robotic technologies and electronics have been integrated to conventional walkers, leading to the emergence of *intelligent walkers* or *Smart Walkers* (SWs).

Within this context, the AGoRA Smart Walker, developed in the scope of the AGoRA Project, constitutes a mobility assistive device that integrates robotic technology to improve the existing HRi and REi interfaces found in literature. The AGoRA SW is also intended to broaden the current knowledge on gait training techniques, by empowering health professionals in clinical and rehabilitation scenarios with robotic devices. In this manner, patients, researchers, and clinical staff could benefit from the outcomes of this thesis and the overall AGoRA project, as they seek to better understand and provide a more efficient and natural rehabilitation process.

1.2   Background

This thesis is developed in the context of the research project "*Development of an Adaptable Robotic Platform for Gait Rehabilitation and Assistance*" (AGoRA) supported by the Colombian Administrative Department of Science, Technology and Innovation *Colciencias* (grant 801-2017), as well as, internal funding from the Colombian School of Engineering Julio Garavito (ECIJG).

The AGoRA project is primarily led by Prof. Dr. Carlos A. Cifuentes (professor at the Department of Biomedical Engineering and head of the *Center for Biomechatronics* at ECIJG). The research team of this project is formed by a cooperation network comprising both national and international research groups and institutions. On the one hand, the trauma and rehabilitation group of *La Sabana* University Clinic (led by Dr. Catalina Gómez) constitutes the medical partner of the project. On the other hand, the project team is also composed

of three international research groups, such as: (1) the Neural and Cognitive Engineering group of the Center for Automation and Robotics at the Spanish National Research Council, Spain (led by Dr. Eduardo Rocon), (2) the Institute of Automation of the University of San Juan, Argentina (led by Dr. Ricardo Carelli) and, (3) the Robotics and Industrial Automation Group of the Federal University of Espíritu Santo in Vitória, Brazil (led by Dr. Anselmo Frizera-Neto).

The main goal of the AGoRA project is to deploy and validate a robotic platform for gait rehabilitation and assistance. This objective demands the establishment of an appropriate interaction between the user, the robotic platform and the environment, by means of different communication channels. This is often referred as multimodal HREI, where different sensors and actuators capable of estimating the interaction and responding appropriately to it are used. Within the Human-Robot interface (HRi), two interfaces are conceived: (1) a cognitive Human-Robot interface (cHRi), in which the user controls the robot while receiving feedback from it and (2) a physical Human-Robot interface (cHRi), where there is an exchange of forces between both the user and the platform.
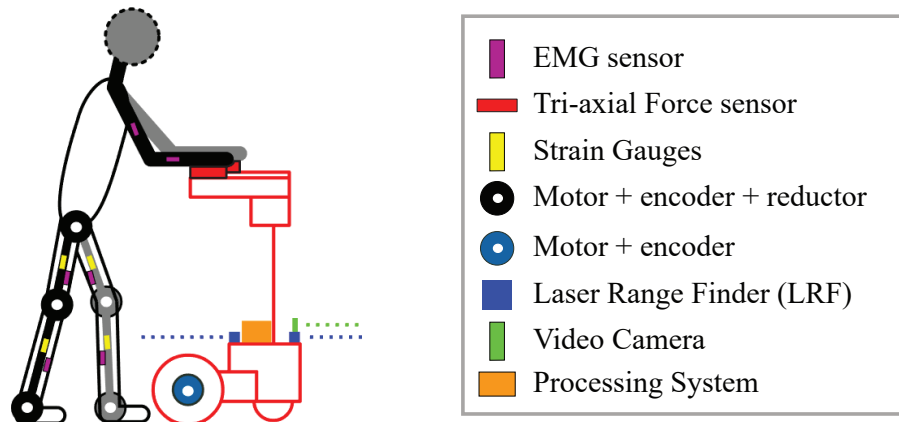
Figure 1.1: Multimodal HREi implemented on the robotic platform of the AGoRA project.

To achieve the purpose of the AGoRA project, the development of a robotic platform composed of two rehabilitation devices will be addressed. Specifically, a robotic or *smart* walker

(SW) and an active lower limb exoskeleton will constitute the final robotic platfom. These devices will be controlled by a HRi serving as a communication channel between the patient and the rehabilitation therapy. Additionally, a second multimodal interface for environment sensing will be coupled. This Robot-Environment interface (REi) will ensure safe interaction and navigation between the patient and the rehabilitation setting. Figure 1.1 illustrates the main elements of the robotic platform and its multimodal HREi. Several sensors and actuators are implemented on the interface providing: (1) electro-mechanical actuation, (2) physical HRI estimation, (3) user's state estimation, and (4) REI. The interface is also equipped with a processing unit supporting the software architecture implemented on the robotic platform.

According to the above and within the scope of the AGoRA project, this master thesis seeks to develop and validate a multimodal HREi on an SW for gait rehabilitation and assistance. In this sense, this work looks forward to answering the following research question: ¿Does the implementation of a HREi in walker-assisted gait provides a natural and efficient gait rehabilitation and assistance?

Finally, later stages of the AGoRA project are aimed at extending the capabilities of the robotic platform by integrating and joining the functionalities of the two rehabilitation devices in clinical scenarios. Thus, the development of novel rehabilitation techniques including robotic devices, as well as, the design of shared high-level control strategies will be addressed.

1.3   Objectives

Bearing in mind the main motivations of this project, it is proposed the development of a HREi for a robotic walker, as well as, its validation for usability and acceptance assessment. Thus, this project seeks not only to provide an SW with a robust, natural and intuitive interface, but also to gather therapists and patients expectancies about the functionalities of gait assistive devices. In order to achieve the project proposal the following objectives are defined.

1.3.1 General Objective

Implement high-level control strategies on a robotic walker for gait assistance, providing a natural and intuitive HREI and validate its functionality within a clinical setting.

1.3.2 Specific Objectives

- Perform a systematic review of literature to understand the existing HRis and REis on SWs.

- Conduct an evaluation of the opinions and expectations of physiotherapists and patients with mobility disorders towards the functionalities and capabilities of the SWs.

- Design and implement shared and autonomous control strategies to provide natural, intuitive and efficient HRI.

- Desing and implement a navigation and safety system to ensure effective and robust REI.

- Develop a social interaction strategy based on a people detection system and people proxemics to ensure social acceptance of the SW.

- Evaluate the functionalities and performance of the HREi on healthy users without any mobility requirements.

1.4 Contributions

The key contributions of this work are framed in the main activities of the AGoRA project, as they pursue the development of a robotic walker for gait rehabilitation and assistance. The fulfillment of this master thesis is accompanied by a series of technical and scientific contributions presented as follows:

1. The design and implementation of a multimodal sensory interface for HREI on a robotic walker, along with the development of low-level control strategies for the device's actu-

ation system. In order to test the HREi performance, it was preliminary implemented on a commercial robotic platform and evaluated under laboratory conditions.

2. The design and development of a software architecture based on the Robotic Operating System (ROS) aimed at integrating high-level control strategies providing both HRI and REI on a robotic walker. The architecture was designed to be modular and easy customizable, in such way that the end user is able to select the desired functionalities of the final HREi.

3. The electronic and software developments related to the robotic walker contributes to the development of associated undergraduate and graduate work in the scope of the AGoRA project. Moreover, the design and implementation of the hardware layer is the result of interdisciplinary work between master students of the AGoRA project.

4. The development of an experimental protocol for the qualitative evaluation of user's perception and platform's usability, regarding the physical and cognitive interaction with the SW.

1.5 Publications

The work presented in this thesis has been reported to the scientific community by means of the following publications:

1. (Conference Proceedings) **Sierra M., S. D.**, Molina, J. F., Gomez, D. A., Múnera, M. C., & Cifuentes, C. A. (2018). Development of an Interface for Human-Robot Interaction on a Robotic Platform for Gait Assistance: AGoRA Smart Walker. In 2018 Technical and Scientific Conference of the Andean Council (IEEE ANDESCON) - Conference Proceedings, 1–7. `https://doi.org/10.1109/ANDESCON.2018.8564594`

2. (Conference Proceedings) **Sierra M., S. D.**, Jimenez, M. F., Múnera, M. C., Frizera-Neto, A., & Cifuentes, C. A. (2019). Remote-Operated Multimodal Interface for Ther-

apists During Walker-Assisted Gait Rehabilitation: A Preliminary Assessment. In 2019 14th ACM/IEEE International Conference on Human-Robot Interaction (HRI), 528–529. `https://doi.org/10.1109/HRI.2019.8673099`

3. (Conference Proceedings) Scheidegger, W. M., C. de Mello, R., **Sierra M., S. D**., Jimenez, M. F., Múnera, M. C., Cifuentes, C. A., & Frizera-Neto, A. (2019). A Novel Multimodal Cognitive Interaction for Walker-Assisted Rehabilitation Therapies. In 2019 IEEE 16th International Conference on Rehabilitation Robotics (ICORR), 905–910. `https://doi.org/10.1109/ICORR.2019.8779469`

4. (Journal Article) **Sierra M., S. D.**; Garzón, M.; Múnera, M.; Cifuentes, C.A. (2019). Human–Robot–Environment Interaction Interface for Smart Walker Assisted Gait: AGoRA Walker. Sensors 2019, 19, 2897. `https://doi.org/10.3390/s19132897`

5. (Conference Proceedings) **Sierra M., S. D.**, Jimenez, M. F., Múnera, M. C., Bastos, T, Frizera-Neto, A., & Cifuentes, C. A. (2019). A Therapist Helping Hand for Walker-Assisted Gait Rehabilitation: A Pre-Clinical Assessment. In 4th IEEE Colombian Conference on Automatic Control (CCAC2019)

6. (Conference Proceedings) C. de Mello, R., **Sierra M., S. D.**, Múnera, M. C., Cifuentes, C. A., Ribeiro, M., & Frizera-Neto, A. (2019). Cloud Robotics Experimentation Testbeds: a Cloud-Based Navigation Case Study. In 4th IEEE Colombian Conference on Automatic Control (CCAC2019)

7. (Congress) Scheidegger, W.; C. de Mello, R.; **Sierra M., S. D.**; Jiménez, M. F.; Múnera, M.; Cifuentes, C. A & Frizera-Neto, A. (2019). A Novel Multimodal Human-Robot Interaction for Walker-Assisted Gait: Merging an Admittance Controller and a Deep Learning Approach. In X Congreso Iberoamericano de Tecnologías de Apoyo a la Discapacidad (IBERDISCAP2019)

1.6   Document Organization

This master thesis document presents the electronic and software design of a multimodal HREi for the AGoRA Smart Walker. Moreover, it is also presented the design and implementation of several high-level control strategies to provide efficient and safe HRI and REI. Finally, it is reported the preliminary validation of the multimodal interface carried out on healthy and elderly subjects. In this sense, the document is structured as follows:

- **Chapter 1** presents the main motivations and research goals of this work. Additionally, this chapter describes the research project in which this thesis is framed, defining the key contributions of this thesis.

- **Chapter 2** introduces the context of gait rehabilitation and assistance scenarios, explaining the primary causes of mobility impairments around the world, as well as, the different gait rehabilitation alternatives and techniques. This chapter is also intended to address the literature review concerning the most representative HRis and REis implemented on existing SWs.

- **Chapter 3** describes the main elements of the proposed multimodal HREi along with the selected design criteria. This chapter is also aimed at presenting the AGoRA Walker sensory interface and its actuation mechanism.

- **Chapter 4** presents a detailed structure of the HRi designed for the AGoRA Walker, describing each module and the outcomes of their individual performance.

- **Chapter 5** addresses the design, development and implementation of REi of the AGoRA Walker. This chapters presents the implementation and adaption of a navigation system widely used in mobile robotic applications to be suitable for an assistive device.

- **Chapter 6** describes the integration of the developed HRi and REi interfaces into a multimodal HREi, by means of a set of high-level control strategies or operation modes. This chapter also describes a preliminary validation study focused at assessing the performance of the proposed interface in healthy subjects.

- **Chapter 7** reports two experimental studies aimed at describing the biomechanical and clinical effects of the AGoRA Walker in two populations of healthy and elderly subjects. This chapter focuses on the description of the impacts of the HRi on the subjects' gait pattern.

- **Chapter 8** summarizes and highlights the main conclusions and remarks of this works. This chapter also proposes a set future works to be addressed with the AGoRA Walker, regarding the conduction of a long term validation study, as well as, its integration with the AGoRA lower limb exoskeleton.

Chapter 2

Human Mobility: Rehabilitation and Assistance

Human mobility is often considered as a key capacity for individuals' development and well-being since it provides autonomy and independence during the activities of daily life. However, different physical and neurological conditions compromise the proper functioning of the systems required for healthy and natural mobility. In this way, several solutions and techniques have been used and deployed to recover and retrain the lost locomotion capacities. This chapter concisely describes the main components of human gait, as well as the main conditions that affect it. Along this chapter, it is also presented a summary of the conventional techniques for gait rehabilitation and assistance, as well as the current trends in robotics-based rehabilitation processes.

2.1 Human Gait

Bipedal walking is one of the most important faculties of humans and is generally described as a complex behaviour that involves not only the musculoskeletal system but also dissociable neuronal systems [35]. The human gait involves the activation of the central nervous

system (CNS), muscular activation, and the integration of sensory information [36]. These systems are aimed at controlling gait initiation, planning, and execution, while adapting them to satisfy motivational and environmental demands of the individual [37]. Despite the evident complexity of gait, individuals usually exhibit smooth, regular, stable and repeating movements during walking [35, 36].

The ability to walk is usually acquired at the first years of life [38]. During this stage, skills such as, body weight balancing and upright standing are learned [39]. Once the individual learns to walk, this ability becomes spontaneous and unconscious, becoming an energy-efficient task [38, 39]. Nevertheless, as the human gait gathers almost of the muscles of the body, as well as involves several cortical and sub-cortical structures, the training processes after physical and neurological injuries are usually challenging and long [38]. In this sense, the gait quality and locomotion capacities constitute important indicators of the overall health of an individual [40]. Thus, the presence of neurological alterations or musculoskeletal pathologies might lead to atypical gait patterns, weakness or loss of motor control [41, 42].

2.2 Conditions Affecting Mobility

Mobility impairments are usually defined as a category of disability, including people with several types of physical and sensory limitations [43, 44]. This type of disability often involves the loss or affectation of upper and lower limb functioning [43]. Several authors also define mobility impairment as the difficulty for walking or inability to ambulate without great complication or assistance [23, 24, 45].

Several health conditions and pathologies affect the key components of mobility [46], such as gait balance, control, and stability [47]. In general terms, these alterations can be classified into neurological or musculoskeletal causes. Among neurological pathologies, Stroke, Spinal Cord Injury (SCI) and Cerebral Palsy (CP) are found to be strongly related to locomotion impairments [7]. Likewise, the progressive deterioration of cognitive functions [37]

(i.e., sensory deficits and coordination difficulties [1]) and the neuromuscular system in older adults [9] (i.e., loss of muscle strength and reduced effort capacity [1]) are commonly related to the partial or total loss of locomotion capacities.

According to the World Health Organization (WHO) the proportion of the mobility impaired population has been experiencing constant and major growth in the last years [11]. Specifically, it has been reported that nearly 15% of the world's population experience some form of disability [10]. Moreover, demographic predictions state that by 2050 the proportion of the world's population over 60 years will nearly double from 12% to 22% [22, 48]. These studies also report that a larger percentage of this growth will take place in developing countries [22]. Therefore, the identification of the causes and conditions that lead to mobility limitations is a public health issue and should be broadly analyzed. This analysis should be aimed at proposing new solutions and strategies for the rehabilitation and assistance of people with mobility disabilities. In this sense, the main conditions and pathologies that lead to mobility impairments are further described and analyzed.

2.2.1   Stroke

Normal functioning of brain relies on the adequate perfusion of oxygen and nutrients to its different tissues. Alterations to proper behaviour of cerebral vessels can result in a cerebrovascular accident or Stroke [49]. Stroke can be divided into two categories: (1) ischemic stroke, caused by a blood clot that blocks a blood vessel in the brain, and (2) hemorrhagic stroke, caused by a ruptured blood vessel that bleeds into the brain [50].

Depending on the affected region after the occurrence of a stroke, different functions of the individual could be affected [51]. For instance, after a stroke the following consequences are commonly found: (1) movement and motor control disorders, (2) sensory and perception impairments, (4) chronic pain, (3) language problems, and (4) cognitive disturbances [52, 53]. Regarding motor control, paralysis is often presented at the side of the body opposite the affected side of the brain. One-sided paralysis is referred as hemiplegia and one-sided

weakness is called hemiparesis [53]. The effects of body paralysis usually result in difficulties in everyday tasks, such as walking and grasping [54]. Moreover, sensory deficits and cognitive impairments in stroke survivors also effect the key characteristics of healthy gait [55]. Stroke survivors also exhibit serious problems regarding balance, coordination, muscular spasticity and propioception [55]. Among the different risk factors of stroke, several birth conditions, diseases, and lifestyle factors are found [56].

According to worldwide statistics, the cerebrovascular accidents constitute the second most common cause of death and the third leading cause of long-term disability in adultness [57,58]. Several global reports state that nearly 15 million people suffer stroke every year, of which 5 million result in death and another 5 million are permanently disabled [59–61]. As found by a recent systematic review of literature, the worldwide stroke incidence rates exhibited a significant 42% decrease in high-income countries. However, during the same period, the incidence rates in low- and middle-income (LMI) countries increased by over 100% [57,58]. In this regard, the WHO estimated, in 2001, that death from stroke in LMI countries accounted for 85.5% of worldwide stroke deaths. In Colombia, it has been reported that nearly 47 thousand cases occur every year, from which 12 thousand cases result in death [60].

2.2.2 Spinal Cord Injury (SCI)

The CNS is mainly constituted by the spinal cord and the brain. Specifically, the spinal cord is made of nerve fibers that transmit impulses back and forth between the body and the brain [62]. Thus, it serves as a center for initiating and coordinating many reflex acts, as well as motor and sensory functions [63]. In this sense, damages or traumas to the spinal cord or nerves roots often result in permanent loss of movement, sensation and other body functions below the site of the injury [62–64].

In general terms, a SCI begins with a sudden, traumatic blow to the spine that fractures the vertebrae. Regarding the causes of the SCI, the National Spinal Cord Injury Association (NSCIA) reports vehicle accidents as the leading cause of injury in young people, followed by

falls (i.e., the main cause after the age of 65), violence acts, and sports [64]. Moreover, the causes of SCI also include diseases (e.g. cancer, arthritis or osteoporosis), infections, blockage of blood supply, and compression by fractured bones or the presence of tumors [65].

The severity or completeness of the SCI defines the loss of functions in the individual, and is usually classified as either complete or incomplete [62]. A complete injury refers to the total loss of motor and sensory function below the level of injury [66]. An incomplete injury occurs when a certain degree of functioning remains below the injury [66, 67].

According to the WHO, between 250.000 and 500.000 cases of SCI are reported around the world [68] and nearly 18.000 new SCI cases occur each year [69]. An epidemiological study found that the proportion of SCI patients doubled between 2003 and 2011 [70]. Moreover, worldwide statistics report an annual global incidence of 40 to 80 cases per million, where the 90% of these cases are due to traumatic causes [62, 68]. Similarly, it has been stated that 80% of new cases are male, and that individuals between the ages of 16 and 30 are more likely to suffer a traumatic SCI [62, 68, 69]. In Colombia, there are no available epidemiological studies of SCI. However, one study reported that SCI occurs in 1 of 40 Colombian patients admitted to a general hospital after trauma [71].

2.2.3   Cerebral Palsy (CP)

The most common cause of disability in childhood is associated with the Cerebral Palsy. This condition is often characterized by a group of disorders affecting the movement, the muscles tone an the posture [72]. This affectations are also accompanied by deficits in sensation, perception, cognition, communication, and behavior [72]. Frequently, CP is the result of abnormal brain development or damage to the developing brain [73]. Although brain damage usually occurs before birth, it can also take place at birth or during the first years of life [74].

The symptoms of CP are not unique, as they affect each person differently [73]. For instance, spastic CP is the most common type and represents the 80% of cases. This type of CP

is characterized by increased muscle tone and can be presented on each side of the body both independently or jointly [73, 75]. People with spastic CP often exhibit problems during standing and walking [76]. Similarly, dyskinetic CP causes problems in the movement and control of hands, arms, feet, and legs, generating difficulties to sit and walk [77]. People with ataxic CP exhibit balance and coordination disturbances, and thus, they usually present unsteady walking [78]. Finally, people with mixed CP present symptoms from more than one type of CP [73].

According to worldwide reports, the prevalence of CP ranges from 1.5 to 4 cases per 1,000 live births or children of a defined age range [20]. Moreover, around 764.000 people currently live with CP, from which 500.000 are children and teens [79]. In Colombia, exact data on the number of people with cerebral palsy are not available.

2.2.4   Elderly

With aging, different health conditions affect people's well-being and overall autonomy. In general, more than half of adults over the age of 65 have three or more medical problems [80]. For instance, older adults often exhibit cardiovascular complications, hormonal disturbances, cancer or musculoskeletal diseases [81, 82]. Similarly, it has been identified that advanced age is a common risk factor for several cardiovascular and neurological diseases [6]. Therefore, the assessment and treatment of the health status of older adults is sometimes challenging [83].

Among the different disorders that occur as people age, mobility and balance are commonly compromised. Specifically, the natural gait pattern and quality are affected by problems in the nervous system, the musculoskeletal apparatus, and the cardio-respiratory system [46]. Additionally, further injuries and severe damages may occur, as balance and gait disorders significantly increase the risk for falls [46, 84].

There are different and important indicators that determine the quality of gait, such as, walking speed, cadence (i.e., number of steps or gait cycles per unit of time), step length, stride length (i.e. linear distance covered by one gait cycle), among others [46]. In this

sense, older adults' gait is usually characterized by decreased speed and step length, while cadence remains stable compared to younger people [46, 85]. Moreover, in order to ensure stability, elderly subjects with gait problems prefer shorter step lengths, as well as, wider stance phases [46].

According to statistical reports, the prevalence of gait and balance disorders increases with age [46, 83]. Between the ages of 60 and 69 years, a prevalence of 10% is usually found, while a prevalence of more than 60% has been reported in people over 80 years of age [3]. Additionally, worldwide statistics state that the proportion of elderly people is increasing [86]. Specifically, it has been asserted that the number of people over 60 years will be larger than the number of children younger than 5 years by 2020 [22]. Moreover, population growth trends also establish that by 2050, the population over 60 will double from 900 million to 2 billion, from which the 80% will live in low- and middle-income countries [22, 86].

2.2.5   Other Conditions

Natural and safe walking requires the proper and intact functionality of the following systems and features: locomotor control, balance, postural reflexes, sensory function and sensory-motor integration, the nervous system, the musculoskeletal system and the cardiovascular system. In this sense, there are several chronic conditions that can also lead to disability and mobility impairments, such as: diabetes, coronary heart disease, heart failure, multiple sclerosis, arthritis, Parkinson's disease, muscular dystrophy and Huntington's disease [87,88].

Moreover, natural and safe gait also requires several cognitive and psychological functionalities, such as attention, executive functioning, perception, and memory [46]. Therefore, the presence of neurocognitive disorders, such as Alzheimer's disease, dementia or mild cognitive impairment syndrome[1], has been reported to affect individuals' mobility and autonomy [90].

---

[1]Mild cognitive impairment is a transitional state between normal aging and early dementia [89]

2.3   Gait Rehabilitation

Physical rehabilitation (i.e., often referred as physiotherapy) is aimed at restoring people's movement and functioning affected by injury, illness or disability [91]. Considering the health condition of each patient, gait rehabilitation and assistance therapies focus on providing, compensating, increasing or re-training the lost locomotion capacities, as well as the cognitive abilities of the individual [92]. Specifically, training interventions seek to improve walking performance by: (1) eliciting voluntary muscular activation in lower limbs, (2) increasing muscle strength and coordination, (3) recovering walking speed and endurance, and (4) maximizing lower limbs range of motion [93]. In this manner, several techniques and approaches have been developed, ranging from overground and conventional gait training to robot-assisted and machine based therapies [94, 95].

2.3.1   Conventional Approaches

There are different techniques and strategies that have been used in conventional rehabilitation settings. Some of the most relevant approaches are described below.

Gait Training Therapies

The most common therapeutic interventions used to improve gait are based on exercise and functional training [96]. These interventions are often complemented by functional electrical stimulation and biofeedback strategies [15]. Moreover, several clinical studies report the use of auditory stimulation, progressive resistive exercises, and visual feedback [97–99].

In general, gait impairments are related to deficits in motor unit recruitment, proprioception, muscle activity, connective tissues, postural reflexes, vestibular function and vision [15]. Therefore, circuit-based strategies are often used to provide parallel training of the affected systems [100]. These strategies include several activities, such as repetive sitting and standing, sit-to-stand tests, step-ups, heel lifts, isokinetic strengthening, obstacles avoidance, as

well as walking over up and down ramps [101,102]. Regarding individual's evolution, the difficulty of these tasks is increased by incorporating endurance elements, functional strengthening, balance challenges and variable speed exercises [15]. Moreover, several studies also report the implementation of intensive training programs, where aerobic exercises (e.g., stationary bicycle) and walking tasks with postural challenges (e.g., walking backwards) are also used [15,103,104].

Regarding neurological patients, several techniques have been widely studied and implemented in rehabilitation scenarios. On the one hand, neurophysiological techniques are aimet at supporting the proper movement patterns of the patients, leaving them as passive actors of the therapy [105]. Some of these techniques are based on proprioceptive stimuli, as well as passive mobilization to suppress spasticity and encourage movement patterns and voluntary activation [106,107]. On the other hand, motor learning techniques are aimed at encouraging the active participation of the patient during the therapy [108]. Some of these techniques are based on task orientated and functional activities (e.g., daily living activities), where verbal, visual and cognitive feedback is used [109].

Mobility Assistive Devices

In addition to the above mentioned techniques and therapeutic interventions, several devices have been developed to assist and support mobility. Concretely, mobility assistive devices are aimed at overcoming and compensating physical limitations by maintaining or improving individual's functioning and independence in both clinical and everyday scenarios [28]. For instance, devices such as canes, crutches, walkers, wheelchairs, as well as ambulatory training devices have been deployed to improve people's life quality [110].

One of the most common types assistive devices is constituted by manual wheelchairs. This type of device is used when locomotion capacities are completely lost [43]. Another simple but effective types of devices are the walking sticks and crutches. These devices increase the patients' base of support, and thereby improve their balance [111]. Another relevant type of

assistive device are the parallel bars. This type of device is usually found in clinical scenarios being used for strength, balance, range of motion, and independence recovering [112]. Similar to this device, treadmills are commonly found in gait training scenarios. The main benefits of treadmills are characterized by the coordinated activation of spinal neural circuits, resulting from the rhythmic and alternating movements of the limbs [113]. Additionally, some studies report the use of body-weight support systems, which may allow the lower functioning of individuals who are not able to stand upright safely [114, 115].

Regarding joint-focused devices, passive orthoses are found. These devices are commonly prescribed to provide functional assistance for patients with lower limb injuries or weakness [116]. Depending on the assisted joints, several types of passive orthoses can be found: (1) Ankle-Foot orthoses (AFO), (2) Knee-Ankle-Foot orthoses (KAFO), and (3) Hip-Knee-Ankle-Foot orthoses (HKAFO) [117].

Finally, an important type of assistive devices is constituted by the walking frames or walkers. These devices improve overall balance by increasing the patient's base of support, enhancing lateral stability, and providing weight bearing [111, 118]. Walkers provide support during bipedestation and use the patient's own remaining locomotion capability to move [112, 118]. In general, these devices exhibit simple mechanical structures and hold a great rehabilitation potential [110, 112]. Considering the mechanical configuration of the supporting points, several types of conventional walkers can be found. Specifically, (1) four-legged frames, (2) front-wheeled walker, and (3) four-wheeled walkers or rollators are commonly found. Despite the advantages of these devices, the use of walkers results in slower, and often abnormal gait patterns [111]. Moreover, these devices often require some degree of upper body strength and cognitive ability [112].

2.3.2 Robot-Assisted Therapy and Modern Approaches

With the rapid advances of technology in the last decades, several devices and strategies have been developed to improve gait training interventions. These new technologies are

mainly constituted by the use of sensing systems, actuators and novel interaction strategies to enhance patient's experience during the rehabilitation process [110]. Moreover, the use of robotic devices allows the implementation of safe, intensive and task oriented therapies.

In general, the integration of technology and robotics enables the following characteristics: (1) Precise and repeatable movement patterns and therapies, (2) intensive activities with programmable and measurable difficulty, (3) online measurement of the performance and physiological state of the patient, (4) motivating and engaging rehabilitation environments through the use of virtual and augmented reality, as well as feedback strategies, (5) reliable assessment of the patient's rehabilitation progress, (6) reduction of the physical effort of the therapists [1, 27, 108, 119].

According to the literature evidence, gait rehabilitation devices and technologies can be classified into different categories based on their behaviour, principle of operation, required assistance, rehabilitation stage, among others [1, 108, 112]. For the purpose of this work, a classification based on the review carried out by Martins et al will be used: (1) robotic alternative devices and (2) robotic augmentative devices. Specifically, alternative devices are used when complete assistance is required, and augmentative devices are used when patients exhibit residual locomotion capacities [112]. Considering the scope of this thesis, the description of the augmentative devices will delve into robotic walkers.

Robotic Alternative Devices

In case of total mobility impairment, several robotic alternative devices have been developed [112]. Specifically, robotic wheelchairs and autonomous vehicles are commonly found. For instance, robotic wheelchairs are based on the principle of operation of the conventional wheelchairs,including actuators, sensory interfaces and advance processing algorithms to provide easier and safer navigation [120]. Moreover, these devices also include multimodal input interfaces, such as joysticks, voice recognition modules, image processing systems, and bio-signals monitoring modules [120]. Regarding autonomous vehicles, robotic scooters and

bipedestation vehicles are also found [112]. These devices include several actuators and multimodal user interfaces to allow intuitive control and interaction. Moreover, these devices may be equipped with lifting mechanisms to provide sit-to-stand capabilities [121].

Robotic Augmentative Devices

These devices exploit the residual locomotion capacities to provide safe, intensive, repetitive and task-oriented rehabilitation interventions [108]. Therefore, these devices encourage patient's active participation during rehabilitation tasks [1,108]. The robotic augmentative devices are generally equipped with control approaches aimed at: (1) allowing a margin of error in patient's performance without providing assistance, (2) triggering assistance in relation to the amount of exerted force or velocity (i.e., intentions of movement), (3) enabling joint compliance, and (4) disabling robotic assistance under specific scenarios [108,110]. According to this, the following devices are found:

Treadmill-based or Stationary Gait Trainers: Similar to the treadmill based approaches in conventional therapies, this technique consists on using a suspension system to provide a symmetrical removal of patients' partial body weight, while a robotic device moves their lower limbs [108]. These type of devices constitute the most common method for mobility training and are mainly aimed at improving functional movements and sensorial stimulation through repetition [1,112]. Several well known and commercial devices are found in literature such as, Lokomat [122], Lokohelp [123], LOPES [124], G-EO [125], ALEX [126], among others [1,112,127].

Ambulatory training devices: These devices use mobile body weight support systems to provide over ground training [112]. These devices are able to provide dynamic assistance, in such a way that the patient learns to walk with proper posture [112].

Wearable Devices: Under this type of devices, active orthoses (i.e., also referred as exoskeletons) and active prostheses are commonly found. These devices are carried by the user

either to improve function of movable parts of the body or to substitute a lost member [112]. Moreover, by means of different types of actuators and sensory interfaces, these devices mechanically compensate and improve the functionality of the affected joints [112,126]. Regarding the control strategies, these devices are usually based on the assist-as-needed control concept, where the active motion of the patient is encouraged [108]. Among the most relevant and notable devices, HAL exoskeleton [128], Ekso Bionics exoskeleton [129], Phoenix [129], MyoSuit [130], Exo H3 [131], ReWalk [132], BLEEX [133], RoboKnee [134], AGoRA exoskeleton [135] and T-FLEX [136] are found.

Robotic or Smart Walkers (SW)

Several issues are often presented in conventional walkers, regarding sensory and cognitive assistance (i.e., required by people with physical limitations) [32–34]. Moreover, natural balance, user's energetic costs, risk for falls and safety issues are often compromised with conventional walkers. In this sense, to outstrip such problems, robotic technologies and electronics have been integrated, leading to the emergence of *robotic walkers* or *Smart Walkers* (SWs).

The SWs are often equipped with actuators and sensory modalities that provide biomechanical monitoring mechanisms and individual's intention estimators for user interaction, as well as several control strategies for movement and assistance level control [30]. Likewise, path following modules are usually included, in addition to safety rules and fall prevention systems [31]. These features enable the SWs to interact in dynamic and complex environments. The particular selection and implementation of such features can be referred to as Human–Robot interaction (HRi) interfaces [137]. Moreover, to provide effective environment sensing and adaption while maintaining safety requirements, Robot–Environment interaction (HREi) interfaces are also required.

Reviewing literature evidence, several SWs and walker based robotic platforms have introduced HRi and REi interfaces. Generally, these systems are aimed at assessing the user's state

(i.e., biomechanical and spatiotemporal parameters), the user's intentions of movement and environment constraints. Likewise, these interfaces and interaction systems are commonly aimed at providing effectiveness, comfort, compliance, safety and different control strategies during rehabilitation and assistance tasks. For this purpose, some sensory modalities are frequently implemented, such as potentiometers, joysticks, force sensors, voice recognition modules and scanning sensors [31].

Some of these HRi and REi interfaces are shown in Table 2.1, where the SWs are characterized by their type (i.e., active for motorized walkers and passive for non–motorized walkers), the sensors used, the internal modules (i.e., main reported functionalities or systems), the reported modes of operation and the implemented shared control strategies.

Platform	Type	Sensory Interface	Internal Modules	Modes of Operation	Shared Control Strategies
GUIDO [138]	Active	- Force sensors - LRF - Sonars - Encoders	- Autonomous navigation - Detection of user's intentions - Sound feedback	- Supervised - Autonomous	-
XR4000 [139]	Active	- Force sensors - LRF - Sonars - Infrared sensors - Encoders	- Autonomous navigation - Detection of user's intentions	- Free - Supervised - Autonomous	- Shared steering
ASBGo++ [137, 140, 141]	Active	- Force sensors - LRF - Sonar - Infrared sensors - Camera - Encoders	- Autonomous navigation - Detection of user's intentions - Gait monitoring - User position feedback	- Free - Supervised - Autonomous	-
JARoW [142, 143]	Active	- LRFs - Infrared sensors - Encoders	- User position estimation - Obstacle avoidance	- Free - Supervised	-
NeoASAS [144]	Active	- Force sensors	- Detection of user's intentions	- Free	-
UFES [30, 145]	Active	- Force sensors - LRF - IMUs - Encoders	- Path following - Obstacle avoidance - Detection of user's intentions - Gait monitoring	- Free - Supervised - Feedback	- Modulated admittance control - Visual feedback
PAMM [146]	Active	- Force sensors - Sonars - Camera - Encoders	- Autonomous navigation - Health monitoring	- User control - Path following control	- Adaptive - Shared admittance controller

MOBOT [32, 147–149]	Active	- Force sensors - LRFs - Cameras - Kinect sensors - Microphones	- Autonomous navigation - Detection of user's intentions - Speech recognition - Gesture recognition - Body pose estimation - Gait monitoring	- Walking assitance - Sit-to-stand assistance - Clinician control	- Adaptive control based on context
CAIROW [150] behaviour	Active	- Force sensors - LRFs	- Environment analyzer - Force analyzer - Gait monitoring	- Context aware mode	- Adaptive
ISR–AIWALKER [151, 152]	Active	- Force sensors - Kinect sensor - Encoders - Leap motion - RGB-D Camera	- Detection of user's intention - Gripping recognition - Gait monitoring - Autonomous navigation	- Supervised - Navigation aided	- Aided user intent by the navigation system
COOL Aide [153]	Passive	- Force sensors - LRF - Encoders	- Autonomous navigation - Detection of user's intentions	- Supervised	- Shared control based on obstacles
Wachaja et al. [154]	Passive	- LRF - Tilting LRF	- 3D Mapping and localization - Obstacle avoidance - Vibrotactile feedback	- Single feedback - Multiple feedback	-
MARC [155, 156]	Passive	- Sonars - Infrared sensors - Encoders	- Path following - Obstacle avoidance	- Warning mode - Safety braking mode - Braking mode - Steering mode	- Shared steering
c-Walker [157]	Passive	- Kinect like sensor - RFID reader - IMU - Camera - Encoders	- Autonomous navigation - People detection and tracking - Guidance	- Acoustic feedback - Mechanic feedback - Haptic feedback	- Shared steering

Table 2.1: Related works involving smart walkers with HREi interfaces.

One of the most notable smart walkers is CO-Operative Locomotion Aide (COOL Aide), which is a three-wheeled passive SW [153] intended to assist the elderly with routine walking tasks. It includes mapping and obstacle detection systems, as well as navigation and guidance algorithms. Additionally, it is equipped with force sensors on its handlebars and a Laser Range Finder (LRF) to estimate the user's desired direction to turn. Although it is a passive walker, shared control strategies are achieved by granting walker control to the platform or to the user.

Other passive walkers, such as those presented in [154, 155], include navigation and guidance algorithms in conjunction with shared control systems. These strategies are based on sharing the steering control between the user and the walker.

Different approaches on active SWs have been developed in the past few years regarding HRi and REi interfaces [137–142,145–148,150]. These interfaces are also equipped with navigation and user interaction systems to provide shared control capabilities. Such strategies are based on granting walker steering to the user or to the SW, depending on the obstacle detection and navigation systems, as well as on changing the walker responses to user's commands (i.e., some strategies are based on inducing the user's actions through haptic communication channels). To this end, user interaction systems are required to manage how user's intentions of movement are interpreted. The estimation of such intentions is commonly achieved by admittance control systems, gait analysis systems, and rule-based algorithms.

In addition, other robotic walkers have been reported in the literature, including different HRi interfaces [158–161]. For instance, the approach developed by Ye et al. [159] includes a width changeable walker that adapts to the user's intentions and environment constraints. Likewise, some REI interfaces have been presented in [162–164]. These approaches intend to assess the environment information to adapt their control strategies. Finally, regarding social interaction approaches, the *c-Walker* [157] includes a social force model that represents pedestrians and desired trajectory paths as repulsive or attractive objects, respectively. Although the *c-Walker* presents both shared control strategies and social interaction, it is a passive walker and its shared strategy is based on brakes control and shared steering of the platform.

Bearing in mind the above mentioned, the main purpose of this work is the design and implementation of a multimodal Human-Robot-Environment interactionHREi interface for an SW. Such implementation is aimed at improving previous implementations of HRi and REi interfaces on SWs, by providing safety, natural user interactions and robust environment interactions.

Chapter 3

AGoRA Walker: Robotic Platform and HREi Description

This chapter introduces the design, development, and implementation of a set of control strategies and interaction systems that establish an HREi on a robotic walker, i.e., the AGoRA Walker. The design criteria were proposed in order to join and improve the multiple advantages of the current HRis and REis. The AGoRA Walker is equipped with a multimodal sensory and actuation interface that enables the implementation of several functionalities. Furthermore, all systems and functions of the device were designed considering that the target population is mainly defined by stroke survivors, SCI patients and older adults.

3.1 Human-Robot-Environment interface (HREi)

As one of the main objectives of this work, a multimodal HREi was designed to provide safety, natural user interactions and robust environment interactions during walker-assisted gait. The HREi was focused on the development of shared control strategies (i.e., natural and intuitive user interaction while multiple systems are running), as well as on the imple-

mentation of a robust Robot–Environment interface (REi) (i.e., a safety system for collision prevention, a navigation system and a social interaction system). Moreover, the interface was designed to be equipped with several strategies for management and supervision by a technical or health care professionals. To this end, several robotic and image processing techniques, as well as different control strategies, were implemented. Navigation and human detection systems were aimed at enabling the AGoRA Walker with social interaction and acceptance capabilities. Additionally, user interaction systems and shared control strategies sought to provide a more natural, intuitive and comfortable interaction.

3.1.1 Interface Design Criteria

In order to meet the functionalities of the proposed HREi, two interface to provide HRI and REI were designed. Regarding the HRi, the device should be able to recognize and estimate the user's intentions of movement from the interaction forces between the user and the platform. Moreover, the walker requires natural and intuitive control strategies to adapt its behavior to the user's navigation commands. Likewise, to provide safety and proper gait assistance, the walker movement should only be allowed when the user is properly interacting with the walker's handlebars (i.e., partially supporting on the platform and standing behind it). Finally, in order to be able to track the user's rehabilitation progress, the user's gait parameters should be estimated. These parameters might contain useful information for the clinical assessment of the user.

Considering the REi functions, several features are required. On the one hand, an accurate and efficient low-level motion controller are required to ensure the execution of desired speed profiles on the walker. On the other hand, to provide safe and effective REI, a navigation system with map building, autonomous localization and path planning capabilities is required. Similarly, to provide social interaction capabilities between the walker and surrounding people, it is needed to differentiate among static and complex objects such as humans to adapt the walker behavior. To this end, the device should be equipped with a robust people de-

tection system and motion adaption system based on social spacing and people proxemics. Finally, to provide proper functioning under failure or malfunctioning of the described systems, a low-level safety system. This system should be computationally inexpensive to assess environment hazards.

In addition to the above, several features such as remote control capabilities, emergency braking and session's data recording are also required. Figure 3.1 depicts the most relevant systems provided by the HRi the REi included in this work.
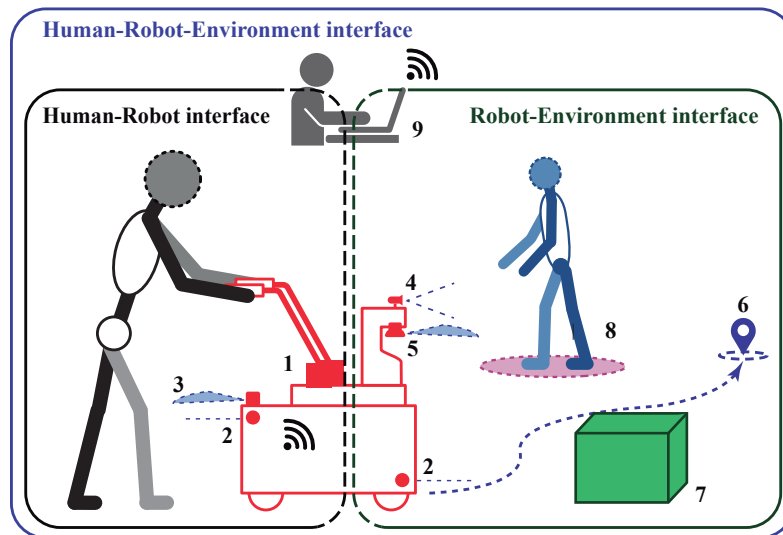
Figure 3.1: Illustration of HRi and REi functionalities: (1) Estimation of interaction forces; (2) low level safety rules; (3) estimation of user's gait parameters; (4) people detection; (5) navigation system; (6) path planning; (7) low-rise obstacle detection; (8) social spacing for people-like obstacles; and (9) platform management and supervision.

3.1.2   Interface Communication Channels

Relying on the different interface functionalities, there are some notable communication channels that take place and provide information exchange between the main components of the interface. In general, a communication channel is one that allows an exchange of information between the user and the device. This communication can be given by different physical elements (e.g., sensors or actuators) or by strategies and behaviors of the robotic walker. The communication channels immersed over the HREi are shown in Figure 3.2.
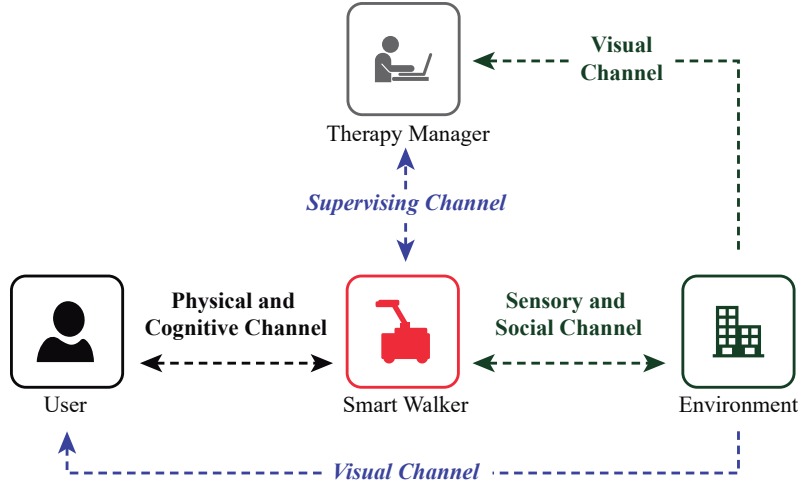
Figure 3.2: Multimodal communication channels over the HREi.

On the one hand, the *user–walker physical and cognitive channel* provides user's information such as, navigation commands, interaction forces, body weight support and gait parameters. Similarly, through this channel, the user is able to sense the walker's behavior according to changes in its mechanical impedance, as well as the responses of the safety restrictions, the guidance system, and the reactions to the navigation commands. Similarly, the *walker–environment sensory and social channel* allows the adaptation of the walker's behavior according to the information retrieved from the environment. Such information is used by the walker's systems to accomplish obstacle avoidance, safety provision, and social interaction.

On the other hand, through the *manager–walker supervising channel*, the therapy manager is able to remotely assess the session data, as well as override or control the walker behavior, if required. Moreover, the therapy manager is able to retrieve environment information through the *manager–environment visual channel*. Such visual sensing allows the manager to set and modify the walker's behavior according to the environment state.

Finally, relying on the natural visual faculty of the user, the environment and walker behavior is cognitively sensed by the user through the *user–walker–environment visual channel*. This natural communication channel takes place over the HREI loop, even though it is not addressed or included in the HREI control strategies.

3.2   AGoRA Smart Walker

To implement the previously described HREi, a robotic platform was adapted to emulate the structural frame of a conventional assistance walker, by attaching two forearm support handlebars on the platform's main deck. The Pioneer LX research platform (Omron, USA), was used to implement and test the interface systems, as shown in Figure 3.3a.

(a) Sensory interface of the AGoRA Walker.

(b) Reference frames on handles.
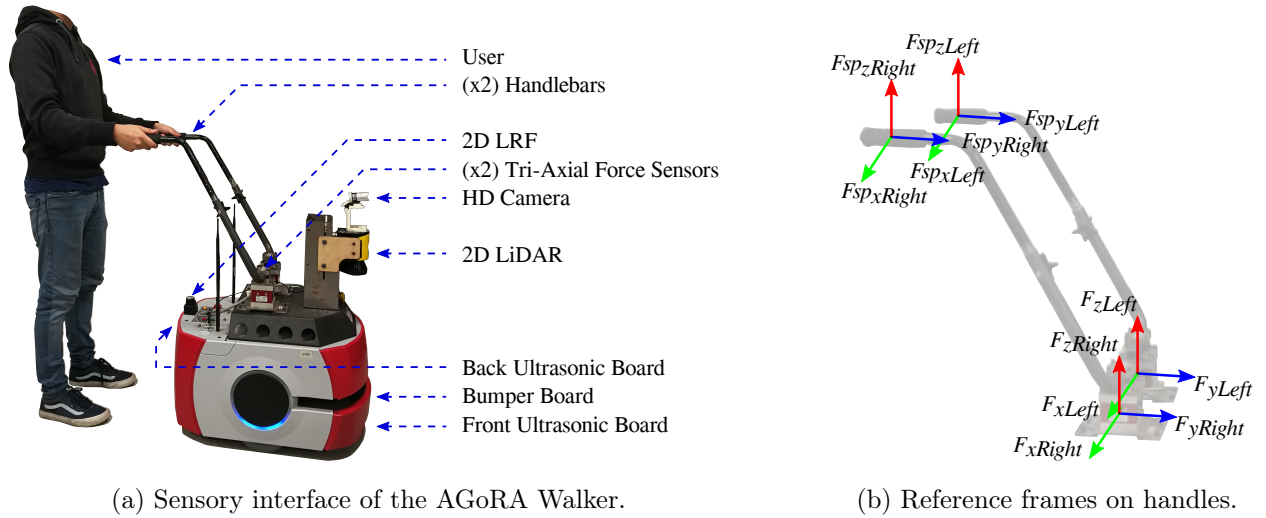
Figure 3.3: (**a**) The AGoRA Walker is mounted on a commercial robotic platform. Several sensors provide user and environment data. (**b**) Reference frames on handlebars and force sensors.

The platform is equipped with: (1) Two motorized wheels and four caster wheels; (2) two encoders, one Inertial Measurement Unit (IMU) and two hall sensors to measure walker's overall position and speed[1]; (3) a 2D Light Detection and Ranging sensor (LiDAR) (S300 Expert, SICK, Germany) for environment sensing; (4) two ultrasonic boards for user and low-rise obstacles detection[1]; (5) a bumper panel to stop the platform under collisions[1]; (6) two tri-axial load cells (MTA400, FUTEK, USA) to estimate the user's navigation commands; (7) a camera (LifeCam Studio, Microsoft, USA) to sense people in the environment; and (8) a 2D Laser Range-Finder (LRF) (URG-04LX, Hokuyo, Japan) for user's gait parameters estimation.

---

[1]The manufacturer does not provide more specific information on these sensors.

Moreover, as shown in Figure 3.3b, the position of the force sensors on the platform's deck is not vertically aligned with the actual supporting points of the user on the handlebars. Essentially, the forces in y- and z-axis read by the sensors (i.e., F_{yRight}, F_{yLeft}, F_{zRight} and F_{zLeft}) are a combination of the forces in y- and z-axis at the supporting points (i.e., Fsp_{yRight}, Fsp_{yLeft}, Fsp_{zRight} and Fsp_{zLeft}). The forces in x-axis (i.e, F_{xRight}, F_{xLeft}, Fsp_{xRight} and Fsp_{xLeft}) are discarded, as they do not provide additional relevant information.

The platform is equipped with an on-board computer running a Linux operating system distribution providing support for the Robotic Operating System (ROS) framework. Table 3.1 illustrates the main characteristics of the on-board computer and its processing capabilities [165]. In order to interface the actuation and sensory systems of the robotic platform, the *RosAria* package was used [166]. This package provides a ROS interface for most Adept MobileRobots, MobileRobots Inc., and ActivMedia mobile robot bases supported by Adept MobileRobot's open source ARIA library [166].

Feature	Description
Processor	Intel® D252 64-bit Dual Core™ 1.8 GHz Atom
Graphics	Integrated Intel® Graphics
RAM	2GB DDR3-1066
Operating System	Ubuntu 14.04 LTS
Connectivity	802.11 a/b/g Wireless Card
	Gigabit Ethernet Ports (x2)
I/Os	USB 2.0 (x3)
	RS-232 (x2)
Hard Disk Drive	16 GB

Table 3.1: Technical features of the on-board computer of the AGoRA Walker.

Additionally, to leverage the AGoRA Walker processing capabilities, an external computer is used for running several systems (i.e, OMEN by HP-15-ce003la, USA). Table 3.2 describes the main characteristics of the external computer [167]. The communication with the external

CPU is achieved through the walker's Ethernet and Wi-Fi modules.

Feature	Description
Processor	Intel® Core™ i7-7700HQ @ 2.8GHz (8 CPUs)
Graphics	NVIDIA® GeForce® GTX 1060 6GB
RAM	16 GB SDRAM DDR4-2133 (2 x 8GB)
Operating System	Ubuntu 16.04 LTS
Connectivity	802.11 /b/g/n/ac (2x2) Wireless Card
	Bluetooth® 4.2 Intel®
	Integrated LAN 10/100/1000 GbE
I/Os	USB 3.1 (x3)
Hard Drive	1 TB SATA and 128 GB SSD

Table 3.2: Technical features of the external computer used along with the AGoRA Walker.

Regarding the operating environment and technical features, Table 3.3 describes several characteristics of the AGoRA Walker. Finally, further specifications of the measurement and actuation systems of the AGoRA Walker can be found in the document's Appendix A.

	Variable	Minimum Value	Typical Value	Maximum Value	Units
Dimensions	Length	-	805	-	mm
	Width	-	483	-	mm
	Height	-	1045	-	mm
	Weight	-	70.2	-	kg
Mobility Overview	Translational Speed	- 0.1	-	1.8	m/s
	Rotational Speed	- 5.236	-	5.236	rad/s
	Turning Radius	-	0	-	mm
	Payload	-	60	-	kg
	Position Accuracy	-		-	

Power	Battery	22	24	30	VDC
	Type	-	LiFePO4	-	-
	Capacity	-	60	-	Ah
	Run Time	-	13	-	hours
	Energy	-	1.5	-	kWh
	Recharge Time	-	3.5	-	hours
	Auxiliary Power	-	5, 12, 20	-	VDC
Environment	Slope	-	1:1	1:12	-
	Terrain	-	Wheelchair accesible	-	-
	Temperature	5	-	40	°C
	Humidity	5	-	95	%
	IP Rating	-	IP-40	-	-

Table 3.3: Technical specifications of the AGoRA Walker robotic platform.

Chapter 4

Human-Robot interface (HRi) and Therapists Accompanying

The interaction between users and assistive devices is a key research topic in the development of SWs. Specifically, SWs are often equipped with a wide range of sensors and actuators, as well as, several interaction strategies to provide both physical and cognitive support to their users (See Chapter 2). Thus, these strategies are also aimed at allowing a more natural and intuitive assistance and rehabilitation process, in clinical and daily life scenarios. This chapter presents the implementation of the HRi previously described in Chapter 2 to interact with users, as well as the description of its internal systems and modules. Moreover, the design and implementation of a Physical and Cognitive interface (PCi) to involve clinicians and therapy managers is also presented.

4.1   HRi Interface for User Interaction

Based on the physical interaction between the user's upper limbs and the walker's handle-bars, the HRi is composed of two main systems: (1) a user's intention detector; and (2) a admittance control system.

4.1.1 User's Intention Detector

During gait, the movement of the human trunk and center of mass describe oscillatory displacements in the sagittal plane [168]. Thus, in walker assisted gait, the interaction forces between the user and the walker handlebars are associated to the movements of the user's upper body [161].

In this sense, to implement a proper control strategy based on such interaction forces, a filtering and gait parameter extraction process is required. Consequently, the estimation of the user's intentions of movement and the user's navigation commands could be achieved with ease and less likely to be misinterpreted.

According to the above, to carry out filtering processes, a gait cadence estimator (GCE) was implemented. The GCE addresses the gait modeling problem, which is reported in the literature to be solved with several applications of the Kalman filter and adaptive filters [169]. In fact, the Weighted-Fourier Linear Combiner (WFLC) is and adaptive filter for tracking quasi-periodic signals [169], such as gait related signals (e.g., the interaction force on walker's handlebars). Therefore, based on the on-line method proposed by Frizera-Neto et al. [170], a GCE was integrated into the HRi interface. This method uses a WFLC to estimate gait cadence from upper body interaction forces.

In the AGoRA Walker, the force applied by the user on the handlebars is decomposed in three components at each force sensor (See Chapter 3). For the purpose of the HRi, the two vertical forces (i.e., F_{zRight} and F_{zLeft}) are computed to obtain a final force, $F_{CAD} = (F_{zRight} + F_{zLeft})/2$[1]. The resulting force, F_{CAD}, is firstly passed through a band-pass filter with experimentally obtained cutoff frequencies of 1 Hz and 2 Hz. This filter allows the elimination of signal's offset and high frequency noise (i.e., mainly due to vibrations between the walker structure and the ground). The filtered force F'_{CAD} is fed to the WFLC, in order to estimate the

---

[1]F_{CAD} refers to the unfiltered force signal with cadence components.

frequency of the first harmonic of F'_{CAD}. Such frequency represents the gait cadence, which is the final output of the GCE. This process is illustrated in Figure 4.1.
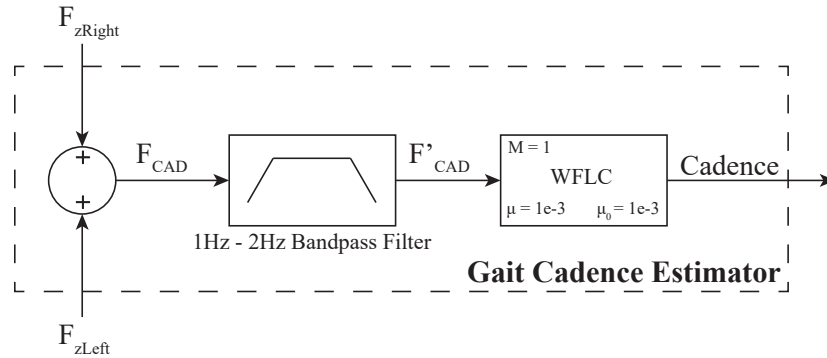
Figure 4.1: The Gait Cadence Estimator (GCE) passes the vertical interaction forces through a filtering process, based on a band-pass filter that eliminates high frequency noise due to walker's vibrations. Then, the Weighted-Fourier Linear Combiner (WFLC) filter adaptively estimates the user's gait cadence.

According to several experimental trials, it has been found that users perform significant forces, related to their intentions of movement, along y-axis (i.e., F_{yLeft} and F_{yRight}, see Chapter 3). It was also observed that the user's navigation commands are mainly included within the y-axis forces. Therefore, the *x-axis* (i.e., F_{xLeft} and F_{xRight}, see Chapter 3) forces were discarded. As previously stated, the interaction force signals require a filtering process to remove high frequency noise and signal offset [170]. Thus, a fourth order *Butterworth* low-pass filter was used.

To remove gait components from the interaction force signals along y-axis, a Fourier Lineal Combiner (FLC) filter in conjunction with the GCE was implemented. Such integration is illustrated in the filtering system (FL) diagram shown in Figure 4.2. The FL is independently applied to both left and right forces, obtaining the filtered forces F'_{yLeft} and F'_{yRight}. Thus, Figure 4.2 denotes $F_{y\Phi}$ as whether F_{yLeft} or F_{yRight}, and $F'_{y\Phi}$ as whether F'_{yLeft} or F'_{yRight}. The final output $F'_{y\Phi}$ of the FL is calculated as the difference between the resulting signal from the low-pass filter (i.e., $F_{y\Phi LP}$) the output of the FLC (i.e., $F_{y\Phi CAD}$ and the cadence signal obtained from each $F_{y\Phi}$ signal).
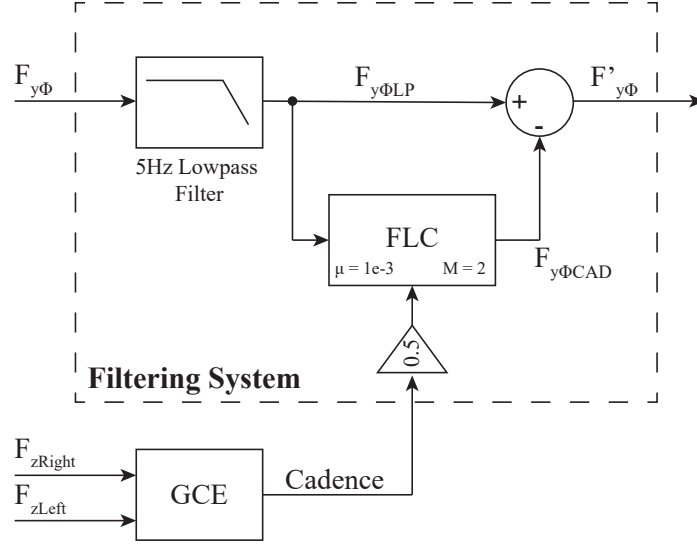
Figure 4.2: Filtering system for y-axis forces (Φ stands for $left$ or $right$). There is an independent FS for each y-axis force signal (i.e., F_{yLeft} and F_{yRight}), composed by a low-pass filter and a FLC filter.

As shown in Figure 4.2, the order M of the FLC filter was experimentally set to 2, and a 0.5 gain was added between the GCE's output and the FLC's frequency input. This gain was set to filter any additional harmonics produced by asymmetrical supporting forces [171]. Moreover, an adaptive gain μ of 0.008 was used.

In order to obtain a general estimation of the physical interaction with the user, the resulting linear force F and torque τ were estimated. These final signals were computed using F'_{yLeft} and F'_{yRight} (i.e., the y-axis forces resulting from the filtering processes) as shown in Equations 4.1 and 4.2 (d is the separation distance between the load cells on the device and is equals to 0.2 m.).

$$F = F'_{yLeft} + F'_{yRight} \tag{4.1}$$

$$\tau = (F'_{yLeft} - F'_{yRight}) * d \tag{4.2}$$

Figure 4.3: Preliminary experiment for the validation of the filtering processes. The user was asked to follow an L-shaped path. Red arrows illustrate impulse forces exerted by the user.

To illustrate the performance of the filtering processes, a simple path following task was proposed to obtain the interaction forces between the device and the user (See Figure 4.3).
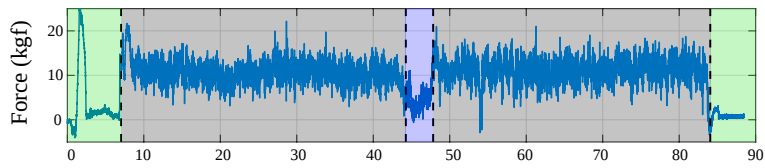
(a) Raw F_{yLeft} signal from left force sensor.
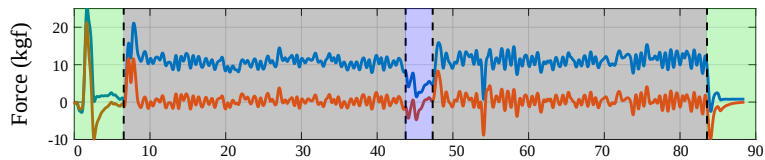
(b) Resulting $F_{yLeftLP}$ signal from the low-pass filter (Blue), and resulting $F_{yLeftCAD}$ signal from the FLC (Red) for left force sensor.
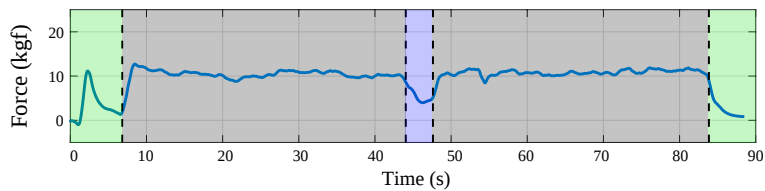
(c) Filtered F'_{yLeft} signal from left force sensor.

Figure 4.4: Filtering process illustration during a preliminary test.

During this experiment the walker brakes were released, in such a way that when the volunteer pushed the device, it moved freely. As a result, the F_{yLeft} signal obtained from the left force sensor and the implementation of the FL is presented in Figure 4.4. The signal obtained corresponds to the readings of the force sensor during the walk along the L-shaped path. Different zones are illustrated in the figure: (1) the green zones show the start and end of the path, where a peak is observed at the start of the test due to first contact with the device; (2) the gray areas denote straight parts of the path; and (3) the blue zones correspond to the curve to the right, where a decrease in the signal amplitude is observed.

4.1.2 Admittance Control System

Starting from the linear force signal and the torque signal, two admittance controllers were implemented to generate walker's linear velocity and angular velocity from the user's intentions of movement. This type of controllers has been reported to provide natural and comfortable interaction in walker assisted gait [7, 145, 163, 172], as they take the interaction forces to generate compliant walker behaviors. The implemented admittance controllers emulate dynamic systems providing the user with a sensation of physical interaction during gait assistance. These systems are modeled with two *mass–damper–spring* second-order systems, whose inputs are the resulting force F and torque τ (i.e., the force and torque applied to the walker by the user), from the filtered y-axis forces. The outputs of these controllers are the linear (v) and angular (ω) velocities, meaning the user's navigation commands.

On the one hand, the transfer function that models the linear system is described by Equation (4.3) ($L(s)$ stands for Linear System), where m is the virtual mass of the walker, b_l is the damping ratio and k_l is the elastic constant. On the other hand, Equation (4.4) ($A(s)$ stands for Angular System) shows the transfer function that models the angular system, where J is the virtual moment of inertia of the walker, b_a is the damping ratio, and k_a is the elastic constant for the angular system. Thus, the dynamic behavior, meaning the mechanical impedance of the walker, could be changed by the modification of the controllers parameters.

$$L(s) = \frac{v(s)}{F(s)} = \frac{\frac{1}{m}}{s^2 + \frac{b_l}{m}s + \frac{k_l}{m}} \tag{4.3}$$

$$A(s) = \frac{\omega(s)}{\tau(s)} = \frac{\frac{1}{J}}{s^2 + \frac{b_a}{J}s + \frac{k_a}{m}} \tag{4.4}$$

Empirically, it was realized that the values of $m = 15$ Kg, $b_l = 5$ N·s/m, $J = 5$ Kg·m^2 and $b_a = 4$ N·m·s/rad were appropriate for the purposes of this work. Moreover, k_l and k_a were used for the walker's behavior modulation. Figure 4.5 shows how the two FLs of the GCE and the user's intention detector are connected.
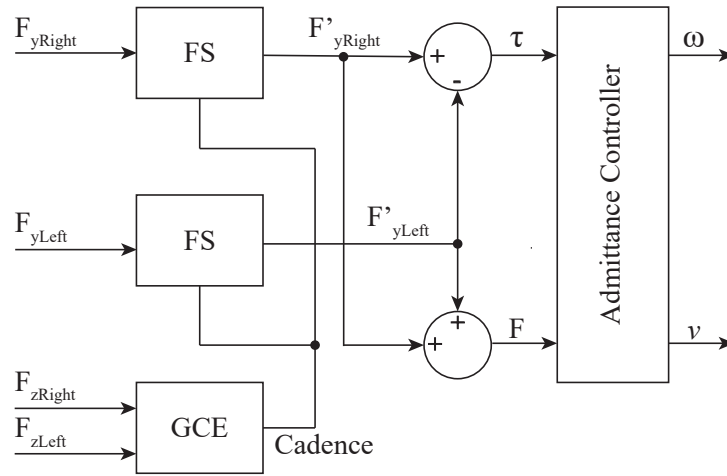
Figure 4.5: Connection between the GCE, the FSs and the proposed admittance controllers.

4.2   PCi for Therapist Accompanying

Generally, gait rehabilitation therapies with conventional walkers demand close accompanying of physiotherapists or clinicians, resulting in high physical efforts [173]. Such accompanying is usually characterized by the supporting of patient's body weight, which occasionally might result in hazardous situations for both user and therapist [108]. Although the physical and cognitive interaction with therapists could affect the patient's independence [174, 175], it has been proven the need for close and active accompanying of therapists during therapies [161, 176].
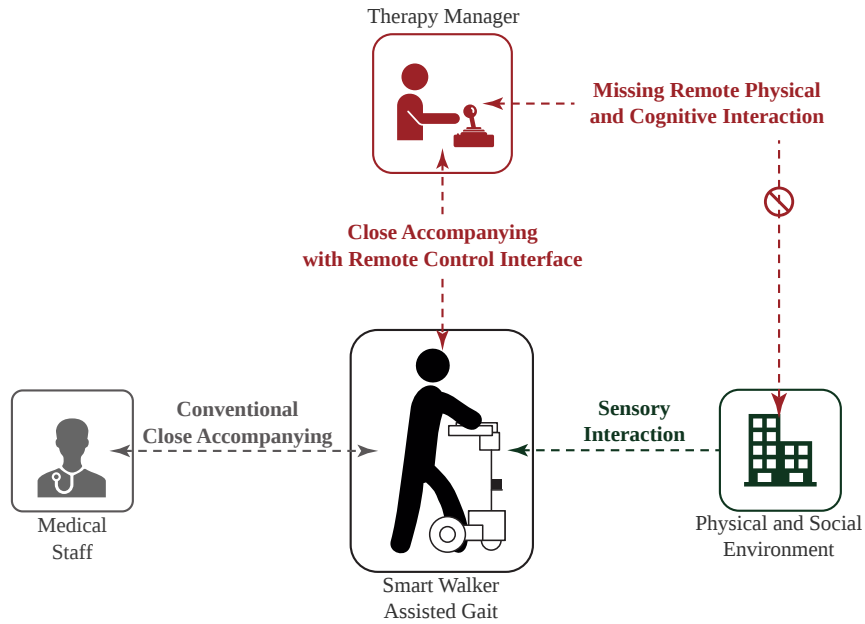
Figure 4.6: Interaction-Loop between therapists, users and environment over a walker-assisted gait therapy.

Bearing in mind such assertions, one of the interactions-loops during walker-assisted gait occurs between the medical staff, the users and the environment (See Figure 4.6). The environment is perceived by the SW's sensory interface [31] and such information is communicated to the user relying on the HRi (See Section 4.1). Moreover, conventional close accompanying of the therapist is based on verbal communication and physical interaction with the user. Therefore, having an additional device, for remote control and monitoring of the SW, may represent a promising option to increase therapies' safety and provide additional control channels, as well as, reduce physical efforts on therapists.

A Physical and Cognitive interface (PCi) was designed to provide the medical staff with a remote device for SW control. In particular, a scenario was proposed where the SW should guide a virtual user through a predetermined path. Thus, the therapist should have a remote device that allows him to modify the movement of the SW, when the user deviates from the desired path. The strategy uses a joystick with haptic and visual feedback to advise how to generate movement commands on the SW.

4.2.1   Path Following Task

To emulate a walker-assisted gait therapy, a path following task was proposed. The user had to generate the linear movement and the therapist had to control the turns of the walker. Particularly, the user was simulated by generating virtual forearm support and impulse forces, and the therapist was in charge of controlling the horizontal movement of the joystick to generate virtual torques on the SW. Subsequently, the admittance controller described in section 4.1 was used to only obtain linear and angular velocities. A a set of navigation paths were predefined and fed to a path following algorithm (See Figure 4.7).
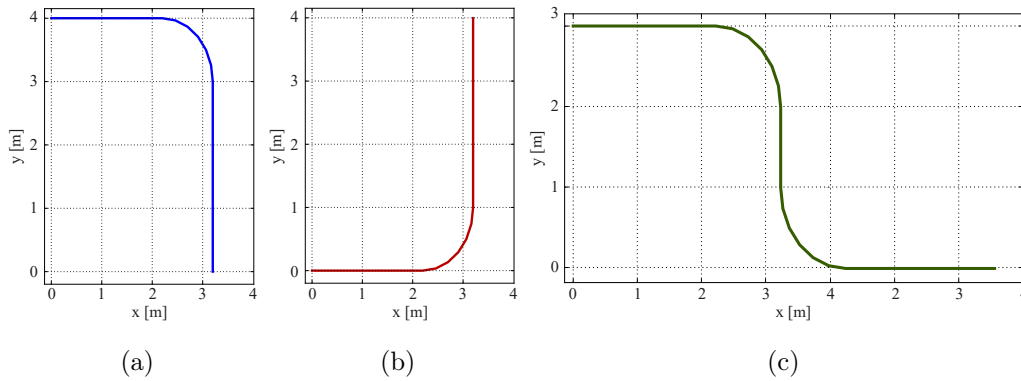
Figure 4.7: Designed trajectories for the path following task.

The path following controller developed by *Andaluz et al.* [177] was used to on-line calculate the desired walker orientation (θ_d). Such desired orientation was used to estimate the angular position error $(\tilde{\theta})$ as $\tilde{\theta} = \theta_d - \theta$.

4.2.2   Testing Environment and Haptic Device

A simulation environment and a haptic joystick were required[2] (See Figure 4.8). The PCi was equipped with an standard workstation constituted by an Intel® Core™ i5-2500 with 4 cores at 3.30GHz with 8 GB of RAM memory. The CPU was configured to run a Linux operating system distribution, providing support for the ROS framework.

---

[2]This implementation was made in collaboration with the Assistive Technology research laboratory (NTA) of the Federal University of Espírito Santo (UFES), Vitoria, Brazil
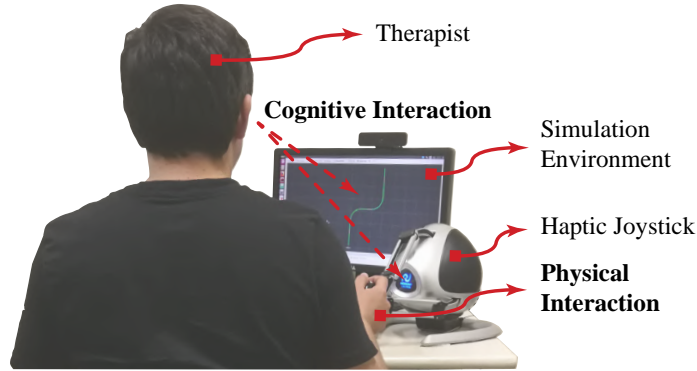
Figure 4.8: Illustration of the testing environment and the interactions between the therapist and the haptic device.

Moreover, a simulation software was configured. The ROS 3D visualization tool was used for presenting a simulated walker on a computer Screen (i.e., rviz). Additionally, the walker odometry and kinematic information were artificially generated by the *MobileSim* simulator and the *RosAria* ROS package. Finally, the The Novint Falcon haptic device was used. The device has 3 translational degrees of freedom DOF. The open-source *libinifalcon* driver was used and an adaption of the *rosfalcon* ROS package was made to fulfill the system requirements.

4.2.3 Feedback Strategies

The angular position error ($\tilde{\theta}$) was fed back to the therapist by means of three strategies implemented on the joystick.

No Feedback Mode

Under this mode, the therapist was only retrieved with therapy information by a path shown in the simulation environment (i.e. no feedback was provided by the joystick).

Visual and Kinesthetic Feedback Mode

Under this mode, the angular position error was fed back to the therapist, by means of two strategies. At first, the $\tilde{\theta}$ value was mapped to an horizontal position on the joystick (i.e. if an error was perceived, the joystick would automatically move along the x axis). The equation 4.5 describes the mapping of $\tilde{\theta}$ to an horizontal position in the joystick.

$$x_{position} = x_{max} \left(\frac{\tilde{\theta}}{\theta_{max}} \right), \qquad (4.5)$$

For the second strategy, the joystick LEDs were configured to change from *blue*, *green* and *red*, meaning negative, zero and positive $\tilde{\theta}$ errors, respectively. A pair of colored arrows placed at each side of the joystick, were aimed at illustrating the therapist on how to compensate the $x_{position}$ of the joystick (see Figure 4.9). Under this strategy, the therapist was asked to correct the joystick position until the LEDs showed a green color, corresponding to $\tilde{\theta} = 0$.
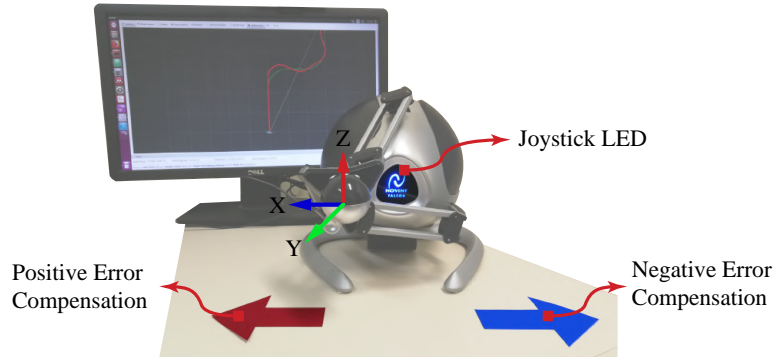
Figure 4.9: Joystick configuration and environment set–up under light feedback mode. The reference frame for the joystick movements is also presented.

Haptic Feedback Mode

Similar to the previous mode, under this mode the value of $\tilde{\theta}$ was used to move the joystick along the x-axis and to generate feedback forces. Specifically, the orientation error was mapped to an $x_{position}$ in the joystick, and once the therapist started to interact with the joystick handle, a feedback force was applied. To determine that the therapists were interacting with the handle, they were asked to press a button that was on the handle. Figure 4.10 shows the feedback force generation from the $\tilde{\theta}$. The function describing the curve in Figure 4.10 is shown in Equation 4.6,

$$F_{haptic} = F_{max} - F_{max} * e^{-\left(\frac{\tilde{\theta}}{d}\right)^2}, \qquad (4.6)$$
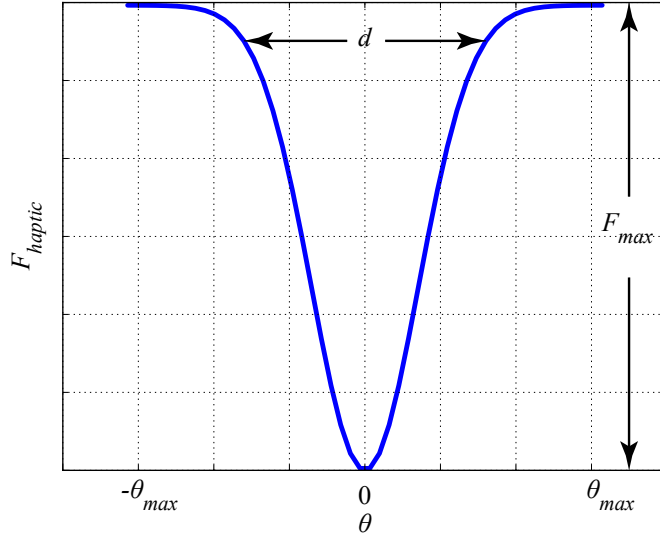
Figure 4.10: Feedback force values from $\dot{\tilde{\theta}}$

where F_{haptic} is the feedback force applied to therapist through the joystick, F_max is the maximum allowed feedback force and d is the parameter that determines the width of the F_{haptic} curve. Under this mode, when $\dot{\tilde{\theta}}$ is zero, the F_{haptic} is minimum, allowing the easy move of the joystick.

4.2.4 Preliminary Validation

To assess the performance and functionalities of the PCi, the haptic strategies were validated on naive users (i.e., users who were neither clinicians nor health professionals).

Experimental Protocol

Participants Recruitment: Participants were all formally recruited to voluntarily participate in the study. The inclusion criteria for the volunteers were that they did not have reported neither upper limb impairments nor cognitive disorders. Specifically, the system was used by 15 users that consented to participate in the study. A single session was carried out for each volunteer, composed by three different trials (i.e. one trial for a different navigation path).

Session Procedure: Prior to the participant arrival, the session environment was adapted to the corresponding feedback mode and corresponding navigation path (See Figure 4.7). At

the participant arrival, the environment was properly adjusted to the participant handedness, and a brief introduction about the use of the joystick and the feedback mode was given. After each trial, a software log was stored containing information regarding to the trial performance and interactions.

Acceptance and Usability Assessment: Based on the UTAUT and UTAUT2 models by [178, 179], as well as, the questionnaire developed by *Heerink et al* [180], an acceptance and usability questionnaire was designed and adapted (See Table 4.1). Several categories were established, in order to evaluate different perception constructs: Facilitating Conditions (FC), Performance and Attitude Expectancy (PAE), Effort expectancy and anxiety (EEA), Behaviour Perception (BP), Trust (TR) and Attitude Towards Using Technology (AT).

Construct	No.	Question
FC	1	I had the necessary knowledge to use the system.
	2	I have previously used similar systems.
PAE	1	If I had to use a joystick as a command interface, the system would be useful to me.
	2	If I had to use a joystick as a command interface, I would like to use this system.
	3	Using the system would enhance my effectiveness over the use of joysticks as command interfaces.
	4	If I use the system, I will increase my skill to use command interfaces.
EEA	1	Learning to operate the system was easy for me.
	2	I think that I quickly learned how to control the system.
	3	I was afraid to make mistakes or break something.
	4	If I were to use the system in a real scenario, I would be afraid to lose the control of the system.
	5	Working with the system was so complicated, it is difficult to understand.
BP	1	I felt understood by the system.

	2	I think that the system was communicating with me.
	3	think that I controlled the robot using the joystick.
	4	I felt that the system helped me to control the simulated robot.
TR	1	I would trust the system if it gave me advice.
	2	I would follow the advice that the system gives me.
AT	1	I had fun using the system.
	2	I think it's interesting how the system interacts with me.
	3	Using the system is frustrating for me.

Table 4.1: Acceptance and usability questionnaire used in the preliminary validation.

Excluding questions *EEA1*, *EEA2* and *AT3*, all questions were positively formulated along each category. The survey was applied to the participants at the end of the session and it was answered using a Likert scale (i.e. Strongly, Disagree, Disagree, Neutral, Agree, Strongly Agree). Regarding the reversely formulated questions, the collected answers were mirrored along the *neutral* scale value for analysis purposes. The questionnaire did not have any clarifications regarding the questions constructs or categories. Furthermore, after the finalization of the survey, open questions were performed, in order to obtain volunteer feedback.

Study Results

Data was collected from 45 trials divided in 15 sessions (i.e., 5 participants per mode).

Performance Assessment: At each session, the first two trials, were aimed at training the participants over the joystick use and the feedback mode. The third task was aimed at assessing the interaction with the joystick (i.e. the feedback understanding). According to this, Figure 4.11 shows a representative result of each feedback strategy.
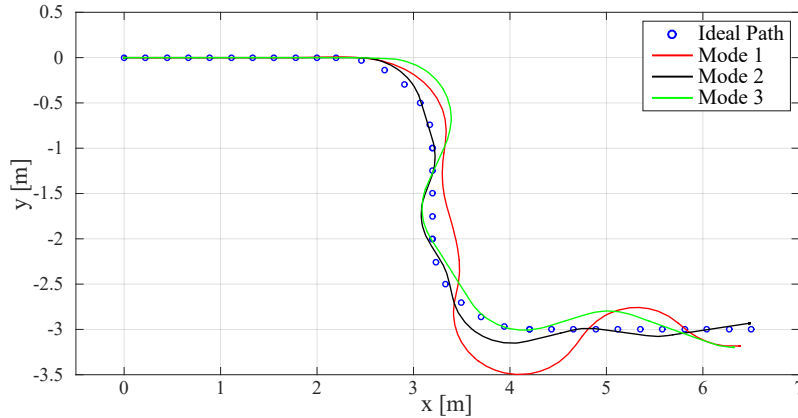
Figure 4.11: Following the virtual navigation path. Mode 1: No feedback mode, mode 2: visual and kinesthetic feedback mode and mode 3: haptic feedback mode.

During the path following task, turns require a more precise control of the SW motion. For instance, when no feedback was given, it was more complex to follow the ideal path by the participants (See Figure 4.11, mode 1). In contrast, when participants interacted under the feedback modes, easier path following was achieved (See 4.11, modes 2 and 3). Moreover, to compare the performance of the participants, the Kinematic Estimation Error (KTE) was calculated as $KTE = \sqrt{|\bar{\varepsilon}|^2 + \sigma^2}$, where $|\bar{\varepsilon}|^2$ is the mean square of the errors between the ideal path and the followed path by the SW, and σ^2 is the variance of this data. Figure 4.12 illustrates the KTE distribution for each feedback mode.
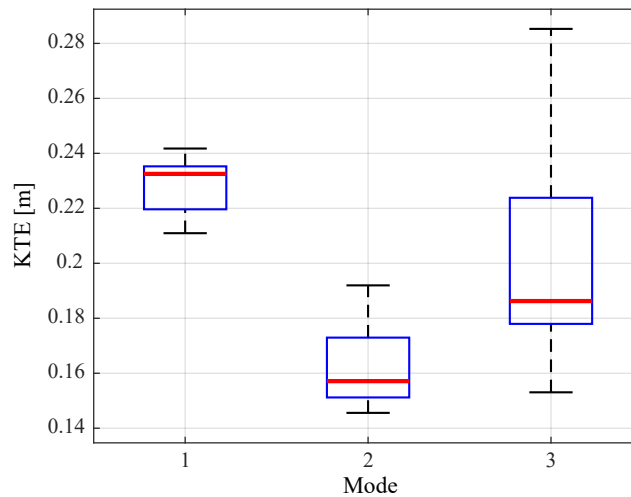
Figure 4.12: Kinematic Estimation Error (KTE) for each feedback mode. Mode 1: no feedback mode, mode 2: visual and kinesthetic feedback mode and mode 3: haptic feedback mode.

A KTE median value of 0.23 was obtained, when no feedback was provided. However, when a feedback strategy was applied, decreased KTE median values were obtained. From Figures 4.11 and 4.12, it can be stated that under mode 2, participants achieved a better performance and thus, lower KTE values were obtained (KTE median value of 0.15). Similarly, despite the maximum KTE value of 0.285 presented under mode 3, the KTE median value of 0.186 is also lower than mode 1. Hence, when a feedback strategy was provided, the participants obtained better results. The maximum KTE value presented at mode 3, was mainly supported by the non understanding of the haptic feedback strategy.

Questionnaire Responses: In order to analyze Likert data from questionnaires, the responses from each mode were studied in pairs. Specifically, the Mann-Whitney-Wilcoxon (MWW) test was used to assess differences between the feedback modes. Table 4.2 summarizes the p values obtained for each paired test between feedback modes.

Construct	Mode 1 vs Mode 2	Mode 1 vs Mode 3	Mode 2 vs Mode 3
FC	0.22	0.19	0.90
PAE	0.52	0.13	0.16
EEA	0.40	**0.007**	**0.009**
BP	0.66	0.23	**0.04**
TR	0.93	0.21	**0.05**
AT	0.65	0.96	**0.05**

Table 4.2: Mann-Whitney-Wilcoxon test p values. Mode 1: no feedback mode, mode 2: visual and kinesthetic feedback mode and mode 3: haptic feedback mode.

Additionally, the survey responses are presented in Figure 4.13, illustrating the percentage of opinions in each category for each Likert item. Negative responses are presented on the left side of the graph and positive responses on the right side. Significant differences encountered in Table 4.2 with a significance level of 0.05 are also illustrated in Figure 4.13.

As it can be seen from Table 4.2 and Figure 4.13, no significant differences were encountered under the FC perception construct. Such similarity, might suggest an homogeneous population for each strategy, in terms of the previous experience and facilitating conditions. Likewise, the PAE category showed a resembling response, with a major positive distribution. Thus, participants exhibited positive attitude, as well as, favorable acceptance towards the system performance. Regarding the effort and anxiety perception (i.e. EEA category), significant differences were encountered between modes 1 and 3, as well as, between modes 2 and 3 (See Table 4.2). These differences, might be supported by the natural effort required under the haptic feedback mode (i.e. mode 3), against the other modes. Moreover, under the EEA category the responses distributions, are mainly left aligned. Hence, the participants perceived considerable anxiety sensations and relevant system use efforts.

Both BP and TR provide the most direct measurement of the communication perception in the experimental sessions. Consequently, significant differences between the feedback modes were found (i.e. mode 1 against mode 2).

The participants stated more positive responses in mode 2 than in mode 3, meaning a better a understanding of the visual and kinesthetic communication strategy. This response distribution supports the better path following results for such mode (See Figure 4.12). Likewise, AT category showed a significant difference between modes 2 and 3. Although, both modes showed neutral and positive values, the results from mode 3 were slightly higher. Therefore, the communication established under these modes had a positive valence, as well as provided natural and intuitive interaction.
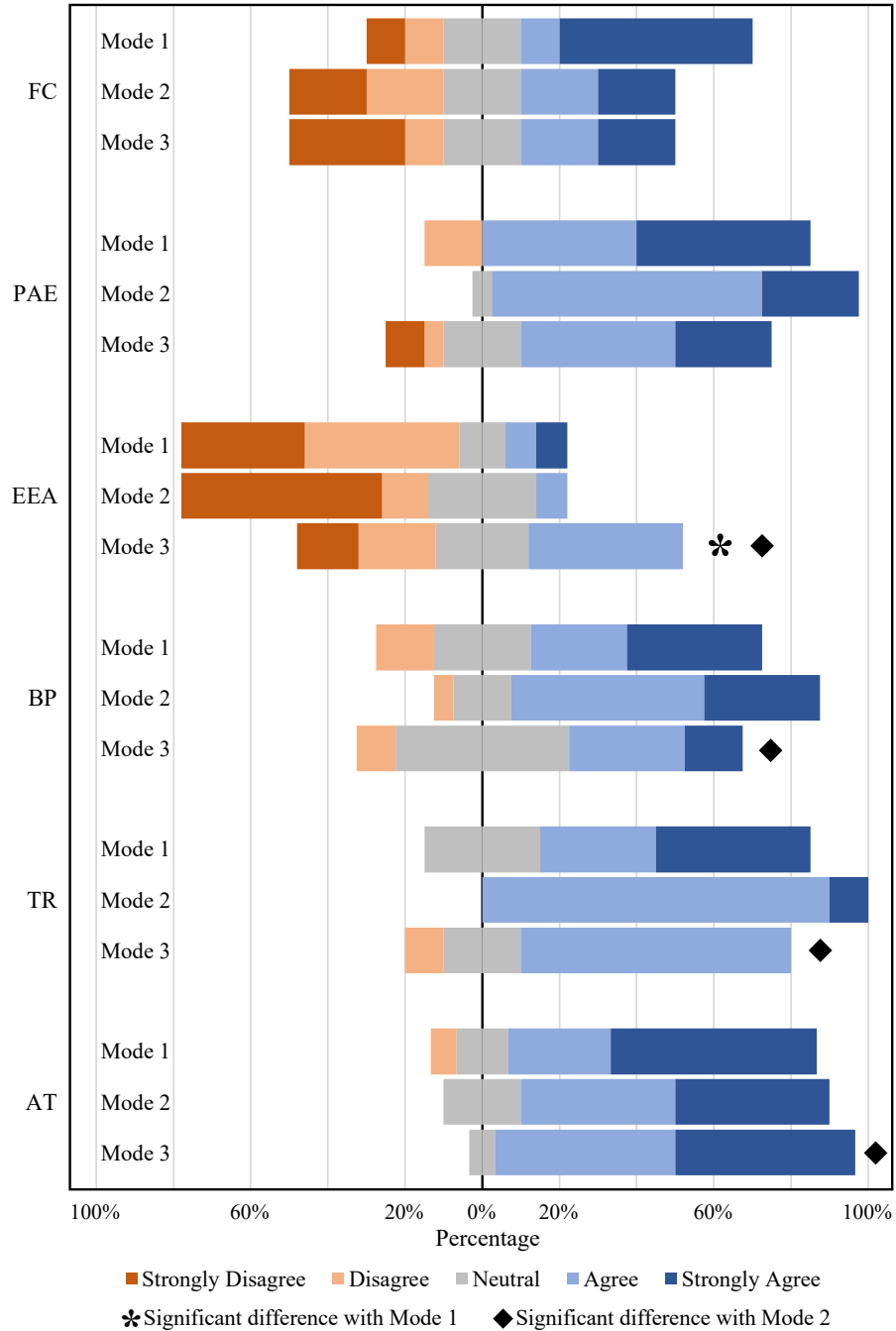
Figure 4.13: Acceptance and usability questionnaire results. Mode 1: no feedback mode, mode 2: visual and kinesthetic feedback mode and mode 3: haptic feedback mode. (Significant difference with $p \leq 0.05$).

Chapter 5

Robot-Environment interface (REi)

Mobile assistive devices are usually deployed in complex and dynamic environments, such as homes, hospitals and rehabilitation centers. Likewise, the SWs are often required to provide cognitive support to the user by assisting them in moving tasks. In this sense, the REi interfaces of the SWs are designed to provide guidance, and path following capabilities. To this end, the SWs should be able to navigate autonomously and effectively, while avoiding static and dynamic obstacles in the environment.

According to the above, this chapter presents the implementation of the REi interface of the AGoRA Walker. This interface is equipped with three main systems: (1) a navigation system; (2) a human detection system; and (3) a low–level safety system.

5.1 Navigation System

Navigation during walker-assisted gait is mainly focused on safety provision while guiding the user through different environments. According to the health condition that is being rehabilitated or assisted, the implementation of goal reaching and path following tasks is

required. Moreover, such navigation tasks on SWs require the consideration of user interaction strategies, obstacle detection and avoidance techniques, as well as social interaction strategies. Particularly, the navigation system presented in this work considers map building, autonomous localization, obstacle avoidance and path following strategies [181].

5.1.1 Map Building and Platform Localization

Relying on the ROS navigation stack, a 2D map building algorithm, that uses a Simultaneous Localization and Mapping (SLAM) technique to learn a map from the unknown environment was integrated. Specifically, the ROS *GMapping* package for map learning was used [182]. This package is aimed at creating a static map of the complete interaction environment. The static map is made off-line and is focused on defining the main constrains and characteristics of the environment. Figure 5.1a shows the raw static map obtained at the Center for Biomechatronics lab. Once this map is saved, it is also used for the walker on-line localization. For this purpose, the Adaptive Monte Carlo Localization Approach (AMCL) [183] was configured and integrated.

(a) Raw static map. (b) Edited static map.
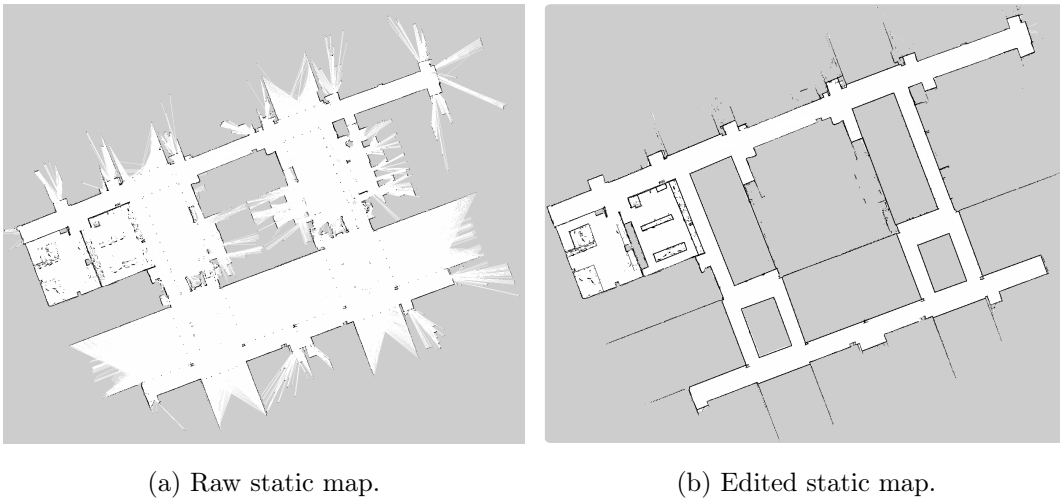
Figure 5.1: (**a**) Navigation raw static map. (**b**) Navigation edited static map. White means non-obstacle zones, gray means unknown zones and black means obstacles.

In general, zones such as stairs, elevator entrances, and corridor railings, among others, are defined as non-interaction zones (i.e., mainly due to the risk of collisions and fallings). These restrictions are achieved by an off-line editing process of the resulting static map. Further modifications are also required, since LiDARs are light-based sensors and the presence of reflecting objects, such as mirrors, affects their readings. As shown in Figure 5.1b, the map constitutes a grayscale image, therefore modifications were made by changing colors in the map.

5.1.2   Path Planning and Obstacle Detection

To achieve path planning, 2D *cost-maps* are elaborated from the previous edited map. These *cost-maps* consist of 2D occupancy grids, where every detected obstacle is represented as a cost. These numerical costs represent how close the walker is allowed to approach to the obstacles. Specifically, local and global *cost-maps* are generated. The local *cost-map* is made using readings from the LiDAR that rely on a portion of the edited map, while the global *cost-map* uses the whole edited map. Moreover, these *cost-maps* semantically separate the obstacles in several layers [184]. The navigation system integrated in this work was configured with an *static map layer*, an *obstacle layer*, a *sonar layer* and an *inflation layer* [184]. During the path planning process, the global *cost-map* is used for the restriction of global trajectories. The local *cost-map* restricts the planning of local trajectories, which are affected for variable, moving and sudden obstacles.

The Trajectory Rollout and the Dynamic Window approach (DWA) were used to plan local paths, based on environment data and sensory readings [185]. As presented in the research of Rösmann et al. [186], this local planner is optimized using a Time Elastic Band (TEB) approach. The information of the environment and global cost-map is used by a global path planner. This planner calculates the shortest collision-free trajectory to a goal point. To do this, the *Dijkstra's* algorithm was used. Finally, a motion controller takes into account both trajectory plans and generates linear and angular velocity commands to take the walker to

each plan's positions. Figure 5.2 shows the trajectories planned by the local and global planner, the positions estimations calculated by the AMCL algorithm, a current goal and the cost-map grid.
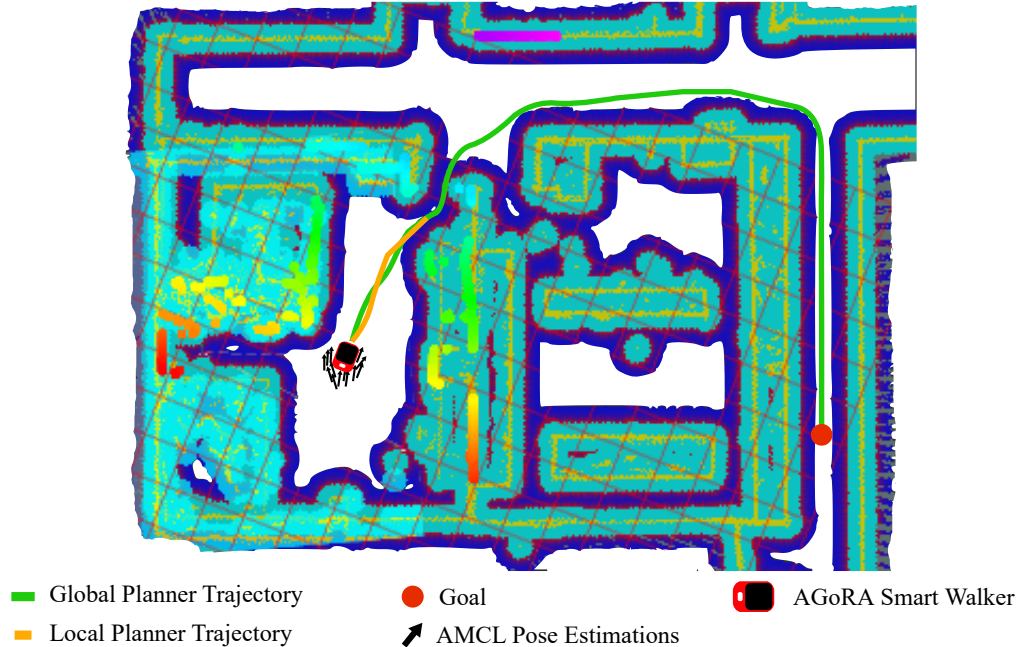
Figure 5.2: Illustration of a navigation task for the AGoRA Smart Walker reaching an specific goal. Green and orange lines represent local and global trajectories calculated by the path planning system. Light blue and dark blue zones represent the 2D *cost-map* occupancy grid.

5.2 Low–Level Safety System

The AGoRA Walker is aimed to be both remotely supervised by a therapy manager, as well as to be controlled by the user's intentions of movement (See Chapter 4). Thus, some safety rules were included to constraint the walker's movement.

5.2.1 User Condition

The walker movement is only allowed if the user is supporting itself on the walker handlebars, as well as standing behind it within an established distance.

5.2.2   Warning Zone Condition

The maximum allowed velocity of the walker is constrained by its distance to surrounding obstacles. A squared shape warning zone is defined in front of the walker, and its dimensions are proportionally defined by the walker's current velocity. If an obstacle yields within the warning zone, the maximum velocity is constrained.
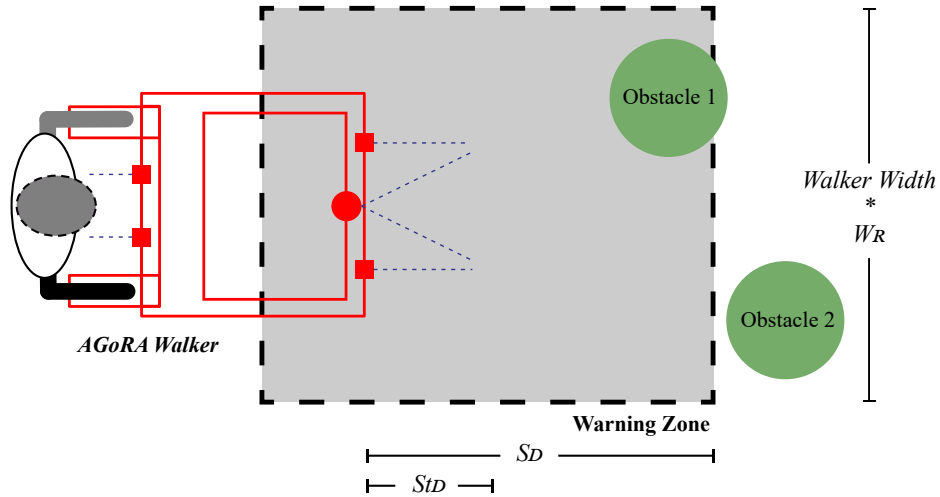
Figure 5.3: Warning zone shape and parameters for velocity limitation during obstacles presence.

Figure 5.3 illustrates the warning zone shape and its parameters that change according to the walker's velocity. The Stop Distance Parameter (STD) determines the minimum distance of the walker to an obstacle before absolute stopping. The Slow Distance Parameter (SD) determines the distance at which obstacles will begin to be taken into account before velocity limitation. Hence, if an obstacle is at distance SD, the walker's velocity will be slowed. The Width Rate (WR) parameter is the multiplying factor of the warning zone width. When an obstacle is detected within the warning zone, the velocity is limited as described in Equation (5.1).

$$V_{max} = Slow_{vel} \cdot \frac{D_{obs} - STD}{SD - STD} \qquad\qquad (5.1)$$

D_{obs} is the distance to the nearest obstacle and $Slow_{vel}$ is the maximum allowed velocity when an obstacle is in the warning zone. Additionally, the $Slow_{vel}$ is continuously adapted by the walker's velocity, as shown in Table 5.1. Such values were defined after several experimental trials, in such a way that the warning zone ensures proper stopping of the walker at each velocities range.

| Walker's | Warning Zone Parameters | | |
Velocity (m/s)	STD (m)	SD (m)	WR
≤ 0.3	0.3	0.6	1.0
≤ 0.4	0.3	0.8	1.2
≤ 0.5	0.3	1.0	1.4
≤ 0.6	0.3	1.2	1.5
≤ 0.8	0.3	1.4	2.0
> 0.8	0.3	2.0	3.0

Table 5.1: Warning zone parameters adaption according to the walker's velocity.

5.2.3 Additional Rules

In order to guarantee the user's balance when interacting with the device, some rules were established for the movement of the device. The device is only allowed to make curves with a minimum turning radius of 15 cm. Backward movements or negative speeds are disabled. Finally, the device has an emergency button to activate the brakes, as well as a remote stop service that can be executed from the external computer.

5.3 Human Detection System

Several techniques have been developed in order to detect people using different sensors, such as, laser based, camera based and both laser and camera based. As described in [187], the

combination of individual techniques constitutes a high performance and low cost computational approach, since the benefits of one technique overcome the weaknesses of the other one. Specifically, *Arras et al.* proposed a method for human detection based on clustering and classification techniques [188]. This technique was based on information regarding the geometrical characteristics of the environment and it has been proved to work efficiently indoors. However, as mentioned in [187] some problems were encountered using this technique outdoors. Likewise, in [189] the benefits of camera data for human recognition have been presented. Nevertheless, the processing of every whole image may result in a low performance of the detection system.

In this manner, the main goal of this module achieve human detection in environment both efficiently and effectively. Moreover, this module complements the capabilities of the navigation system in the distinction of obstacles regarding to people from simple obstacles (i.e., stationary or mobile objects). This distinction enables the walker with social acceptance and social interaction skills. To achieve this, the human detection system implemented in this work was based on the techniques proposed by Fotiadis et al. [187] and Garzón et al. [190]. Such approaches exploit the localization information provided by the laser of potential humans, in order to reduce the processing time of the camera data. This sensory fusion requires a proper process of calibration. Hence, an extrinsic calibration method was implemented for the laser-camera information fusion. Figure 5.4 illustrates the methodology of the integrated people detection system.
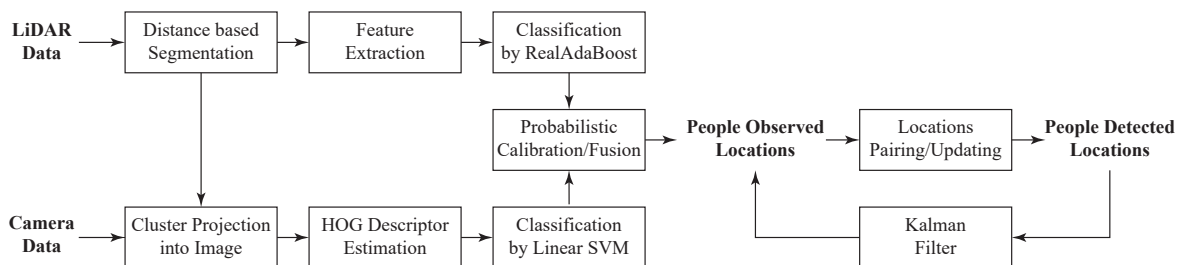
Figure 5.4: Outline of the people detection system.

5.3.1   Detection Approach

The people detection system begins with the segmentation of laser data into clusters, based on Euclidean distance differences. These laser clusters are inputs of a process of characteristic extraction [188]. Consequently, these features feed a classification algorithm based on *Real AdaBoost* [191], which is trained off-line with several laser clusters. In parallel, a camera based detection process starts from the projection of each laser cluster into the image frames. As previously mentioned, this projection is accomplished thanks to a calibration process that provides a set of rotation and translation matrices. Such matrices allow the transformation of laser points into the camera frame [192]. From the localization of each cluster, a region of interest (ROI) is defined for the calculation of a Histogram of Oriented Gradients (HOG) descriptor [193]. This descriptor is used by a Linear Support Vector Machine (SVM), which is aimed at classifying the descriptor outputs.

As also proposed in [187], to increase the possibilities to detect a person, the ROI is defined by several adaptive projections, resulting in a group of ROIs in which a person might be.

Both classifiers, *Real AdaBoost* and Linear SVM, are not completely probabilistic methods, since they produce probability distributions that are typically distorted. Such distortions take place as the classifiers outputs constitute signed scores representing a classification decision [194]. To overcome this, a probabilistic calibration method is implemented. The calibration of *Real AdaBoost* scores is achieved by a logistic correction and for the Linear SVM a parametric sigmoid function is used [187]. Afterwards, the outputs of each classifier are passed through an information fusion system, in order to get a unique probabilistic value from both detection methods, resulting in a decision about the presence of people in the environment.

Finally, a tracking process takes into account the previous people observations to generate a final decision about pedestrian locations. Specifically, a Kalman filter instance is created for each detection, including those that rely out the image frame [190]. Based on each person's

current and previous position, the filter uses a linear model to calculate people velocities, and consequently achieve the tracking task. A location pairing–updating process is carried out, as presented in [190]. This process is aimed at adding new people locations, updating previous locations, scoring, and removing them.

Figure 5.5a shows several laser clusters obtained from a LiDAR reading. Figure 5.5b explains the projection of the clusters into the image, where possible. Specifically, three moving people were detected out four. The laser cluster related to the non-detected person included additional points belonging to walls, therefore its detection was not achieved.

(a) Laser clusters.   (b) Detection scenario in stationary position.
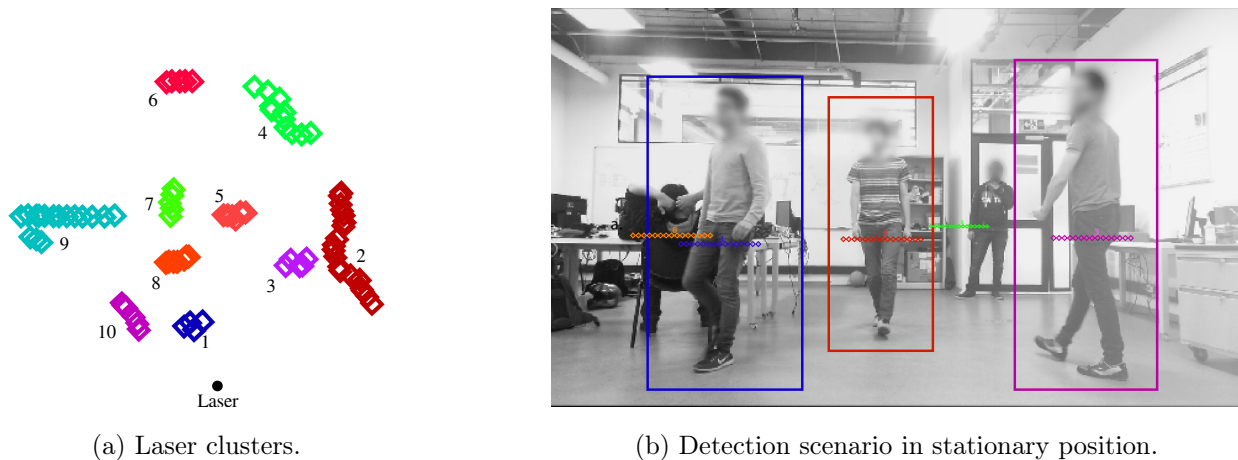
Figure 5.5: (**a**) Clusters obtained from the segmentation process of laser's data. (**b**) Three people detected in stationary position.

5.3.2   Social Interaction

The navigation system and people detection system are integrated to enable the AGoRA Walker with social interaction and social acceptance skills. This is accomplished by adjusting how obstacles are understood by the navigation system. Through the modification of the navigation 2D *cost-map*, these changes are achieved. As described in the navigation system, the obstacles detected in the environment, including people, are represented as equal costs in the 2D *cost-maps*. Therefore, it is necessary to inflate the costs corresponding to a person, to

avoid the interruption of social interaction zones in the environment. The inflation is made to match the social interaction zone of each person. This is achieved using the information provided by the people detection system, and passing people locations to navigation system. The criteria to inflate the costs are defined by strategies of adaptive spacing in walker–human interactions, as described in [195].

Chapter 6

Control Strategies and Experimental Trials

As previously explained in Chapter 3, the HREi integrates functions from the HRi and REi to provide efficient, safe and natural interaction with the user and the environment. To this end, this chapter presents the design and implementation of three control strategies, as well as their validation through several experiments with healthy patients.

6.1   Control Strategies

6.1.1   User Control

By the implementation of the HRi, the users are able to control the walker's motion according to their intentions of movement (See Chapter 4). Specifically, the user's intentions detector and the admittance controller are capable of generating velocity commands from the interaction forces. Under this control strategy, the safety rules are left active to ensure a secure interaction with the environment.

6.1.2 Navigation System Control

Under this control strategy, the REi is configured to have total control of the walker's movement, providing secure user guidance (i.e., the user's intentions of movement are ignored). The guidance goals can be whether programmed or on-line modified, while the navigation and social interaction system ensure safety paths. Additionally, the safety rules are also active ensuring that the walker moves only if the user is supporting and standing in front of the walker.

6.1.3 Shared Control

This strategy combines the navigation velocity commands and the user's intentions of movement for walker's control granting. The user's intentions are calculated using F and τ, as a vector of magnitude equals to the normalized F, with a proportional orientation to the exerted τ. Equation 6.1 illustrates the calculation of the intention vector's orientation, where Max_{angle} is the maximum turn angle allowed and MET is the maximum exerted torque.

$$\theta(t)_{usr} = Max_{angle} \cdot \frac{\tau(t)}{MET} \tag{6.1}$$

To estimate the control granting (i.e., if the walker is controlled by the user or by the navigation system), the user's intentions are compared with the navigation path, obtaining the final goal to be followed by the walker. Specifically, as shown in Figure 6.1, for the nearest path point (x_{nav}, y_{nav}) to the current walker position at (x_{sw}, y_{sw}), a range of possible user intentions is calculated (i.e., the range where the control is granted to the user). The positions are calculated in the map coordinate reference frame, since the navigation system generates the path plans in such reference frame.

The range of possible intentions is calculated as a triangle-shaped window, which is formed

by: (1) θ_{sw}, the current orientation of the walker; (2) θ_{usr}, the current user's intention of movement; (3) θ_{nav}, the orientation of the next and nearest path point; and (4) d, the Euclidean distance from the walker position to the next pose.
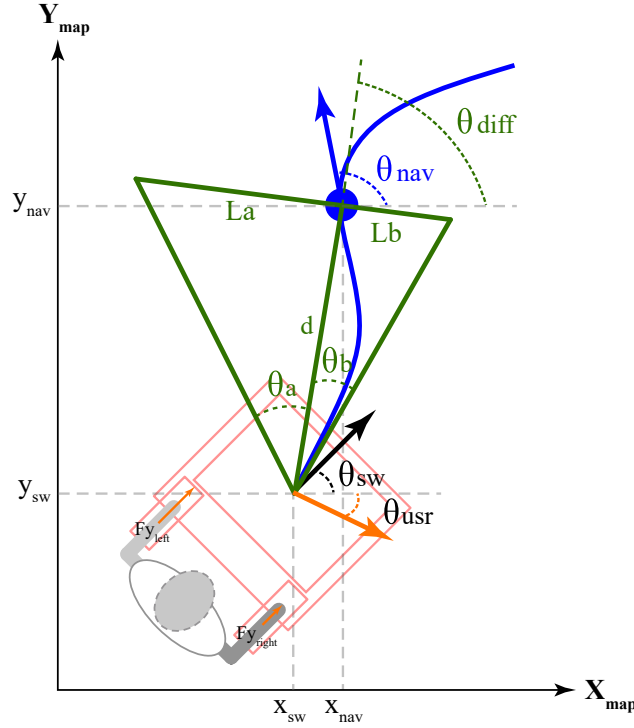
Figure 6.1: Estimation of possible user's intentions area.

The geometric parameters for the window formation are described in Equations 6.2–6.5. A window scaling factor $Wind_{width}$ is used to adapt the window area. Graphically, the window is formed by two right-angled triangles. These smaller triangles are constituted with height d, bases La and Lb, and auxiliary angles θ_a and θ_b.

$$L_a = \frac{Win_{width} \cdot (\theta_{nav} - \theta_{sw})}{Max_{angle}} \tag{6.2}$$

$$L_b = Win_{width} - L_a \tag{6.3}$$

$$\theta_a = tan^{-1}\left(\frac{L_a}{d}\right) \tag{6.4}$$

$$\theta_b = tan^{-1}\left(\frac{L_b}{d}\right) \tag{6.5}$$

If the user's intention of movement lies in the described window, the control is granted to the user. Otherwise, if the user's objective lies outside the area of possible movements, a new path pose is computed. This new pose is calculated to be within the area of possible movements. To this end, both x_{nav} and y_{nav} define the new pose position and the new pose orientation (θ_{nxt}) is defined as presented in Equation 6.6:

$$\theta_{nxt} = \begin{cases} \theta_{nav}, & if \quad \theta_{diff} - \theta_a \leq \theta_{usr} \leq \theta_{diff} + \theta_b \\ \theta_{diff} - \theta_a, & if \quad \theta_{usr} < \theta_{diff} - \theta_a \\ \theta_{diff} + \theta_b, & if \quad other \end{cases} \tag{6.6}$$

where θ_{diff} is estimated as shown in Equation 6.7 and represents the relative center of the window of possible movements.

$$\theta_{diff} = sin^{-1}\left(\frac{y_{nav} - y_{sw}}{d}\right) \tag{6.7}$$

6.2 Experimental Trials

To evaluate the described HREi, several performance and usability tests were proposed, regarding the control strategies previously described. The main goal of these tests was to assess the performance of every module of the AGoRA Walker, both independently and simultaneously. A group of healthy subjects was recruited to voluntarily participate in the validation study. Specifically, seven volunteers conformed the validation group (6 males, 1 female, 33.71 $\pm$ 16.63 y.o., 1.69 $\pm$ 0.056 m, 65.42 $\pm$ 7.53 kg) with no gait assistance requirements (See Table 6.1).

Subject	Age (y.o.)	Height (m)	Weight (kg)	Gender
1	23	1.76	65	Male
2	23	1.77	72	Male
3	23	1.65	62	Female
4	61	1.67	65	Male
5	23	1.72	69	Male
6	59	1.60	50	Male
7	24	1.70	75	Male

Table 6.1: Summary of volunteers who participated in the study.

The experimental trials took place at the laboratories building of the Colombian School of Engineering. A total of 21 trials divided into 7 sessions were performed. Every session consisted in three different trials of each specific control mode (i.e., user control, navigation system control and shared control). At the beginning of each session, the order in which the control modes were going to be evaluated was randomized. Likewise, before each trial the volunteers were instructed in the behavior of the control mode, allowing them to interact with the platform. At the end of each trial, a data log including user and walker's information was stored for analysis purposes.

According to this, the obtained results under each control mode are presented in the following sub-sections.

6.2.1   User Control Tests

The volunteers were asked to follow a square-shaped trajectory by reaching several landmarks. Figure 6.2a illustrates the reference trajectory to be followed by the participants and Figure 6.2b shows the achieved trajectories by the participants. Under this control mode, the only active systems were those corresponding to the HRi interface. The trajectory was aimed at assessing the capabilities of the interface to respond to the users' intentions of movement and

adapt to their gait pattern. Specifically, the gait parameter estimator was responsible for acquiring and filtering the force and torque signals due to the physical interaction between the walker and the user.

(a) Reference path

(b) Participants' trajectories
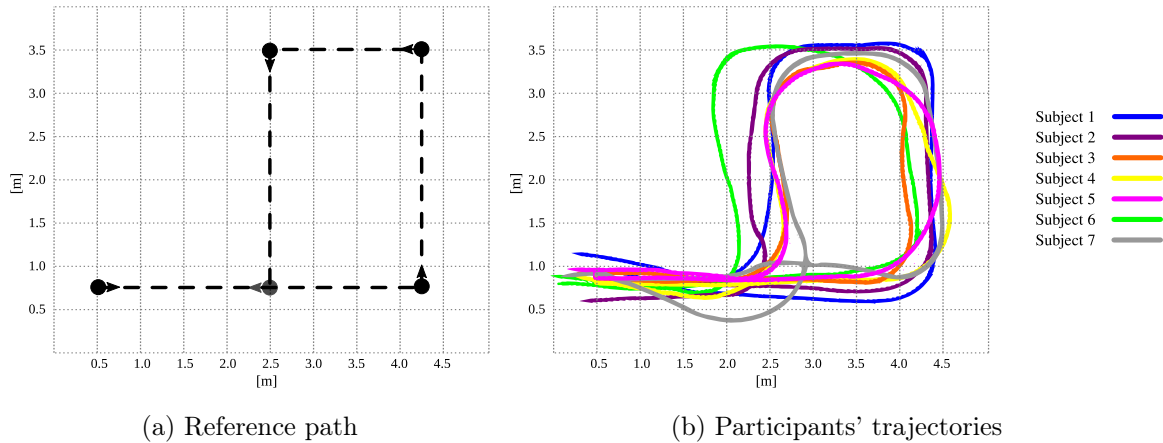
Figure 6.2: (**a**) Reference path for user control tests based on a square-shaped trajectory. (**b**) Trajectories achieved by the nine participants under user control trials.

As an explanatory result, Figure 6.3a shows the filtered signals regarding to force and torque for subject 1. The user's intentions detector was in charge of generating the linear and angular speed control signals of the walker, as shown in Figure 6.3b. Similarly, the low level safety system was running in parallel, in such a way that collisions were avoided. Specifically, no collisions took place during these trials.

During the execution of the user control trials, higher differences were encountered between the ideal and the achieved paths at the trajectory corners. Accordingly, the 90-degree turns were more difficult to accomplish by the participants, as the AGoRA Walker axis of rotation is not aligned with the user's axis of rotation. In fact, such kind of turns are avoided by the device as they risk user's stability and balance. Thus, less steep turns are more natural and safer for the users.
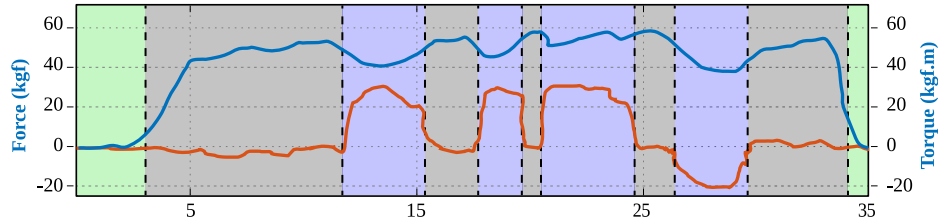
(a) Force and torque signals for the first subject.
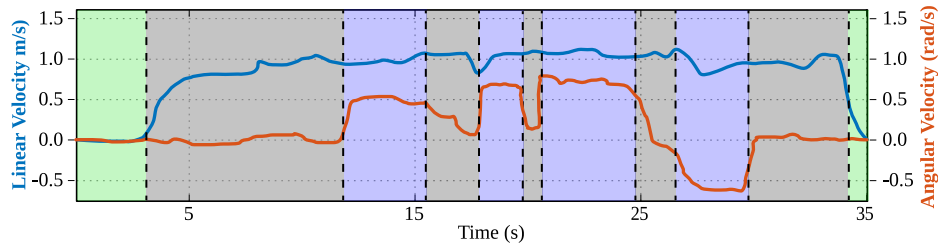
(b) Responses from the admittance controller for the first subject.

Figure 6.3: (**a**) Force (blue) and torque (orange) signals for the first subject. (**b**) Linear (blue) and angular (orange) velocities from the admittance controller for the first subject.

6.2.2   Navigation System Control Tests

The guiding capability of the navigation system was validated on the seven volunteers who participated in the study. Specifically, the predefined path goals presented in Figure 6.4 were configured in the navigation system to form a desired trajectory. The reference trajectory was designed to be similar to the reference path used for the user control trials. However, the trajectory corners were designed as soft turn curves, in such a way that the user's balance and stability were not compromised. During the seven trials, no significant differences were encountered in the achieved trajectories, no collisions took place and the mean guidance task time was 53.06 ± 2.15 s.

Additionally, to evaluate the path following and safety restrictions capabilities alongside the people detection system, a preliminary guidance trial with one subject was performed in presence of people. The volunteer was guided through a random path previously programmed, while overcoming both regular and people obstacles in the environment. The navigation system was configured with: (1) minimum turning radius of 15 cm, to avoid steeped curves;

(2) local planner frequency of 25 Hz; (3) global planner frequency of 5 Hz; and (4) maximum linear velocity of 0.3 m/s and maximum angular velocity of 0.2 rad/s.
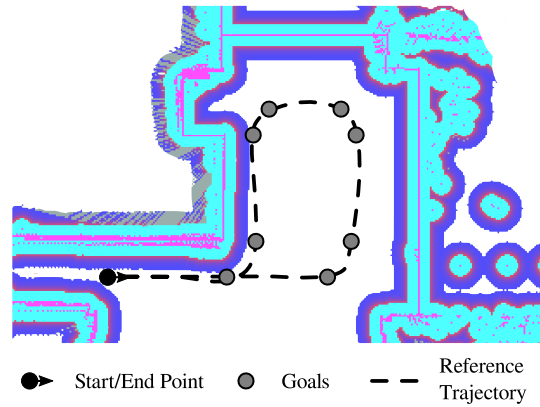
Figure 6.4: Reference trajectory and goals for the guiding task.
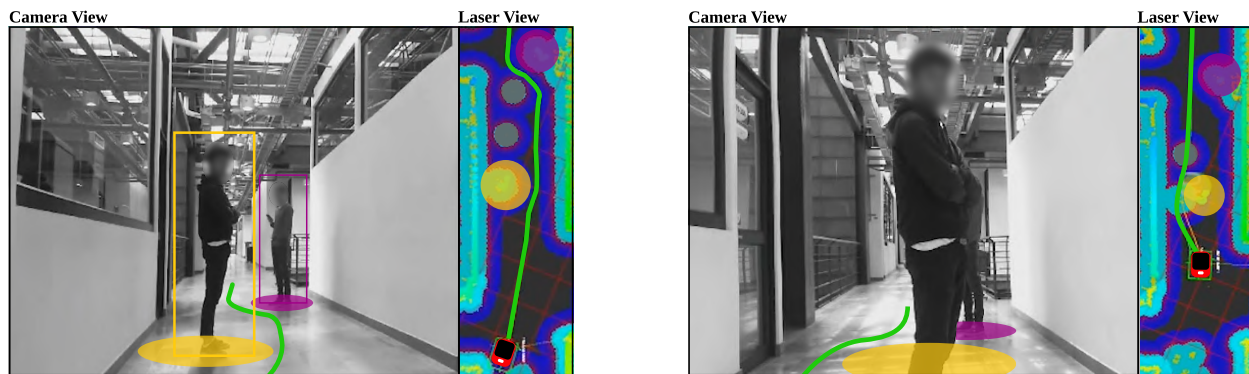
(a) Overcoming two detected people.

(b) Path update after new people locations.
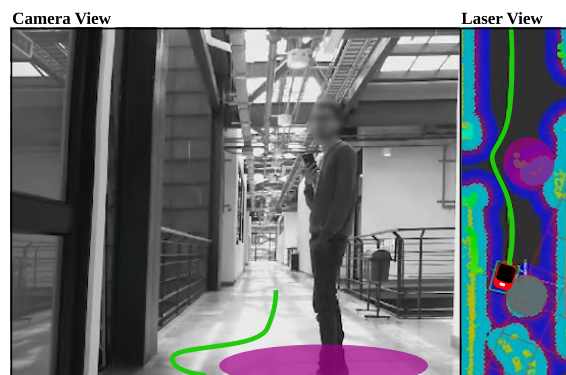
(c) Final path planning update.

Figure 6.5: Navigation and people detection systems during guidance task. Yellow and purple squares represent people obstacles detected by both camera and laser, while circles represent people obstacles only detected by the laser. Gray circles show old obstacles that will be removed once the walker senses such areas again. Green line illustrates the path.

Figure 6.5 illustrates the carried out test in three different states. The first state shows the planned trajectory according to the initial environment sense, as shown in Figure 6.5a. The second state in Figure 6.5b presents an update in the trajectory due to new people locations. Although the most proximate person to the walker is not detected by the camera, laser readings allows the person's position tracking and therefore its detection. Finally, Figure 6.5c illustrates the avoiding of another person, while continuing with the guidance task.

6.2.3   Shared Control Tests

To assess the shared control performance, each volunteer was asked to follow the reference trajectory previously presented in Figure 6.4. Under this control mode, the participants were partially guided by the navigation system. Likewise, before each trial the volunteers were informed that their intentions of movement would be taken into account. Table 6.2 summarizes main findings for each trial.

Subject	Achieved Goals	Task Time (s)	Mean Linear Speed (m/s)	Percentage of User Control (%)
1	10	63.94	0.34	69.19
2	10	71.46	0.34	71.63
3	10	48.38	0.46	53.66
4	10	83.45	0.23	62.55
5	10	64.54	0.34	68.25
6	8	80.8	0.21	73.99
7	10	60.29	0.37	67.71

Table 6.2: Summary of the results obtained for shared control trials.

The results presented in Table 6.2 suggest proper capabilities of the shared control strategy to effectively guide the participants through a specific trajectory. Six subjects achieved the full reference path by reaching its ten intermediate goals. In contrast, one subject did

not complete the task by only reaching eight goals. This result is due to a random false obstacle perceived at the ninth goal, resulting in the blocking of the path planning module. Regarding the task completion times, the mean task time obtained for all the participants was 67.55 $\pm$ 11.25 s. The differences among these times is mainly supported by the fact that the linear speed was totally controlled by the user. Accordingly, the obtained mean linear speed was 0.33 $\pm$ 0.07 m/s. Finally, to evaluate the control granting behavior under this mode, the percentage of user control was estimated. This ratio was calculated taking into account the total time of user control and the overall task time. A mean percentage of 66.71 $\pm$ 6.26 % was obtained. The user control occurred mainly in the straight segments of the trajectory, since at the trajectory curves the users' intentions of movement did not completely matched the planned path.

6.2.4 Acceptance and Usability Assessment

Similar to the perception study presented in Chapter 4, the interactions between the participants and the AGoRA Walker under the control modes were qualitatively assessed. At the end of each trial, the volunteers were asked to fill out a usability and acceptance questionnaire to obtain instant perceptions of the mode of operation. The participants were also encouraged to highlight perceptions regarding the interaction with the smart walker. The questionnaire was designed to be relevant to the interaction with the AGoRA Walker (See Table 6.3) and was based on the the UTAUT models presented in [178, 179]. Moreover, the questions were formulated to be answered using a five-item Likert scale.

No.	Question
Q1	I think the robotic device makes me feel safe
Q2	I think the robotic device was easy to use
Q3	I think most people would learn to use this device quickly, it is intuitive
Q4	I think the device guides me well
Q5	I think my experience interacting with the device was natural

Q6	I think my experience interacting with the device was intuitive
Q7	I think my experience interacting with the device was stressful.
Q8	In this session, I felt that I had control of the device
Q9	In this session, I felt that the device had the control of the path to be followed
Q10	In this session, I felt that the device control was shared with me

Table 6.3: Acceptance and usability questionnaire used in the study.

For analysis purposes, the answers from Questions Q1–Q4 were grouped into a single category (C1), since they evaluated the attitude towards the device and the expected performance. Similarly, the answers from Questions Q5–Q7 were grouped into another category (C2), as they evaluated the perceived effort and anxiety of the interaction with the device. Finally, Questions Q8–Q10 were aimed at assessing the behavior perception of each control mode. The answers from these question (i.e., Q8–Q10) were independently analyzed, to find differences between them. Figure 6.6 illustrates the questionnaire responses, showing the percentage of opinions in each category (i.e., C1 and C2), as well as in Questions Q8–Q10 for each Likert item.
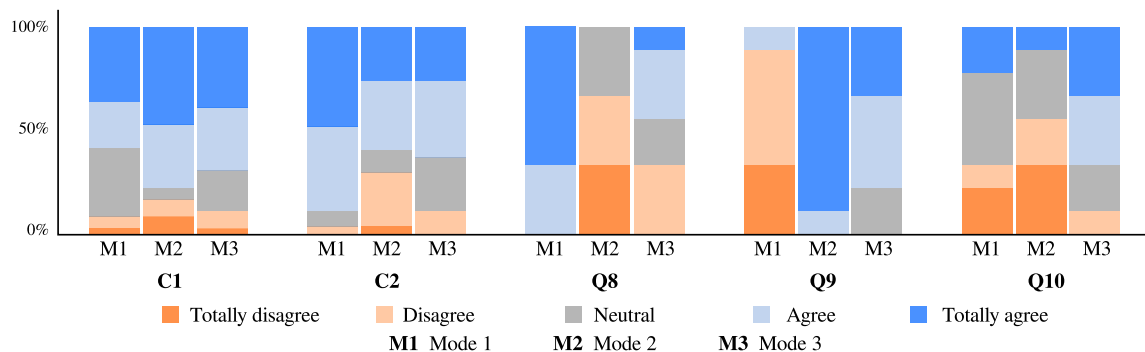
Figure 6.6: Acceptance and usability questionnaire results: Mode 1, user control; Mode 2, navigation system control; Mode 3, shared control.

Relying on the questionnaire responses for categories C1 and C2, a direct measure of the interaction perception in the experimental sessions can be obtained. Consequently, resembling survey answers were obtained under each control mode with major positive distributions.

These results might suggest safe, natural and intuitive interactions perceived by the volunteers who participated in the study. Moreover, some participants stated additional comments regarding to the navigation control mode. Specifically, the volunteers suggested that at specific trajectory points the device stopped, in such a way that the path following task was not very comfortable. These impressions occurred at several trajectory goals, since the navigation system was configured to reach them at specific orientations.

To analyze the participants' behavior perception under each control mode, the responses from questions Q8–Q10 were statistically analyzed. The MWW test was used to assess differences in the perception of each control mode [196, 197]. Specifically, Table 6.4 summarizes the p values obtained for each paired test between control modes (i.e., Mode 1, user control; Mode 2, navigation system control; and Mode 3, shared control).

Question	Mode 1 vs. Mode 2	Mode 1 vs. Mode 3	Mode 2 vs. Mode 3
Q8	**0.02**	**0.02**	**0.05**
Q9	**0.02**	**0.02**	0.08
Q10	0.37	0.136	**0.04**

Table 6.4: Mann–Whitney–Wilcoxon p values for paired tests among Q8, Q9 and Q10. p values in bold illustrate significant differences encountered, meaning $p \leq 0.05$.

As it can be seen in Table 6.4 and Figure 6.6, significant differences were encountered among all participants responses for question Q8. Such outcome may suggest that all participants perceived the ability of the interface to respond to their intentions of movement. Similarly, responses for question Q9 showed significant differences between two paired tests (i.e., Mode 1 vs. Mode 2 and Mode 1 vs. Mode 3), indicating that participants perceived modifications in the walker behavior. Finally, regarding question Q10, a significant difference was only obtained for paired test between Mode 2 and Mode 3. Such behavior might be supported by the fact that both navigation system control and user control work together under the shared control mode.

Chapter 7

Biomechanical and Clinical Trials

Several setups and tools allow the understanding of physical interaction between the SWs and its users. Among these, motion capture systems based on cameras and force platforms are often referred as the gold standard for biomechanical analysis purposes [198, 199]. Moreover, several studies have been focused on validating the performance of the user during daily living activities. To this end, the user's state and performance is assessed through different physiotherapy and mobility scales [200]. In this sense, this chapter presents two validation scenarios aimed at assessing the physical interaction between the AGoRA Walker and two groups of users.

7.1 Biomechanical Validation

To analyze the kinematics of the assistance provided by the AGoRA Walker, a biomechanical assessment was carried out on a group of healthy subjects. Using the HRi described in chapter 4, different assistance levels were configured on the SW during walking tests with turnings. Moreover, a motion capture system was used to obtain the biomechanical measurements of the user and the device.

7.1.1 Experimental Protocol

Interaction Strategy

To apply different assistance levels on the SW, an admittance controller based on the strategy presented in Chapter 4 was used. This approach was aimed at giving the user the sensation of dynamic physical interaction during gait assistance. The inputs of the controller were the force (F) and torque (τ) applied to the walker by the user, and the outputs of the controller were the linear velocity (v) and the angular velocity (ω).

For the purpose of these trials, the controller presented in Chapter 4 was modified by removing the gain corresponding to the spring element. This alteration was made to guarantee the comparability of the results with literature evidence [145]. Moreover, this modification simplifies the tuning process of the controller for each patient. Specifically, the equations that describe this controller are presented as follows:

$$L_1(s) = \frac{v(s)}{F(s)} = \frac{\frac{1}{m}}{s + \frac{b_l}{m}} \tag{7.1}$$

$$A_1(s) = \frac{\omega(s)}{\tau(s)} = \frac{\frac{1}{J}}{s + \frac{b_a}{J}} \tag{7.2}$$

where m is the virtual mass of the walker, J is the virtual moment of inertia of the walker, and b_l and b_a are damping ratios. Considering this, the assistance level or mechanical stiffness of the walker can be changed by the modification of the controller parameters. Thus, the assistance levels were configured as follows:

1. Assistance Mode (AM): $m = 0.5\ kg$, $b_l = 4\ N.s/m$, $J = 2.1 kg.m^2/rad$ and $b_a = 2\ N.m.s/rad$.

2. Resistance Mode (RM): $m = 10kg$, $b_l = \beta\ N.s/m$, $J = 2.1kg.m^2/rad$ and $b_a = 7\ N.m.s/rad$, where β was estimated according to the subject's weight:

$$\beta = 0.375 * weight - 12.5^1 \qquad\qquad (7.3)$$

3. Passive Mode (PM): the admittance controller and the device's brakes were disabled.

Subjects and Intervention Description

A group of 11 healthy male volunteers was recruited to participate in the study (23.36 ± 2.11 y.o., 1.76 ± 0.06 m, 71.72 ± 18.91 kg). The subjects did not report any history of injuries or musculoskeletal dysfunctions. Table 7.1 describes demographic data of the participants.

Subject	Age (y.o.)	Height (m)	Weight (kg)
1	23	1.8	72
2	26	1.79	70
3	28	1.79	90
4	20	1.87	95
5	23	1.78	72
6	24	1.76	62
7	23	1.62	28
8	23	1.79	90
9	22	1.68	60
10	23	1.76	65
11	22	1.74	85

Table 7.1: Summary of volunteers who participated in the biomechanical validation study.

The experimental trials took place at the Motion Capture and Analysis laboratory of the

---

[1]This relationship was found empirically, so that a subject with a maximum weight of 110 kg and a subject with a minimum weight of 55 kg could move the device with moderate resistance.

Colombian School of Engineering Julio Garavito. Each session was composed of four types of trials corresponding to the three assistance levels and an additional trial without the SW (i.e., referred as Unassisted Mode (UM)). The user was asked to follow simple paths with turnings, as shown in Figure 7.1. Specifically, the users were instructed to follow at their preferred speed each path 3 times under each stiffness mode and without the SW. Additionally, before recording the data of each mode, a training period was allowed to ensure understanding of the assistance level.
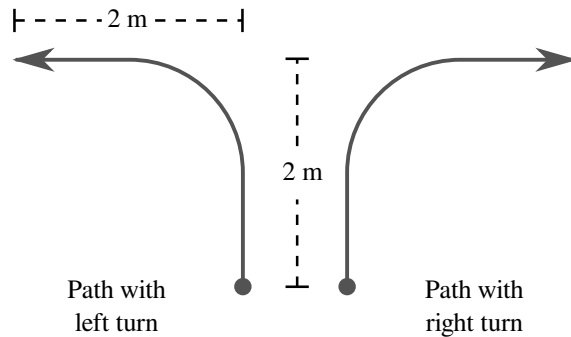
Figure 7.1: Reference paths for the biomechanical validation study.

Gait and Biomechanical Analysis Systems

The subjects were fitted with 64 reflecting markers (14 mm diameter), according to the full body set-up described by [201] (See Figure 7.2a). Similarly 8 markers were placed on the SW, using the set-up shown in Figure 7.2b.

Data were acquired with a seven-camera VICON (Oxford, UK) motion analysis system operating at 120 Hz. The motion analysis system and the *AGoRA walker* internal system were synchronized using an external event (i.e., a stick hit the force sensors while the cameras were capturing its motion). In this sense, the AGoRA Walker sensors were configured to capture user's interaction forces and spatiotemporal parameters. Moreover, prior to the experiments, the VICON active wand was used to calibrate the motion analysis system. To estimate joints degrees of freedom, a multibody kinematics optimization approach performed on OpenSim software [202, 203] using a fullbody model was implemented [204, 205].
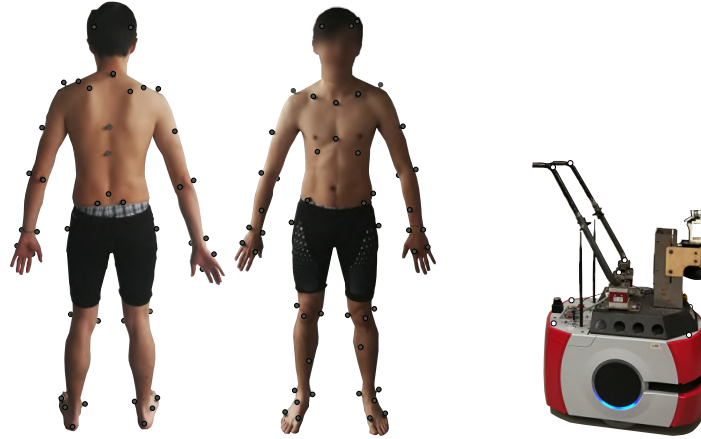
Figure 7.2: (a) Marker's set-up on subject (Markers in gray). (b) Marker's set-up on the SW (Markers in white).

7.1.2   Results and Discussion

A total of 264 trials divided into 11 sessions (i.e., one session per subject) were performed and successfully recorded. Several kinematic and biomechanical parameters were measured: users' gait spatio-temporal parameters, the interaction force and torque, the elbow and knee average range of motion (ROM) and trial average duration. In this sense, Table 7.2 describes a summary of the different kinematic and interaction parameters that were acquired during trials. In order to test the normality of each variable, the Shapiro-Wilk test was used.

Furthermore, to evaluate the difference between the experimental modes, a one way ANOVA with repeated measures for parametric data was used. In case of non-parametrical data, the Friedman test was used. The parameters shown in bold were found to be significantly different with $p \leq 0.05$ among the different modes.

Parameter	AM	PM	RM	UM
SW Speed [m/s]	0.41±0.15	0.40±0.15	0.26±0.13	-
User Speed [m/s]	0.41±0.14	0.42±0.15	0.28±0.14	0.70±0.27 *
Cadence [Steps/min]	49.20±18.47 *	45.27±16.28 *	36.33±20.35 *	48.93±17.00 *
Cycle Duration [s]	1.07±0.38 *	1.14±0.40 *	1.22±0.68 *	1.03±0.36

No. Cycles	6.47±2.66 *	6.12±2.48	6.70±3.86 *	3.91±1.42 *
Knee ROM [°]	54.38±18.83 *	54.71±19.15 *	47.81±24.26	59.17±20.80 *
Elbow ROM [°]	60.16±29.88 *	57.93±31.36 *	58.97 ±38.73*	17.34±10.72 *
Trial Duration [s]	13.43±4.57 *	13.25±4.70 *	14.99±7.57	7.88±2.99 *
Max. frc$_y$ [N]	6.07±3.18 *	5.93±2.40 *	9.85±5.84 *	-
Mean frc$_y$ [N]	1.08±0.54 *	1.77±0.69 *	3.50±2.06 *	-
Max. trq$_z$ [N.m	4.35±2.13 *	2.30±0.96 *	5.92±3.50 *	-
Mean trq$_z$ [N.m]	0.88±0.58 *	0.50±0.25 *	1.60 ±1.00 *	-
Distance [m]	5.24±1.76 *	5.20±1.74 *	4.51 ±2.25 *	-

Table 7.2: Kinematics and interaction data for all experimental conditions of the biomechanical validation study: Assisted Mode (AM), Passive Mode (PM), Resistance Mode (RM), Unassisted Mode (UM). Asterisks mean that the variable is normally distributed. Parameters in bold indicate significant differences between modes ($p - value \leq 0.05$).

According to these results, it can be seen that changes in the device stiffness impact the physical interaction, as well as the kinematics of the user. Significant differences were found under all the experimentation modes. For instance RM mode required greater efforts from the user to move the device. Specifically, the RM trials required higher interaction forces and torques compared to the AM and PM trials. Moreover, lower user speeds were achieved under the RM trials. Analyzing the literature evidence, the AGoRA Walker allows slower speeds than the average unassisted walking speed [206]. However, the AGoRA Walker is a rehabilitation device aimed at being used in clinical scenarios, where medical staff often require slower and controlled speeds to correct inappropriate gait patterns [206].

As an illustration, Figure 7.3a shows some of the paths achieved by one user during the different modes of operation. Figure 7.3b shows the behavior of the force exerted by the same user during a left-turn path. It can be seen that the user required a considerably higher force to move the device during the RM mode. Similarly, Figure 7.3c shows the behavior of the torque exerted by the user during the left-turn path. Although it is not possible to observe a different behavior between AM and RM modes, once the user reaches the turn,

additional efforts are required to stabilize the walker.
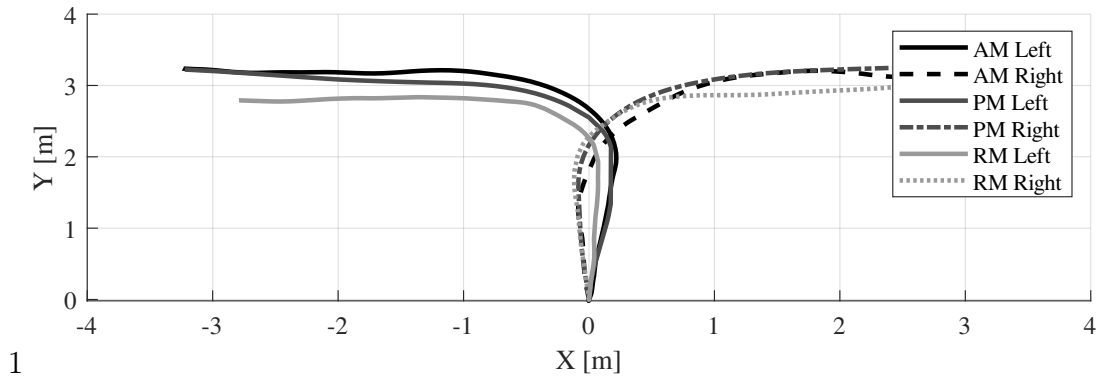
(a) Performed path.
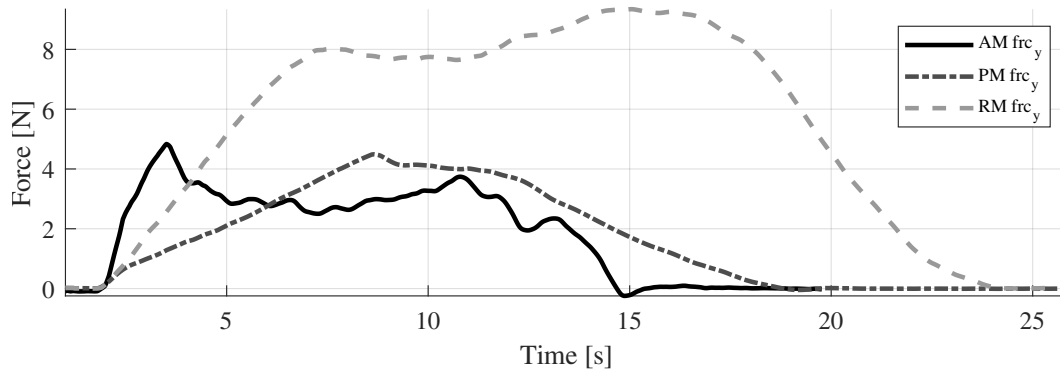
(b) Force signals on the handlebars during the left-turn path.
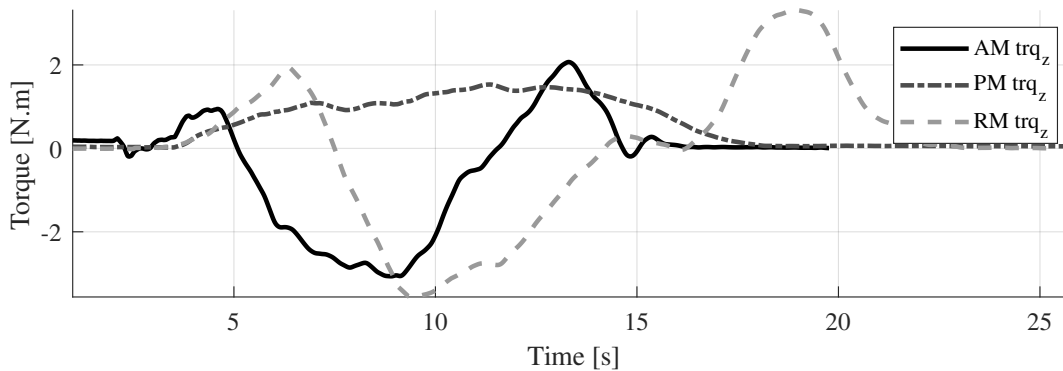
(c) Torque signals on the handlebars during the left-turn path.

Figure 7.3: Illustration of kinematic and interaction data for one subject. AM stands for assistive mode, PM stands for passive mode, and RM stands for resistive mode.

One of the main findings of this study is related to the behavior of kinematic and user interaction parameters during the RM. Specifically, this mode could be very useful in patients at an early stage of the rehabilitation process. In general terms, this interaction mode fosters

muscle training and ensures slower and safer gait patterns. In the same way, the AM and the PM may be useful in patients with lower assistance requirements, as the device allows faster and less controlled movements.

Finally, by comparing the behavior of the AM and PM modes, AM can be beneficial to users as it allows the dynamics of the device to be removed. Specifically, the AGoRA Walker is a device mounted on a fairly heavy commercial robotic platform, thus the implementation of the admittance controller facilitates the user's interaction with the device.

7.2 Clinical Trials

In order to validate the functioning and performance of the AGoRA Walker in a clinical setting, a second study was proposed involving patients who are actively attending a rehabilitation processes. Specifically, elderly subjects and Parkinsonian patients with mobility impairments were recruited.

7.2.1 Experimental Protocol

Interaction Strategy

According to the results obtained in the biomechanical validation study, the same HRi strategy was implemented. Specifically, the controller gains of the AM were modified following the concept of a physiotherapist to ensure that the device was easy for patients to maneuver. Regarding the RM tuning, Equation 7.3 was used to modify the controller gains according to the subject's weight. Moreover, to ensure subject's safety and avoid collisions, the low-level safety system described in Chapter 5 was activated. Specifically, this system was intended to limit speed when subjects came too close to an object, as well as to stop the device in case of imminent collisions. This mode was configured as a supervisor of the admittance controller, in such a way that it only modified the speed of the device when speed restrictions were violated.

Subjects and Intervention Description

A group of subjects that were actively attending a rehabilitation program was formally recruited to participate in the clinical study. Specifically, 14 subjects conformed the validation group (6 males, 8 females, 65.07 ± 8.44 y.o, 1.6 ± 0.08 m, 67.71 ± 14.93 kg), where 5 subjects suffered from Parkinson's disease. Table 7.3 describes demographic data of the participants.

Subject	Age (y.o.)	Height (m)	Weight (kg)	Gender	Pathology
1	69	1.62	69.5	Male	Tibial fracture
2	67	1.58	56.6	Female	Hypothyroidism Osteoporosis
3	46	1.72	90.2	Male	Overweight
4	72	1.64	70.3	Male	High blood pressure Diabetes
5	56	1.56	96.6	Female	Lymphatic Disorder
6	67	1.47	44.8	Female	Ankle fracture
7	71	1.53	60.9	Female	Hypothyroidism Osteoporosis
8	68	1.5	55.6	Female	High blood pressure Osteoarthritis
9	70	1.63	57	Female	High blood pressure Diabetes Parkinson
10	71	1.66	59.2	Male	High blood pressure Parkinson
11	65	1.59	58.1	Female	Epicondylitis Parkinson
12	70	1.70	81.8	Male	Parkinson
13	70	1.73	82.6	Male	Parkinson
14	49	1.53	64.8	Female	-

Table 7.3: Demographic data of the volunteers who participated in the clinical study.

The experimental trials took place at the Motion Capture and Analysis laboratory of the Center for Innovation and Technological Development (CiDT) at the Technological University of Pereira (UTP). Additionally, the experimental tests were supported and accompanied by students and physiotherapy professors from the Areandina University Foundation of Pereira. Each session was composed of two parts.

On the one hand, similar to the study carried out with healthy subjects, the HRI assessment part was aimed at assessing path following capabilities by the user (See Figure 7.1). Additionally, the patients were instructed to follow each path 3 times under each stiffness mode with the AGoRA Walker, and without it. Moreover, the subjects were encouraged to walk at their preferred speed and the training period was also allowed.

On the other hand, to assess the AGoRA Walker performance in everyday scenarios, the Daily Living Activities part was proposed. During this part, several test were proposed. Firstly, the subjects were asked to walk up (RUT) and down (RDT) a ramp with the AGoRA Walker. Each user had to walk 3 times on the ramp up and then 3 times on the ramp down. Figure 7.4a describes the shape and size of the ramp.

Secondly, the Timed Up & Go test (TUG) was implemented to assess balance and walking ability of the subjects [200]. A modified version of this test was used, in order to be suitable during walker-assisted gait. Specifically, the subjects were asked to rise from an chair, walk at their usual pace a distance of 3 meters, make a u-turn around a cone, walk back to the chair, and sit down [200]. Due to the use of the walker, users had to make a final turn before reaching the chair. Figure 7.4b illustrates the setup for this test. The participants were asked to repeat this test 3 times.

Moreover, the 10 Meters Walk test (10MWT) was implemented, where the subjects were asked to walk in a 10 meter straight line at their preferred speed being assisted by the SW. The participants were asked to repeat this test 3 times. Finally, the Six Minutes Walking test (6MWT) was implemented to assess endurance and overall physical performance and

mobility in the subjects [200]. In this sense, the participants were instructed to walk over a flat hallway without running or jogging, and they were allowed to stop and rest during the test. Considering the duration of the test, a walking circuit was used, where the subject had to make a u-turn every 30 meters. Figure 7.4c illustrates the test setup. Moreover, to avoid the patient's loss of motivation, two standardized phrases were used: "You're doing very well!" and "Keep going, there are only X minutes left!". This test was done without the AGoRA Walker.
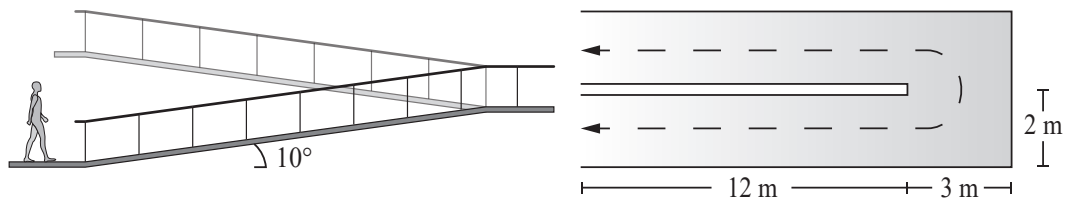
(a) Ramps test setup.
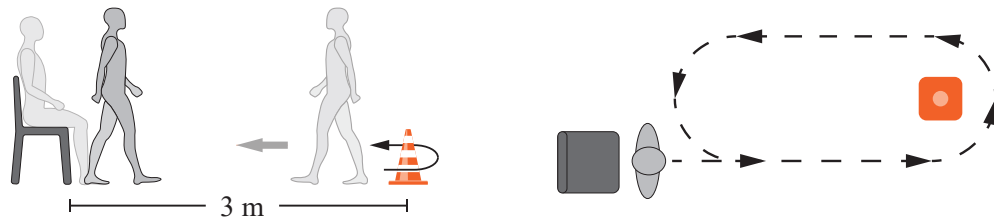
(b) Timed Up & Go test setup.
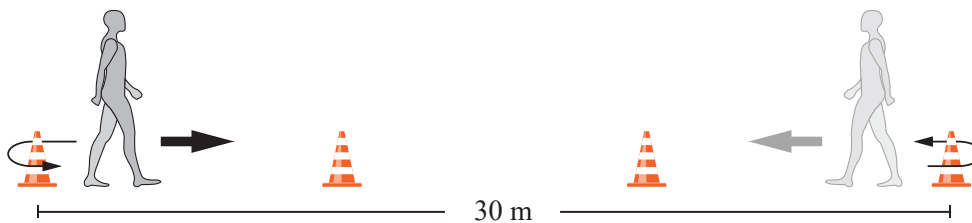
(c) 6 Minutes Walking test setup

Figure 7.4: Illustration of experimental setups of the daily living activities part.

Gait Analysis Systems

Data were acquired through the sensory interface of the AGoRA Walker. The interaction force and torque, walker speeds and trial duration were recorded. To estimate additional

parameters of the subject, the G-WALK sensor was used. This device supplied relevant parameters related to each trial such as, subject's speed, cadence, and gait cycles [207].

7.2.2 Results and Discussion

A total of 546 trials divided into 14 sessions (i.e., one session per subject) were performed. Several kinematic and interaction parameters were measured such as, users' gait spatio-temporal parameters, interaction force and torque, trial duration, and walked distance.

HRi Assessment Part

The subjects successfully completed all the trials regarding to this part of the study. Table 7.4 summarizes the main outcomes of several kinematic and interaction data of this part.

Parameter	AM	PM	RM
SW Speed [m/s]	0.38±0.09 *	0.39±0.08 *	0.34±0.10 *
User Speed [m/s]	0.34±0.09 *	0.35±0.08 *	0.31±0.10 *
Trial Duration [s]	17.82±6.77 *	15.72±7.48 *	17.65±7.39 *
Max. frc_y [N]	6.73±2.34 *	6.59±2.25 *	8.48±2.81 *
Mean frc_y [N]	1.67±0.63 *	2.18±1.23 *	3.39±1.61 *
Max. trq_z [N.m]	7.19±2.92 *	3.49±1.97 *	9.97±4.16 *
Mean trq_z [N.m]	1.86±1.68 *	0.70±1.04 *	3.60±2.76 *
Distance [m]	5.78±2.86 *	5.13±3.32 *	5.24±3.13 *

Table 7.4: Kinematics and interaction data for the HRi assessment part of the clinical study: Assisted Mode (AM), Passive Mode (PM), Resistance Mode (RM). Asterisks mean that the variable is normally distributed. Parameters shown in bold indicate significant differences with a Greenhouse-Geisser correction ($p - value \leq 0.05$)

To test the normality of each variable, the Shapiro-Wilk test was used. Normally distributed parameters are indicated with an asterisk in Table 7.4. To assess differences between the

experimentation modes, one way ANOVA with repeated measures for parametric data was used. The parameters shown in bold were found to be significantly different with $p \leq 0.05$.

Similar to the study conducted with healthy subjects, it can be established from Table 7.4 that tests with the RM were more difficult for users to perform. In essence, due to the configuration of the admittance controller, subjects had to exert greater forces and torques on the device in order to interact with it. Moreover, another interesting result of this study is related to the duration of the trials and the speeds of the subjects. The trials duration was not found to be statistically different, however the average speed was found significantly different for all stiffness modes. This result can be supported by the fact that some older adults prefer slower and more cautious gait patterns [46, 84].

Additionally, it is also interesting to note that the average impulse forces are higher in the study with patients compared to the study with healthy subjects. This behavior may be mainly supported by the fact that older adults and Parkinsonian patients tend to rely more on assistive devices compared to healthy subjects [144]. Specifically, due to the structural configuration of the handlebars of the AGoRA Walker, the vertical supporting forces of the patients result in components along the y-axis on the force sensors. As an illustration of the execution of this trials, Figure 7.5 shows several kinematic and interaction parameters for one subject.

Figure 7.5a depicts some of the paths achieved by a user during the different modes of operation. Figure 7.5b shows the behavior of the force exerted by the user during a left-turn path. Based on the results obtained during the AM tests, it is possible to establish that once the user overcomes the minimum inertia to move the device, the admittance controller allows him to interact with the device easily and effortlessly. Similarly, Figure 7.3c illustrates the behavior of the torque exerted by the user during the left-turn path.

(a) Performed paths.
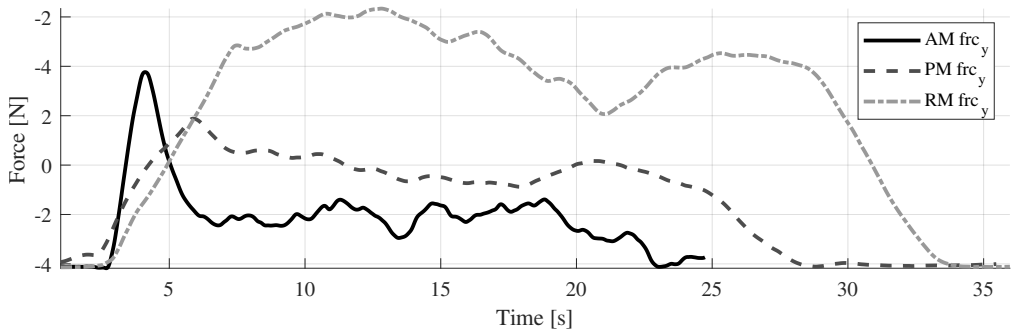
(b) Force signals on the handlebars during the left-turn path.
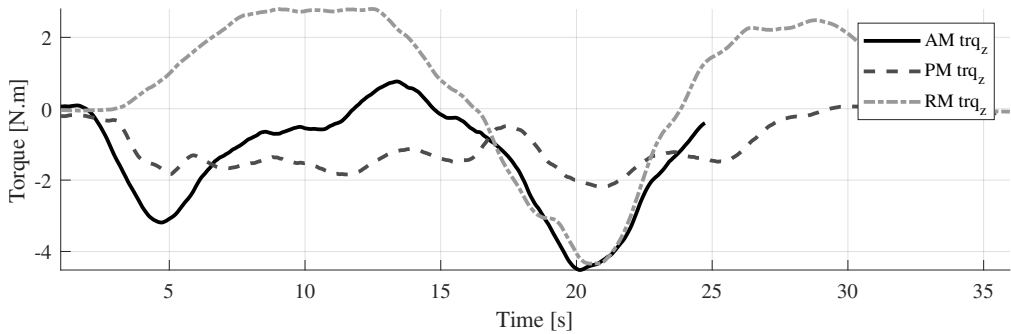
(c) Torque signals on the handlebars during the left-turn path.

Figure 7.5: Illustration of kinematic and interaction data for one subject during the HRi assessment part. AM stands for assistive mode, PM stands for passive mode, and RM stands for resistive mode.

Daily Living Activities Part

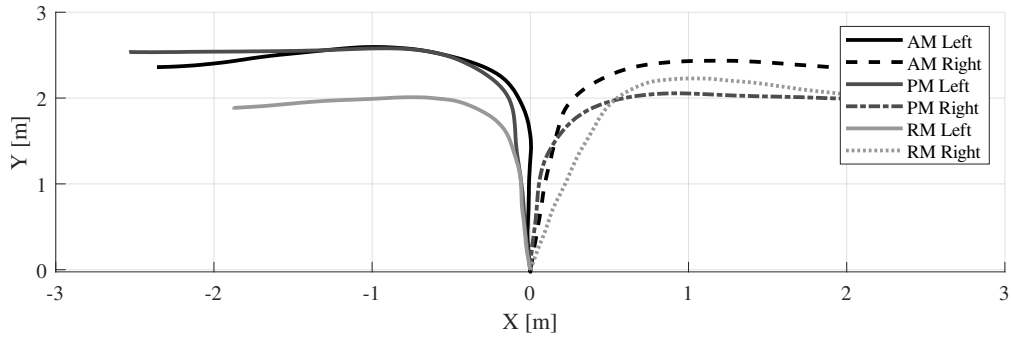Table 7.5 summarizes the main outcomes of several kinematic and interaction data of the trials. To test the normality of each variable, the Shapiro-Wilk test was used. Normally distributed parameters are indicated with an asterisk in Table 7.5. To assess differences between

the experimentation modes, one way ANOVA with repeated measure for parametric data was used. The parameters in bold were found to be significantly different with $p-value \leq 0.05$.

	RUT	RDT	10MWT	6MWT
SW Speed [m/s]	0.66±0.08 *	0.63±0.06 *	0.37±0.09 *	-
User Speed [m/s]	0.64±0.08 *	0.61±0.06 *	0.33±0.10 *	1.23±0.46 *
Cadence [Steps/min]	85.67±5.10 *	102.42±8.21 *	117.04±15.26 *	128.54±23.64 *
Cycle Duration [s]	1.41±0.08 *	1.18±0.10 *	1.04±0.15 *	0.96±0.13 *
No. Cycles	36.47±4.12 *	46.71±8.32 *	8.99±2.40 *	385.63±70.93 *
Trial Duration [s]	52.13±6.79 *	54.99±6.87 *	9.3±2.43 *	360
Max frc_y [N]	8.47±2.86 *	8.22±2.49 *	7.23±2.83 *	-
Mean frc_y [N]	2.63±0.49 *	2.49±0.48 *	1.49±0.57 *	-
Max. trq_z [N.m]	5.07±1.99 *	9.66±2.47 *	5.36±2.65 *	-
Mean trq_z [N.m]	0.37±0.63 *	1.70±0.62 *	-0.33±1.26 *	-
Distance [m]	33.57±0.87 *	32.16±0.95 *	11.02±1.28 *	442.03±166.83 *

Table 7.5: Kinematics and interaction data for the Daily Living Activities part (i.e., except the TUG test) of the clinical study: Ramp-Up test (RUT), Ramp-Down test (RDT), 10 Meters Walking test (10MWT), 6 Minutes Walking test (6MWT). Asterisks mean that the variable is normally distributed. Parameters shown in bold indicate significant differences with $(p-value \leq 0.05)$

By comparing the behavior of the kinematic parameters only during ramp tests, very similar results concerning user speeds were observed. However, slight changes were obtained in the cadence, the duration of the gait cycle and the number of cycles. Specifically, these results are supported by the fact that the positive inclination of the path induced slower gait patterns and longer steps on the subjects. Moreover, the maximum torque exerted by the users was considerably higher in the down-ramp tests. Since, the device presented greater moments of inertia during the down-tests, the subjects required greater efforts to make the turn in the middle of the ramp.

As an illustration of the results of the ramp tests, Figure 7.6 shows several kinematic and

interaction parameters acquired by the AGoRA Walker. Specifically, Figure 7.6a shows the performed trajectories for one subject during the RUT and RDT tests. Moreover, Figure 7.6b describes the linear and angular speeds recorded during the RUT trial. Finally, Figure 7.6c illustrates the behaviour of the force and torque signals during the RUT trial.
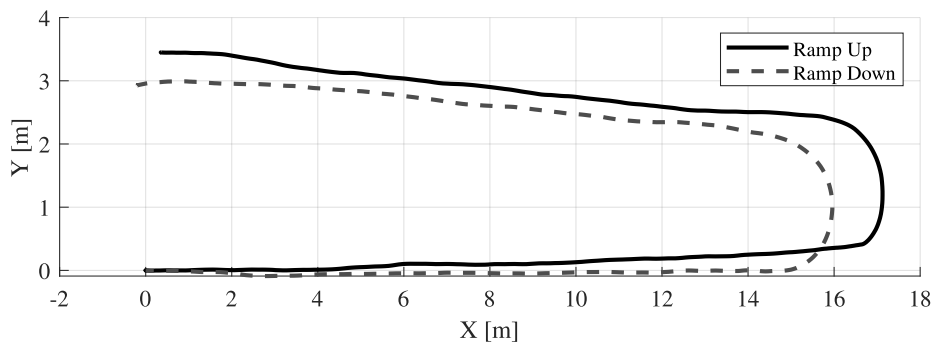
(a) Performed paths.
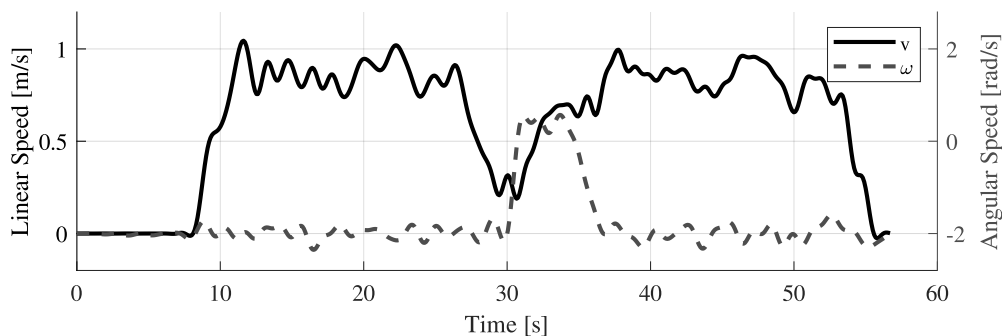
(b) Linear and angular speed signals during the ramp up trial.
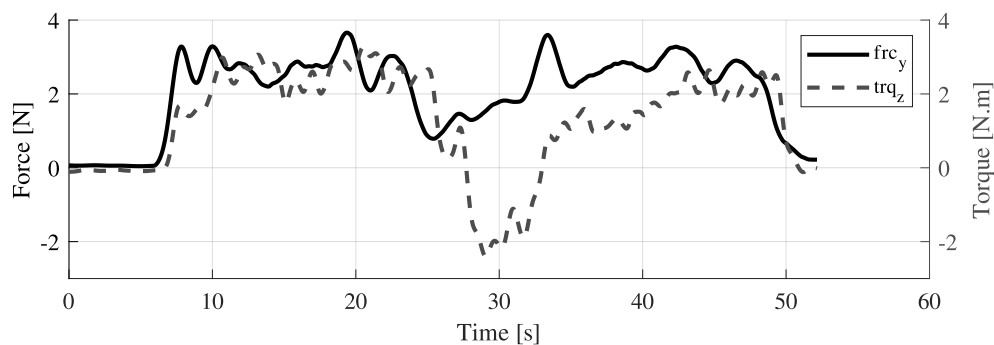
(c) Force and torque signals on the handlebars during the ramp up trial.

Figure 7.6: Illustration of kinematic and interaction data for one subject during ramp tests.

An important finding during ramp tests is primarily related to the behavior of the walker on

inclined trails. Specifically, the admittance controller was observed to respond in a similar manner to tests performed on flat surfaces. This may be a promising feature of the AGoRA, as this results suggest the capability of the device to interact in complex and everyday scenarios without modifying the control strategy.

As an illustration of the 10MWT trials, Figure 7.7 shows several kinematic and interaction parameters acquired by the AGoRA Walker.

(a) Performed path.

(b) Force and torque signals on the handlebars.

(c) Linear and angular speed signals.
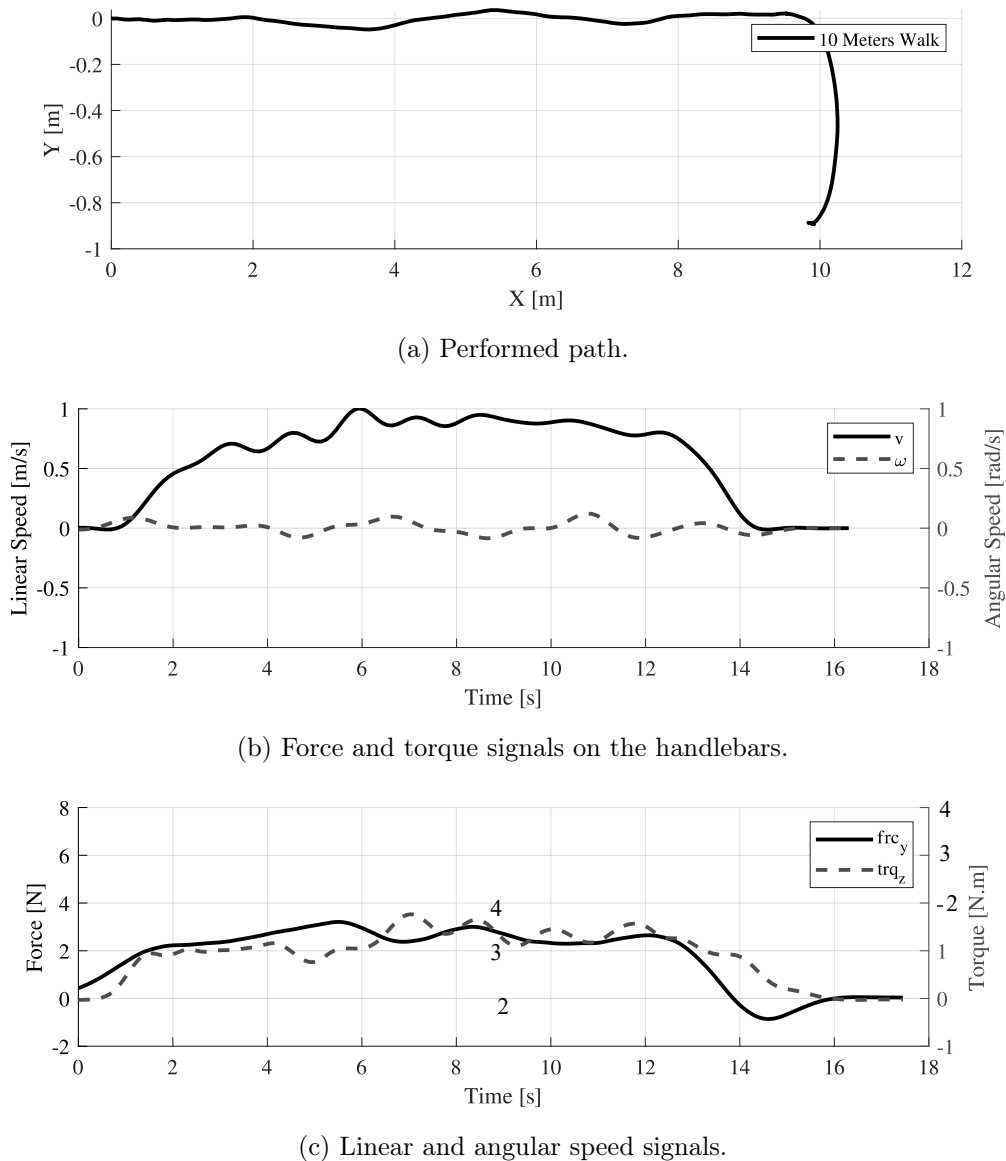
Figure 7.7: Illustration of kinematic and interaction data for one subject during the 10 Meters Walk test.

Figure 7.7a shows the performed trajectory for one subject during the 10MWT test. More-over, Figure 7.7b describes the linear and angular speeds recorded during the 10MWT trial. Finally, Figure 7.7c illustrates the behaviour of the force and torque signals during the 10MWT trial. Analyzing the results obtained for the different tests, relevant changes in the user's walking speed were observed. The lowest speeds were obtained during the 10MWT test and the highest speeds were obtained during the 6MWT tests. It can be asserted that this behavior is related to the duration of the tests. Specifically, shorter tests presented lower speeds, and longer tests presented higher speeds. Similarly, as the 6MWT test did not require the of use the AGoRA Walker, users could walk much more freely and faster.

Regarding the kinematic and interaction parameters acquired during the TUG test trials, Table 7.6 summarizes this information. No statistical tests were applied to the outcomes of the TUG test, as it may not be comparable with the other tests.

Parameter	TUG
SW Speed [m/s]	0.35+0.05
User Speed [m/s]	0.32+0.05
Sit-to-Stand Time [s]	1.25 + 0.3
Trial Duration [s]	36.72+7.90
Max frc_y [N]	7.23+2.83
Mean frc_y [N]	1.49+0.57
Max. trq_z [N.m	5.36+2.65
Mean trq_z [N.m]	-0.33+1.26
Distance [m]	11.02+1.28

Table 7.6: Kinematics and interaction data for the Timed Up & Go (TUG) test of the clinical study.

In order to illustrate the TUG trial, Figure 7.4b depicts several kinematic and interaction parameters during the trial for one subject. The performed trajectory is shown in Figure 7.8a, where it can be seen that the user had to make an additional turn at the end of the

test to sit down. Figure 7.8b illustrates the behavior of the walker linear and angular speeds during the trial. Finally, Figure 7.8c depicts the force and torques exerted by the user.
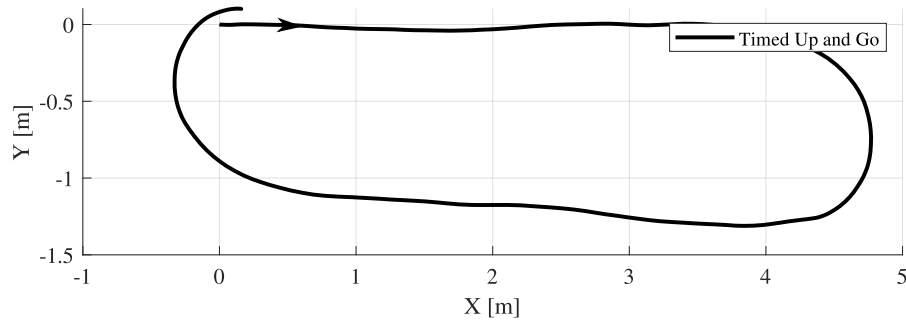
(a) Performed path.
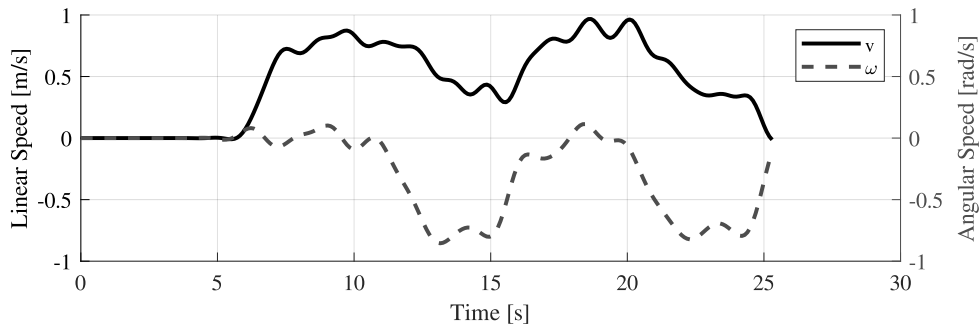
(b) Force and torque signals on the handlebars.
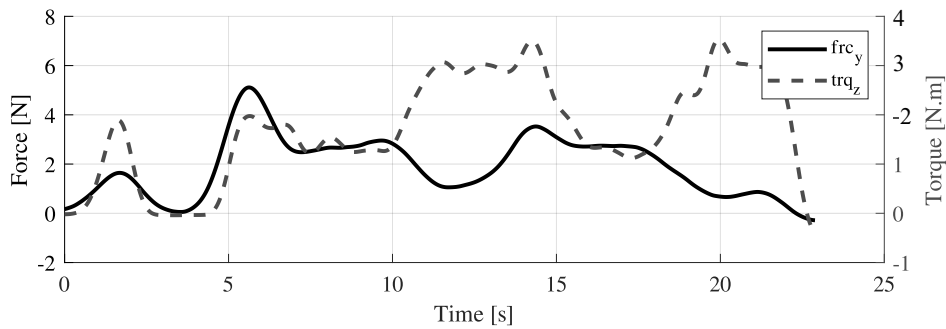
(c) Linear and angular speed signals.

Figure 7.8: Illustration of kinematic and interaction data for one subject during the Timed Up & Go test activities.

During these tests, users were asked to lean on the device to stand up from the chair. This supporting event was observed as an initial peak in the force and torque signals. To prevent the admittance controller from generating speeds, the device's motors were remotely disabled. Once the user was fully upright, the motors were re-enabled.

Chapter 8

Conclusions and Future Works

A Human-Robot-Environment interface (HREi), composed by a Human-Robot interface (HRi) and a Robot-Environment interface (REi), was developed and implemented on a robotic platform for walker assisted gait. Within the HREi design criteria, the following functions are found: estimation of user's intentions of movement, providing of safe and natural HRI, implementation of a navigation system alongside a people detection system for social interaction purposes, and the integration of a set of control strategies for intuitive and natural interaction. These functions were proposed according to the findings of the performed review of literature described in Chapter 2. As presented in 3, the robotic platform was equipped with two handlebars for forearm support and several sensory modalities to emulate the performance and capabilities of an SW.

In addition to the description of the HRi presented in Chapter 4, an additional strategy for therapists interaction through a command interface was described. Specifically, taking advantage of the haptic and visual capabilities of a joystick device, a physical and cognitive interface (PCi) was implemented. A set feedback strategies were configured, in order to provide different levels of communication. Moreover, to address the qualitative perceptions of therapists, an acceptance and usability questionnaire was implemented on 15 participants

that completed several trials. The participants found the PCi as an intuitive remote device, however several improvements should be addressed to enhance the feedback capabilities. Although this implementation was completely simulated, the use of haptic and visual feedback strategies on remote control devices, contribute to research areas such as tele-management.

As presented in Chapter 6, to validate the platform performance and interaction capabilities, preliminary tests were conducted under laboratory conditions. Particularly, a set of shared and autonomous control strategies were designed. Data were collected from 21 trials, where 7 healthy participants interacted with each control mode. According to the participants' performance under the user control mode, preferences for less steeped curves were found. Concretely, the participants did not strictly execute 90-degree turns at trajectory corners. Such behavior is mainly supported by the not aligned axes of rotation of the walker and the users. Moreover, ignoring path corners allowed the participants to ensure balance and stability during walking.

The preliminary validation trials were also aimed at assessing the performance of the navigation system presented in Chapter 5. Specifically, a path following task, as well as the evaluation of the performance of the navigation and people detection systems working together were proposed. An isolated preliminary test with a volunteer was carried out to evaluate the capabilities of the platform for overcoming environments with people, even when sudden changes in obstacles locations. In the preliminary test, both navigation and people detection systems were executed at a maximum frequency of 4 Hz, due the on-board computational limitations. To ensure user's balance and stability, the trajectory planning was configured to prefer curves with minimum turning radius of 15 cm. Although collisions and system clogging were not presented, the implementation of the REi on clinical or crowded scenarios may require higher computational resources. Regarding the trials with the 7 healthy volunteer users, a reference trajectory composed by 10 intermediate goals was proposed. All participants experienced the navigation system control completely achieving the reference

path with no collisions.

Regarding the assessment of the shared control mode, a path following task was also proposed. Under this control mode, the participants' intentions of movements and the navigation system cooperatively controlled the platform. Specifically, the linear speed was totally controlled by the users, and the angular speed was controlled according to the shared control strategy estimations. To ensure participant's balance and stability, a minimal turning radius of 15 cm was also configured. Among the participants trials, a mean percentage of user control of 66.71 ± 6.26 was obtained. Concretely, the control of the platform was mainly granted to the user at straight segments of the trajectory, since the participants' did not have exact information about the reference trajectory. According to the geometrical model implemented for the shared control strategy, more strict or more flexible behaviors can be configured by modifying the dimensions of the interaction window. Such modifications can potentially be implemented in rehabilitation scenarios in order to provide different levels of assistance. Specifically, early stages of physical and cognitive rehabilitation processes might benefit from more rigorous or narrow interaction windows, ensuring a higher percentage of control of the navigation system.

A qualitative assessment of the platform performance and interaction capabilities relying on an acceptance and usability questionnaire was carried out. The participants' attitude towards the device, as well as the performance and behavior perception were evaluated. According to the survey responses, the participants perceived a mostly positive interaction with the platform. Specifically, the questionnaires showed natural, safe and intuitive interactions under all the control modes. Regarding the behavior perception, significant differences were statistically found between the control modes. The questions aimed at evaluating effort and anxiety perceptions showed slightly negative responses. Particularly, two volunteers stated that the navigation system suddenly stopped at specific points of the trajectory. Such behavior was mainly due to the system configuration to reach goals at specific orientations.

Similar to these evaluations, biomechanical validation and clinical trials were presented in Chapter 7. Trials were conducted with healthy subjects for the biomechanical validation study and with older adults and Parkinson's patients for the clinical study. Regarding the biomechanical study, different stiffness or assistance levels were configured on the device. These levels were aimed at providing whether resistance, assistance or no assistance at all. In this sense, the physical interaction between the SW and the users was assessed, by means of several kinematic parameters. The user walking speed was compared between the different stiffness levels, finding higher values at the low stiffness mode and the passive mode. The interaction forces were found to be considerably higher under the high stiffness mode. These findings support the fact that the impact of the stiffness level on user's gait is mainly represented by a decrease in the walking speed and the increase of the energetic expenditure.

Regarding the clinical trials, two experimental parts were proposed. In the first part, a study similar to the one carried out with healthy subjects was executed, where the impact of the assistance levels in pathological patients was evaluated. For this group of tests, similar results were obtained compared to the biomechanical study. Specifically, it was found that it was more difficult for patients to interact with the AGoRA Walker with the resistance mode. However, this is a promising interaction strategy, as it promotes muscle and energetic training. In the second part, a group of activities were proposed in order to analyze the behavior of the device in everyday scenarios. Specifically, users were asked to walk on ramps, perform the 10-Meter Walking test (10MWT), perform the Timed Up & Go (TUG) test, and perform the 6-Minute Walking test (6MWT). In general, the device allowed tests to be carried out safely. However, the SW was found to favour a slower and more cautious gait compared to tests without it. In addition, it was found that the user's speed may be related to the duration of the tests. Specifically, longer tests allowed the user to achieve higher speeds with greater comfort.

Future works will address extensive evaluations of social interactions between the walker and

people in the environment, by implementing several avoidance strategies, as well as algorithms for recognition of social groups interactions. Moreover, the implementation of the AGoRA Walker's interface will be achieved on a custom frame, and thus removing the commercial robotic platform. In this sense, further long-term validations of the HREi will be achieved in post-stroke patients and SCI patients. Future works will also address the integration of the custom SW with the AGoRA exoskeleton. Finally, the integration of a cloud based system could leverage processing capabilities, resulting in better performance results.

Appendix A

Sensors Description

A.1   Tri-axial Load Cells

As previously described in Chapter 2, there is a wide range of sensory interfaces used to measure the physical interaction between the users and the SWs. Among these, load cells are often found to be suitable for force measurement on the SWs.

A load cell can be defined as a transducer that measures force, and outputs such force as an electrical signal [208]. In general terms, these type of sensors can be broadly classified into hydraulic, pneumatic and electronic load cells [209]. However, the electronic load cells based on strain gauges are of special interest, as they represent the most practical means of weighing [209].

Operating Principle: An strain gauge is mainly constituted by a wire or foil bonded to a spring element (e.g., commonly made of steel or aluminum). This wire is usually disposed in a grid pattern in such a way that its cross section varies as the spring element is strained. Thus, a relationship between the electrical resistance of the wire and the deformation force can be estimated [209]. Typically, to measure such resistance variations, the strain gauges

configurations are based Wheatstone bridges [210]. Depending on the selected configuration and design, the load cells might be able to measure forces in two or more axes.

Figure A.1: MTA400 Triaxial load cell from FUTEK, USA.

Selected Sensor: In order to accurately measure the forces exerted by the user on the handlebars, the MTA400 tri-axial load cell (FUTEK, USA) was selected [211] (See Figure A.1). This sensor decomposes the force applied to it into three orthogonal components using an array of strain gauges. The MTA400 is made from Aluminum, weighs 907.185 g and uses metal foil strain gauge technology [211]. Specifically, a pair of these sensors were placed on the platform's main deck serving as a contact point between the handlebars and the device. Some technical features of the sensor such as, dimensions, channel sensitivity, channel range, input and output nominal resistances and excitation voltage are shown in the Table A.1.

	Variable	Minimum Value	Typical Value	Maximum Value	Units
Dimensions	Length	-	74.9	-	mm
	Width	-	74.9	-	mm
	Height	-	76.2	-	mm
	Weight	-	0.907	-	kg
Performance	Capacity (Fx, Fy)	-113.4	-	113.4	kg
	Capacity (Fz)	-226.8	-	226.8	kg

Electrical	Rated Output (Fx, Fy)	-	1.5	-	mV/V
	Rated Output (Fz)	-	0.75	-	mV/V
	Excitation	1	-	18	VDC
	Input Resistance	-	253	-	Ω
	Output Resistance	-	700	-	Ω
	Connection	-	10 pin LEMO® [1]	-	-
Environment	Temperature	-51	-	93	°C
	IP Rating	-	IP-40	-	-

Table A.1: Technical specifications of the MTA400 tri-axial load cell.

In this type of sensor, the analog voltage output is linearly related to changes in the internal resistance of each channel, thus an instrumentation circuit is required to properly acquire the output signal. Specifically, the full bridge strain gauge signal conditioning voltage amplifier IAA100 was selected [212] (See Figure A.2).
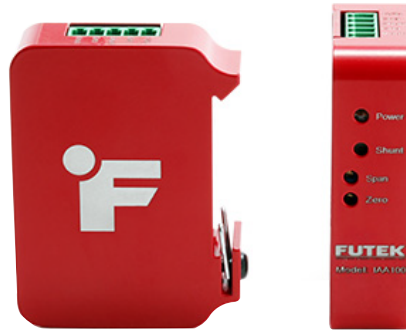
Figure A.2: IAA100 Signal conditioning amplifier from FUTEK, USA.

The IAA100 amplifier is able to measure input signals precisely with a total error of 0.005% [212]. Table A.2 describes the main technical features of this amplifier [212].

---

[1]LEMO® connector scheme is described at https://www.futek.com/store/product/FSH04139

	Variable	Minimum Value	Typical Value	Maximum Value	Units
Dimensions	Length	-	51.82	-	mm
	Width	-	17.78	-	mm
	Height	66.04	-	84.33	mm
	Weight	-	0.104	-	kg
Performance	Input Range	0.5	-	10	mV/V
	Bandwidth	-	1000	-	Hz
Electrical	Power Supply	16	-	26	VDC
	Current Consumption	-	30	100	mA
	Bridge Excitation	-	5, 10	-	VDC
	Load Impedance	14000	-	-	Ω
	Sensor Impedance	75	-	5000	Ω
Environment	Temperature	0	-	70	°C
	IP Rating	-	IP-50	-	-

Table A.2: Technical specifications of the IAA100 signal conditioning amplifier.

According to the above, the AGoRA Walker is equipped with two pairs of signal conditioning amplifiers, i.e., one pair for each tri-axial load cell. Moreover, an analog-to-digital converter (ADC) was used to digitalize the analog signal obtained in each instrumentation amplifier. For the purpose of this work, the multifunction data acquisition device (DAQ) NI USB-6008 was selected (National Instruments, TX, USA). Figure A.3 illustrates the mentioned device [213].

The NI USB-6008 device is equipped with several analog and digital input/output ports. Moreover, the communication protocol of this device is based on a USB 2.0 full-speed interface, providing a straightforward way to retrieve the information registered by the device. Table A.3 describes some of the technical features of this device [213] focusing on the analog

Figure A.3: NI USB-6008 digital-to-analog converter from National Instruments, USA.

inputs characteristics. In order to obtain a better conversion resolution, the analog inputs of the device were configured in differential mode. In this way, only the information from the Fy and Fz channels of each sensor was acquired (i.e.,forces in x-axis were discarded).

	Variable	Minimum Value	Typical Value	Maximum Value	Units
Dimensions	Length	-	85.1	-	mm
	Width	63.5	-	81.8	mm
	Height	-	23.2	-	mm
	Weight	0.054	-	0.084	kg
Analog Input	Inputs	-	4	-	-
	Resolution	-	12	-	bits
	Input Range	1	-	20	V
	Impedance	-	144	-	kOhm
	Overvoltage protection	- 35	-	+ 35	V
	System Noise	0.5	-	5	mVrms
	Sample Rate	-	10	-	kS/s
Electrical	Power Supply (USB)	4.1	-	5.25	VDC
	Current Consumption	-	80	500	mA
Environment	Temperature	0	25	55	°C

Table A.3: Technical specifications of the NI DAQ USB-6008 multifunction device.

A.2   Scanning Laser Rangefinders

Laser based systems or laser rangefinders are optical sensors that use infrared laser beams for distance measurement in two dimensions. In general, these systems consist of a transmitter of light pulses arranged on a rotation system that allows distance measurements at different angles.

Operating Principle: Among the most common operating principles of laser based sensors, triangulation, time-of-flight and confocal chromatic perception measurements are commonly found [214]. In particular, the laser sensors used in this work are based on the time-of-flight principle. Under this method, the time it takes for the light beam to travel to a target and return is measured. This time can be obtained both directly or indirectly. If it is done indirectly, as the intensity of the beam changes over time, the flight time is measured by comparing the laser signal at a certain instant with the delayed returning signal [214]. This approach is often referred as phase measurement. On the other hand, if the time-of-flight is measured directly, at the instant in which the light pulse is sent, an electronic chronometer is started that waits until the signal returns [215].

The data delivered by the laser sensors can be organized as an ordered sequence of points in polar coordinates (S), as shown in Equation A.1, where ρ corresponds to the measured distance and θ to the angle.

$$S = [s_1, s_2, \ldots, s_n], \;\; s_i = (\rho, \, \theta) \tag{A.1}$$

In some applications implemented in this work it is useful to express the points acquired by the laser in Cartesian coordinates. Taking into account that the plane of laser readings corresponds to the XY plane, Equation A.2 illustrates this conversion.

$$P = [(x_1, y_1), (x_2, y_2), \ldots, (x_n, y_n)], \; : \; x_i = \rho sin(\theta), \; \rho cos(\theta) \qquad \text{(A.2)}$$

Selected Sensors: In order to meet the functionalities of the HREi interface, two laser based sensor were implemented on the AGoRA Walker. On the one hand, to measure and estimate surrounding obstacles, the safety laser scanner S300 Expert (SICK, USA) was used (See Figure A.4).

Figure A.4: Safety laser scanner S300 Expert from SICK, Germany.

The S300 Expert laser scanner is capable of detecting objects at a maximum distance of 30 m in both indoors and outdoors. Table A.4 describes some technical features of this device [215]. The device was placed on the platform's main deck at height of **X** m, by means of a support structure made of steel. Since one of the functionalities of the AGoRA Walker is to detect people in the environment, this positioning of the laser allows to detect them in a simpler way. Specifically, each person in the sensor field of view will be defined as single group of points.

	Variable	Minimum Value	Typical Value	Maximum Value	Units
	Length	-	106	-	mm
	Width	-	102	-	mm
Dimensions	Height	-	152	-	mm

	Weight	-	1.2	-	kg
Performance	Measuring Range	-	30	-	m
	Scanning Angle Range	-	270	-	°
	Resolution	30	-	150	mm
	Angular Resolution	-	0.5	-	°
	Response Time	-	80	-	ms
	Connectivity	RS-232, RS-422, CANOpen, Ethernet			-
Electrical	Power Supply	16.8	24	30	VDC
	Current Consumption	0.33	-	1.7	A
Environment	Temperature	-10	25	50	°C
	IP Rating	-	IP-65	-	-

Table A.4: Technical specifications of the SICK S300 Expert laser scanner.

On the other hand, to estimate relevant characteristics of the user's gait, an additional laser scanner was placed pointing towards the user's legs. Specifically, the URG-04LX-UG01 (Hokuyo, Japan) laser scanner was selected (See Figure A.5) [216].

Figure A.5: URG-04LX-UG01 laser scanner from Hokuyo, Japan.

This device is widely used in stand-alone robot applications due to its features and ease of use. Table A.5 describes the main technical characteristics of this sensor [216].

	Variable	Minimum Value	Typical Value	Maximum Value	Units
Dimensions	Length	-	50	-	mm
	Width	-	50	-	mm
	Height	-	70	-	mm
	Weight	-	0.160	-	kg
Performance	Measuring Range	-	5.6	-	m
	Scanning Angle Range	-	240	-	°
	Resolution	-	1	-	mm
	Angular Resolution	-	0.36	-	°
	Response Time	-	100	-	ms
	Connectivity	USB 2.0 Full Speed			-
Electrical	Power Supply (USB)	4.75	5	5.25	VDC
	Current Consumption	-	0.5	0.8	A
Environment	Temperature	-10	25	50	°C
	IP Rating	-	IP-64	-	-

Table A.5: Technical specifications of the Hokuyo URG-04LX-UG01 laser scanner.

In order to integrate the URG-04LX-UG01 laser scanner into the ROS architecture, the *hokuyo_node* package was used. This package is included and available in the open source repository of the ROS community [217][2].

A.3   Camera Vision System

Vision systems are one of the most useful and innovative technologies of robotic and automatic systems. In particular, cameras allow robots to better identify objects, navigate, inspect,

---

[2]Newer distributions than ROS Indigo might require the *urg_node* package

and interact with complex and unknown scenarios [218]. Thus, a camera was added to the AGoRA Walker sensory interface to provide people detection capabilities, as well as, environment surveillance during monitoring tasks.

Operating Principle: In the imaging process, 3D geometric features of objects in the world are projected into 2D features on an image. Essentially, the objects reflect off the light rays and these are concentrated by the lenses present in the cameras. Afterwards, light rays reach an imaging sensor, where the amount of light is controlled by the duration of the exposure and is then processed by a set of sense amplifiers [219]. There are two main types of sensor used in cameras, charge-coupled devices (CCD) and complementary metal oxide on silicon (CMOS) [220]. Specifically, in CMOS the photons affect the conductivity of a photo-detector and then an ADC is used to generate the raw image [219].

In general, the key factors that affect the output of the imaging process in digital cameras are the shutter speed, duration of exposure, sensor active size an resolution, amplification scheme, sensor noise, and the resolution of the ADC [219, 220].

Selected Sensor: In particular, the HD camera LifeCam Studio (Microsoft, USA) was integrated to the AGoRA Walker [221]. This device was placed on top of the frontal laser scanner (i.e., the S300 Expert) by means of a 3D printed structure. Figure A.6 illustrates this device.

Figure A.6: LifeCam Studio camera from Microsoft, USA.

The main physical and electronic characteristics of this camera are detailed in Table A.6. As previously stated, this camera is based on a CMOS sensor and it is equipped with built-in pre-processing system in charge of image enhancing and auto-focusing. Moreover, in order to integrate this device into the ROS architecture of the AGoRA Walker, the *usb_ cam* package was used [222].

	Variable	Minimum Value	Typical Value	Maximum Value	Units
Dimensions	Length	-	114	-	mm
	Width	-	60	-	mm
	Height	-	45	-	mm
	Weight	-	0.128	-	kg
Performance	Sensor	-	CMOS	-	-
	Field of View	-	75	-	°
	Resolution	-	-	1920x1080	pixels
	Auto focus	0.1	-	10	m
	Response Time	1	-	30	frames/s
	Connectivity	USB 2.0 Full Speed			-
	Operating Systems	Windows, Mac OS X, Ubuntu			-
Electrical	Power Supply (USB)	4.75	5	5.25	VDC
	Current Consumption	-	0.5	0.8	A
Environment	Temperature	0	25	40	°C

Table A.6: Technical specifications of the Microsoft LifeCam Studio.

A.4   Additional Sensors

As noted above, the robotic platform used for the implementation of the AGoRA Walker (i.e., the Pioneer LX) has several built-in sensors. For instance, the platform is equipped with encoders and hall sensors in the wheels, an IMU, a frontal bumper board, and two ultrasonic boards (i.e., frontal and rear)[3]. This group of sensors is integrated into the ROS architecture of the AGoRA Walker by means of the *RosAria* package [166].

---

[3]The manufacturer of the platform does not specify any technical characteristics of these devices.

Glossary

ADC Analog-To-Digital Converter.

ADL Activies of Daily Living.

AFO Ankle-Foot orthoses.

AGoRA In Spanish *Desarrollo de una plataforma robótica adaptable para rehabilitación y asistencia de la marcha*.

AMCL Adaptive Monte Carlo Localization Approach.

AT Attitude Towards Using Technology.

BP Behaviour Perception.

CCD Charged-Coupled Devices.

cHRi Cognitive Human-Robot interface.

CiDT Center for Innovation and Technological Development.

CMOS Complementary Metal Oxide on Silicon.

CNS Central Nervous System.

Colciencias In Spanish *Departamento Administrativo de Ciencia, Tecnología e Innovación*.

CP Cerebral Palsy.

DAQ Data Acquisition.

DOF Degrees of Freedom.

DWA Dynamic Window approach.

ECIJG In Spanish *Escuela Colombiana de Ingeniería Julio Garavito*.

EEA Effort Expectancy and Anxiety.

FC Facilitating Conditions.

FL Filtering System.

FLC Fourier Linear Combiner.

GCE Gait Cadence Estimator.

HKAFO Hip-Knee-Ankle-Foot orthoses.

HOG Histogram of Oriented Gradients.

HREI Human-Robot-Environment Interaction.

HREi Human-Robot-Environment interface.

HRI Human-Robot Interaction.

HRi Human-Robot interface.

IMU Inertial Measurement Unit.

KAFO Knee-Ankle-Foot orthoses.

KTE Kinematic Estimation Error.

LiDAR Light Detection and Ranging.

LMI Low- and Middle-Income.

LRF Laser Range-Finder.

MET Maximum Exerted Torque.

MWW Mann-Whitney-Wilcoxon.

NSCIA National Spinal Cord Injury Association.

PAE Performance and Attitude Expectancy.

PCi Physical and Cognitive interaction.

REI Robot-Environment Interaction.

REi Robot-Environment interface.

ROI Region of Interest.

ROS Robotic Operating System.

SCI Spinal Cord Injury.

SD Slow Distance Parameter.

SLAM Simultaneous Localization and Mapping.

STD Stop Distance Parameter.

SVM Support Vector Machine.

SW Smart Walker.

TR Trust.

TX Texas.

UN United Nations.

USA United States of America.

UTP Technological University of Pereira.

WFLC Weighted-Fourier Linear Combiner.

WHO World Health Organization.

WR Width Rate.

YLD Years Lived with Disability.

Bibliography

[1] T. Mikolajczyk, I. Ciobanu, D. I. Badea, A. Iliescu, S. Pizzamiglio, T. Schauer, T. Seel, P. L. Seiciu, D. L. Turner, and M. Berteanu, "Advanced technology for gait rehabilitation: An overview," *Advances in Mechanical Engineering*, vol. 10, no. 7, pp. 1–19, 2018.

[2] M. Akhtaruzzaman, A. A. Shafie, and M. R. Khan, "Gait Analysis: Systems, Technologies, and Importance," *Journal of Mechanics in Medicine and Biology*, vol. 16, p. 1630003, nov 2016.

[3] P. Mahlknecht, S. Kiechl, B. R. Bloem, J. Willeit, C. Scherfler, A. Gasperi, G. Rungger, W. Poewe, and K. Seppi, "Prevalence and Burden of Gait Disorders in Elderly Men and Women Aged 60–97 Years: A Population-Based Study," *PLoS ONE*, vol. 8, p. e69627, jul 2013.

[4] World Bank Group, "Disability Inclusion," 2019.

[5] L. Kraus, E. Lauer, R. Coleman, and A. Houtenville, *2017 Disability Statistics Annual Report*. Durham: Durham, NH: University of New Hampshire, 2018.

[6] A. H. Snijders, B. P. van de Warrenburg, N. Giladi, and B. R. Bloem, "Neurological gait disorders in elderly people: clinical approach and classification," *The Lancet Neurology*, vol. 6, pp. 63–74, jan 2007.

[7] C. A. Cifuentes and A. Frizera, *Human-Robot Interaction Strategies for Walker-Assisted Locomotion*, vol. 115 of *Springer Tracts in Advanced Robotics*. Cham: Springer International Publishing, 2016.

[8] J. A. Cohen, J. Verghese, and J. L. Zwerling, "Cognition and gait in older people," *Maturitas*, vol. 93, pp. 73–77, nov 2016.

[9] R. Gheno, J. Cepparo, C. Rosca, and A. Cotten, "Musculoskeletal Disorders in the Elderly," *Journal of Clinical Imaging Science*, vol. 2, no. 3, p. 39, 2012.

[10] World Health Organization, *World Report on Disability 2011*. WHO Press, 2011.

[11] World Health Organization , "Disability and Health," 2018.

[12] World Health Organization, "The need to scale up rehabilitation," *Rehabilitation 2030: A Call for Action*, 2017.

[13] M. Katan and A. Luft, "Global Burden of Stroke," *Seminars in Neurology*, vol. 38, pp. 208–211, apr 2018.

[14] The Internet Stroke Center, "Stroke Statistics," 2018.

[15] J. J. Eng and P.-F. Tang, "Gait training strategies to optimize walking ability in people with stroke: a synthesis of the evidence," *Expert Review of Neurotherapeutics*, vol. 7, pp. 1417–1436, oct 2007.

[16] B. Ovbiagele and M. N. Nguyen-Huynh, "Stroke Epidemiology: Advancing Our Understanding of Disease Mechanism and Therapy," *Neurotherapeutics*, vol. 8, pp. 319–329, jul 2011.

[17] World Health Organization, "Spinal cord injury," 2013.

[18] M. Fehlings, A. Singh, L. Tetreault, S. Kalsi-Ryan, and A. Nouri, "Global prevalence and incidence of traumatic spinal cord injury," *Clinical Epidemiology*, p. 309, sep 2014.

[19] N. Sezer, "Chronic complications of spinal cord injury," *World Journal of Orthopedics*, vol. 6, no. 1, p. 24, 2015.

[20] M. Stavsky, O. Mor, S. A. Mastrolia, S. Greenbaum, N. G. Than, and O. Erez, "Cerebral Palsy—Trends in Epidemiology and Recent Development in Prenatal Mechanisms of Disease, Treatment, and Prevention," *Frontiers in Pediatrics*, vol. 5, feb 2017.

[21] N. Paneth, T. Hong, and S. Korzeniewski, "The Descriptive Epidemiology of Cerebral Palsy," *Clinics in Perinatology*, vol. 33, pp. 251–267, jun 2006.

[22] World Health Organization, "Ageing and health," 2018.

[23] C. J. Brown and K. L. Flood, "Mobility limitation in the older patient: A clinical review," *JAMA - Journal of the American Medical Association*, vol. 310, no. 11, pp. 1168–1177, 2013.

[24] M. M. Pedersen, N. E. Holt, L. Grande, L. A. Kurlinski, M. K. Beauchamp, D. K. Kiely, J. Petersen, S. Leveille, and J. F. Bean, "Mild cognitive impairment status and mobility performance: An analysis from the Boston RISE study," *Journals of Gerontology - Series A Biological Sciences and Medical Sciences*, vol. 69, no. 12, pp. 1511–1518, 2014.

[25] N. E. Groce, "Global disability: an emerging issue," *The Lancet Global Health*, vol. 6, pp. e724–e725, jul 2018.

[26] United Nations, "Factsheet on Persons with Disabilities," 2016.

[27] S. L. Chaparro-Cárdenas, A. A. Lozano-Guzmán, J. A. Ramirez-Bautista, and A. Hernández-Zavala, "A review in gait rehabilitation devices and applied control techniques," *Disability and Rehabilitation: Assistive Technology*, vol. 0, no. 0, pp. 1–15, 2018.

[28] H. Bateni and B. E. Maki, "Assistive devices for balance and mobility: Benefits, demands, and adverse consequences," *Archives of Physical Medicine and Rehabilitation*, vol. 86, no. 1, pp. 134–145, 2005.

[29] S. F. Tyson and L. Rogerson, "Assistive Walking Devices in Nonambulant Patients Undergoing Rehabilitation After Stroke: The Effects on Functional Mobility, Walking Impairments, and Patients' Opinion," *Archives of Physical Medicine and Rehabilitation*, vol. 90, pp. 475–479, mar 2009.

[30] A. F. Neto, A. Elias, C. Cifuentes, C. Rodriguez, T. Bastos, and R. Carelli, "Smart Walkers : Advanced Robotic Human Walking-Aid Systems," in *Springer Tracts in Advanced Robotics 106 Intelligent Assistive Robots Recent Advances in Assistive Robotics*, ch. Smart Walk, pp. 103 – 131, Springer International Publishing, 2015.

[31] M. Martins, C. Santos, A. Frizera, and R. Ceres, "A review of the functionalities of smart walkers," *Medical Engineering and Physics*, vol. 37, no. 10, pp. 917–928, 2015.

[32] M. Geravand, C. Werner, K. Hauer, and A. Peer, "An Integrated Decision Making Approach for Adaptive Shared Control of Mobility Assistance Robots," *International Journal of Social Robotics*, vol. 8, no. 5, pp. 631–648, 2016.

[33] T. L. Mitzner, T. L. Chen, C. C. Kemp, and W. A. Rogers, "Identifying the Potential for Robotics to Assist Older Adults in Different Living Environments," *International Journal of Social Robotics*, vol. 6, pp. 213–227, apr 2014.

[34] S. Jenkins and H. Draper, "Care, Monitoring, and Companionship: Views on Care Robots from Older People and Their Carers," *International Journal of Social Robotics*, vol. 7, no. 5, pp. 673–683, 2015.

[35] C. L. Vaughan, "Theories of bipedal walking: an odyssey," *Journal of Biomechanics*, vol. 36, pp. 513–523, apr 2003.

[36] L. M. Decker, F. Cignetti, and N. Stergiou, "Complexity and Human Gait," *Revista Andaluza de Medicina del Deporte*, vol. 3, no. 1, pp. 2–12, 2010.

[37] A. S. Buchman, P. A. Boyle, S. E. Leurgans, L. L. Barnes, D. A. Bennett, B. AS, B. PA, L. SE, B. LL, and B. DA, "Cognitive Function is Associated with the Development of Mobility Impairments in Community-Dwelling Elders," *Am J Geriatr Psychiatry*, vol. 19, no. 6, pp. 571–580, 2011.

[38] É. Watelain, "Human gait: From clinical gait analysis to diagnosis assistance," *Movement & Sport Sciences*, vol. 98, no. 4, p. 3, 2017.

[39] K. E. Adolph, W. G. Cole, M. Komati, J. S. Garciaguirre, D. Badaly, J. M. Lingeman, G. L. Y. Chan, and R. B. Sotsky, "How Do You Learn to Walk? Thousands of Steps and Dozens of Falls per Day," *Psychological Science*, vol. 23, pp. 1387–1394, nov 2012.

[40] S. Schmid, K. Schweizer, J. Romkes, S. Lorenzetti, and R. Brunner, "Secondary gait deviations in patients with and without neurological involvement: A systematic review," *Gait & Posture*, vol. 37, pp. 480–493, apr 2013.

[41] G. Malanga and J. A. DeLisa, "Clinical Observation," in *Gait Analysis in the Science of Rehabilitation* (T. T. Sowell, ed.), pp. 1–10, Baltimore: Department of Veterans Affairs, 1998.

[42] M. Roberts, D. Mongeon, and F. Prince, "Biomechanical parameters for gait analysis: a systematic review of healthy human gait," *Physical Therapy and Rehabilitation*, vol. 4, no. 1, p. 6, 2017.

[43] Disabled World, "Physical and Mobility Impairment: Information & News," 2019.

[44] G. Sammer, T. Uhlmann, W. Unbehaun, A. Millonig, B. Mandl, J. Dangschat, and R. Mayr, "Identification of Mobility-Impaired Persons and Analysis of Their Travel Behavior and Needs," *Transportation Research Record: Journal of the Transportation Research Board*, vol. 2320, pp. 46–54, jan 2012.

[45] E. M. Simonsick, A. B. Newman, M. Visser, B. Goodpaster, S. B. Kritchevsky, S. Rubin, M. C. Nevitt, and T. B. Harris, "Mobility Limitation in Self-Described Well-Functioning Older Adults: Importance of Endurance Walk Testing," *The Journals of Gerontology Series A: Biological Sciences and Medical Sciences*, vol. 63, pp. 841–847, aug 2008.

[46] W. Pirker and R. Katzenschlager, "Gait disorders in adults and the elderly," *Wiener klinische Wochenschrift*, vol. 129, pp. 81–95, feb 2017.

[47] P. Bamberski, "Analysis of stability of the human gait.," *Journal of Theoretical and Applied Mechanics*, vol. 45, no. 1, pp. 91–98, 2007.

[48] The World Bank, "Disability Inclusion," 2018.

[49] C. Chrissobolis, Sophocles Sobey, "Vascular Biology and Atherosclerosis of Cerebral Vessels," in *Stroke: Pathophysiology, Diagnosis, and Management* (J. C. Grotta, G. W. Albers, J. P. Broderick, S. E. Kasner, and E. H. Lo, eds.), ch. Pathophysi, pp. 3 – 12, New York: Elsevier, 6 ed., 2016.

[50] NIH: National Institute of Neurological Disorders and Stroke, "Stroke," 2018.

[51] D. Kasper, E. Braunwald, A. Fauci, S. Hauser, D. Longo, and J. Jameson, "Stroke," in *Harrison's Manual of Medicine* (D. Kasper, E. Braunwald, A. Fauci, S. Hauser, D. Longo, and J. Jameson, eds.), ch. Section 2:, pp. 58 – 65, New York: McGraw-Hill, 16 ed., 2005.

[52] B. P. B. Carvalho-Pinto and C. D. C. M. Faria, "Health, function and disability in stroke patients in the community," *Brazilian Journal of Physical Therapy*, vol. 20, pp. 355–366, aug 2016.

[53] Spalding Rehabilitation Hospital, "Disabilities Related To Stroke," 2019.

[54] American Stroke Association, "Paralysis," 2019.

[55] S. C. Cramer, S. L. Wolf, H. P. Adams, D. Chen, A. W. Dromerick, K. Dunning, C. Ellerbe, A. Grande, S. Janis, M. G. Lansberg, R. M. Lazar, Y. Y. Palesch, L. Richards, E. Roth, S. I. Savitz, L. R. Wechsler, M. Wintermark, and J. P. Broderick, "Stroke Recovery and Rehabilitation Research," *Stroke*, vol. 48, pp. 813–819, mar 2017.

[56] A. Lindgren, "Risk Factors," in *Oxford Textbook of Sroke and Cerebrovascular Disorders* (B. Norrving, ed.), ch. 2, pp. 9 –18, New York: Oxford University Press, 1 ed., 2014.

[57] V. Feigin and R. Krishnamurthi, "Epidemiology of Stroke," in *Oxford Textbook of Sroke and Cerebrovascular Disorders* (B. Norrving, ed.), ch. 1, pp. 1 – 8, New York: Oxford University Press, 1 ed., 2014.

[58] W. Johnson, O. Onuma, M. Owolabi, and S. Sachdev, "Stroke: a global response is needed," *Bulletin of the World Health Organization*, vol. 94, pp. 634–634A, sep 2016.

[59] The Internet Stroke Center, "Stroke Statistics," 2019.

[60] C. O. Johnson and M. Nguyen, "Global, regional, and national burden of stroke, 1990–2016: a systematic analysis for the Global Burden of Disease Study 2016," *The Lancet Neurology*, vol. 18, pp. 439–458, may 2019.

[61] V. L. Feigin, B. Norrving, and G. A. Mensah, "Global Burden of Stroke," *Circulation Research*, vol. 120, pp. 439–448, feb 2017.

[62] Mayo Clinic, "Spinal cord injury," 2019.

[63] MedlinePlus, "Spinal Cord Injuries," 2019.

[64] University of Alabama at Birmingham, "Spinal Cord Injury Model System," 2019.

[65] Merck Manuals, "Overview of Spinal Cord Disorders," 2019.

[66] American Association of Neurological Surgeons, "Spinal Cord Injury," 2019.

[67] National Institute of Child Health and Human Development, "Spinal Cord Injury (SCI): Condition Information," 2016.

[68] World Health Organization, "Spinal cord injury: Key facts," 2013.

[69] Spinal Cord Injury Information Page, "Spinal Cord Injury Facts & Statistics," 2019.

[70] R. Yang, L. Guo, P. Wang, L. Huang, Y. Tang, W. Wang, K. Chen, J. Ye, C. Lu, Y. Wu, and H. Shen, "Epidemiology of Spinal Cord Injuries and Risk Factors for Complete Injuries in Guangdong, China: A Retrospective Study," *PLoS ONE*, vol. 9, p. e84733, jan 2014.

[71] C. P. Henao-Lema and J. E. Perez-Parra, "Lesiones medulares y discapacidad: revisión bibliográfica," *Aquichan*, vol. 10, no. 2, 2010.

[72] C. L. Richards and F. Malouin, "Cerebral palsy," in *Handbook of Clinical Neurology*, vol. 111, pp. 183–195, Elsevier B.V., 2013.

[73] Center for Disease Control and Prevention, "What is Cerebral Palsy?," 2019.

[74] Healthline, "Cerebral Palsy," 2019.

[75] J. J. Noble, N. R. Fry, A. P. Lewis, S. F. Keevil, M. Gough, and A. P. Shortland, "Lower limb muscle volumes in bilateral spastic cerebral palsy," *Brain and Development*, vol. 36, pp. 294–300, apr 2014.

[76] Cerebral Palsy Alliance, "Spastic Cerebral Palsy," 2018.

[77] G. Jansheski, "Dyskinetic Athetoid Cerebral Palsy," 2019.

[78] Cerebral Palsy Guide, "Ataxic Cerebral Palsy," 2016.

[79] P. Mimi Poinsett, "Cerebral Palsy Prevalence and Incidence," *Cerebral Palsy Guidance*, oct 2019.

[80] Health In Aging, "Living With Multiple Health Problems: What Older Adults Should Know," 2017.

[81] MedlinePlus, "Bone Diseases," 2016.

[82] S. N. Nabili and C. P. Davis, "Senior Health: Successful Aging," 2019.

[83] A. Banerjee, V. Nikumb, and R. Thakur, "Health Problems Among the Elderly: A Cross-Sectional Study," *Annals of Medical and Health Sciences Research*, vol. 3, no. 1, p. 19, 2013.

[84] S. Studenski, "Gait Speed and Survival in Older Adults," *JAMA*, vol. 305, p. 50, jan 2011.

[85] J. O. Judge, "Gait Disorders in Older Adults," 2019.

[86] United Nations, "Ageing," 2019.

[87] U. M. Kujala, P. Hautasaari, H. Vähä-Ypyä, K. Waller, N. Lindgren, P. Iso-Markku, K. Heikkilä, J. Rinne, J. Kaprio, and H. Sievänen, "Chronic diseases and objectively monitored physical activity profile among aged individuals – a cross-sectional twin cohort study," *Annals of Medicine*, vol. 51, pp. 78–87, jan 2019.

[88] L. I. Iezzoni, E. P. McCarthy, R. B. Davis, and H. Siebens, "Mobility difficulties are not only a problem of old age," *Journal of General Internal Medicine*, vol. 16, pp. 235–243, apr 2001.

[89] M. Montero-Odasso, J. Verghese, O. Beauchet, and J. M. Hausdorff, "Gait and Cognition: A Complementary Approach to Understanding Brain Function and the Risk of Falling," *Journal of the American Geriatrics Society*, vol. 60, pp. 2127–2136, nov 2012.

[90] M. Amboni, P. Barone, and J. M. Hausdorff, "Cognitive contributions to gait and falls: Evidence and implications," *Movement Disorders*, vol. 28, pp. 1520–1533, sep 2013.

[91] National Health Service UK, "Physiotherapy," 2018.

[92] M. Martins, A. Frizera-Neto, C. P. Santos, and R. Ceres, "Review and Classification of Human Gait Training and Rehabilitation Devices," in *Assistive Technology Research Series* (IOS Press, ed.), ch. Everyday T, pp. 774 – 781, IOS Press Ebook, 2011.

[93] J. H. Carr and R. B. Shepherd, *Stroke Rehabilitation - Guidelines for Exercise and Training to Optimize Motor Skill*. Butterworth-Heinemann, 1 ed., 2003.

[94] R. A. States, E. Pappas, and Y. Salem, "Overground physical therapy gait training for chronic stroke patients with mobility deficits," *Cochrane Database of Systematic Reviews*, jul 2009.

[95] A. Pollock, G. Baer, P. Campbell, P. L. Choo, A. Forster, J. Morris, V. M. Pomeroy, and P. Langhorne, "Physical rehabilitation approaches for the recovery of function and mobility following stroke," *Cochrane Database of Systematic Reviews*, apr 2014.

[96] I. G. van de Port, S. Wood-Dauphinee, E. Lindeman, and G. Kwakkel, "Effects of Exercise Training Programs on Walking Competency After Stroke," *American Journal of Physical Medicine & Rehabilitation*, vol. 86, pp. 935–951, nov 2007.

[97] M. Thaut, A. Leins, R. Rice, H. Argstatter, G. Kenyon, G. McIntosh, H. Bolay, and M. Fetter, "Rhythmic Auditor y Stimulation Improves Gait More Than NDT/Bobath Training in Near-Ambulatory Patients Early Poststroke: A Single-Blind, Randomized Trial," *Neurorehabilitation and Neural Repair*, vol. 21, pp. 455–459, sep 2007.

[98] D. A. Gelber, B. Josefczyk, D. Herrman, D. C. Good, and S. J. Verhulst, "Comparison of Two Therapy Approaches in the Rehabilitation of the Pure Motor Hemiparetic Stroke Patient," *Neurorehabilitation and Neural Repair*, vol. 9, pp. 191–196, jan 1995.

[99] L. Bradley, B. B. Hart, S. Mandana, K. Flowers, M. Riches, and P. Sanderson, "Electromyographic biofeedback for gait training after stroke," *Clinical Rehabilitation*, vol. 12, pp. 11–22, feb 1998.

[100] Q. U. Ain, A. N. Malik, U. Haq, and S. Ali, "Effect of task specific circuit training on gait parameters and mobility in stroke survivors," *Pakistan Journal of Medical Sciences*, vol. 34, sep 2018.

[101] K. Kim, S. I. Jung, and D. K. Lee, "Effects of task-oriented circuit training on balance and gait ability in subacute stroke patients: a randomized controlled trial," *Journal of Physical Therapy Science*, vol. 29, no. 6, pp. 989–992, 2017.

[102] Physiopedia, "Gait Training in Stroke," 2019.

[103] Y.-R. Yang, R.-Y. Wang, K.-H. Lin, M.-Y. Chu, and R.-C. Chan, "Task-oriented progressive resistance strength training improves muscle strength and functional performance in individuals with stroke," *Clinical Rehabilitation*, vol. 20, pp. 860–870, oct 2006.

[104] M. Y. C. Pang, J. J. Eng, A. S. Dawson, H. A. McKay, and J. E. Harris, "A Community-Based Fitness and Mobility Exercise Program for Older Adults with Chronic Stroke: A Randomized, Controlled Trial," *Journal of the American Geriatrics Society*, vol. 53, pp. 1667–1674, oct 2005.

[105] S. Lennon, "The Bobath concept: a critical review of the theoretical assumptions that guide physiotherapy practice in stroke rehabilitation," *Physical Therapy Reviews*, vol. 1, pp. 35–45, sep 1996.

[106] C. E. Perry, "Principles and Techniques of the Brunnstrom Approach to the Treatment of Hemiplegia," *American Journal of Physical Medicine & Rehabilitation*, vol. 46, no. 1, 1967.

[107] B. Langhammer and J. K. Stanghelle, "Bobath or Motor Relearning Programme? A comparison of two different approaches of physiotherapy in stroke rehabilitation: a randomized controlled study," *Clinical Rehabilitation*, vol. 14, pp. 361–369, aug 2000.

[108] J.-M. Belda-Lois, S. M.-d. Horno, I. Bermejo-Bosch, J. C. Moreno, J. L. Pons, D. Farina, M. Iosa, M. Molinari, F. Tamburella, A. Ramos, A. Caria, T. Solis-Escalante, C. Brunner, and M. Rea, "Rehabilitation of gait after stroke: a review towards a top-down approach.," *Journal of neuroengineering and rehabilitation*, vol. 8, p. 66, jan 2011.

[109] Physio.co.uk, "Carr & Shepherd: What is the Carr and Shepherd approach?," 2019.

[110] S. D. Sierra M., M. Garzón, M. Múnera, and C. A. Cifuentes, "Human–Robot–Environment Interaction Interface for Smart Walker Assisted Gait: AGoRA Walker," *Sensors*, vol. 19, p. 2897, jun 2019.

[111] F. W. Van Hook, D. Demonbreun, and B. D. Weiss, "Ambulatory Devices for Chronic Gait Disorders in the Elderly," *American Family Physician*, vol. 67, no. 8, pp. 1717 – 1724, 2003.

[112] M. M. Martins, C. P. Santos, A. Frizera-Neto, and R. Ceres, "Assistive mobility devices focusing on Smart Walkers: Classification and review," *Robotics and Autonomous Systems*, vol. 60, no. 4, pp. 548–562, 2012.

[113] A. R. Luft, R. F. Macko, L. W. Forrester, F. Villagra, F. Ivey, J. D. Sorkin, J. Whitall, S. McCombe-Waller, L. Katzel, A. P. Goldberg, and D. F. Hanley, "Treadmill Exercise Activates Subcortical Neural Networks and Improves Walking After Stroke," *Stroke*, vol. 39, pp. 3341–3350, dec 2008.

[114] Y.-R. Mao, W. L. Lo, Q. Lin, L. Li, X. Xiao, P. Raghavan, and D.-F. Huang, "The Effect of Body Weight Support Treadmill Training on Gait Recovery, Proximal Lower Limb Motor Pattern, and Balance in Patients with Subacute Stroke," *BioMed Research International*, vol. 2015, pp. 1–10, 2015.

[115] C.-L. Yen, R.-Y. Wang, K.-K. Liao, C.-C. Huang, and Y.-R. Yang, "Gait Training—Induced Change in Corticomotor Excitability in Patients With Chronic Stroke," *Neurorehabilitation and Neural Repair*, vol. 22, pp. 22–30, jan 2008.

[116] E. Russell Esposito, K. A. Schmidtbauer, and J. M. Wilken, "Experimental comparisons of passive and powered ankle-foot orthoses in individuals with limb reconstruction," *Journal of NeuroEngineering and Rehabilitation*, vol. 15, p. 111, dec 2018.

[117] C. McDaid, D. Fayter, A. Booth, J. O'Connor, R. Rodriguez-Lopez, D. McCaughan, R. Bowers, C. P. Iglesias, S. Lalor, R. J. O'Connor, M. Phillips, and G. Ramdharry, "Systematic review of the evidence on orthotic devices for the management of knee instability related to neuromuscular and central nervous system disorders," *BMJ Open*, vol. 7, p. e015927, sep 2017.

[118] R. Constantinescu, C. Leonard, C. Deeley, and R. Kurlan, "Assistive devices for gait in Parkinson's disease," *Parkinsonism & Related Disorders*, vol. 13, pp. 133–138, apr 2007.

[119] L. R. Sheffler and J. Chae, "Technological Advances in Interventions to Enhance Poststroke Gait," *Physical Medicine and Rehabilitation Clinics of North America*, vol. 24, pp. 305–323, may 2013.

[120] J. Leaman and H. M. La, "A Comprehensive Review of Smart Wheelchairs: Past, Present, and Future," *IEEE Transactions on Human-Machine Systems*, vol. 47, pp. 486–499, aug 2017.

[121] R. Bostelman and J. Albus, "Robotic Patient Lift and Transfer," in *Service Robot Applications*, InTech, 2008.

[122] K. Y. Nam, H. J. Kim, B. S. Kwon, J.-W. Park, H. J. Lee, and A. Yoo, "Robot-assisted gait training (Lokomat) improves walking function and activity in people with spinal cord injury: a systematic review," *Journal of NeuroEngineering and Rehabilitation*, vol. 14, p. 24, dec 2017.

[123] S. Freivogel, J. Mehrholz, T. Husak-Sotomayor, and D. Schmalohr, "Gait training with the newly developed 'LokoHelp'-system is feasible for non-ambulatory patients after stroke, spinal cord and brain injury. A feasibility study," *Brain Injury*, vol. 22, pp. 625–632, jan 2008.

[124] J. Veneman, R. Kruidhof, E. Hekman, R. Ekkelenkamp, E. Van Asseldonk, and H. van der Kooij, "Design and Evaluation of the LOPES Exoskeleton Robot for Interactive Gait Rehabilitation," *IEEE Transactions on Neural Systems and Rehabilitation Engineering*, vol. 15, pp. 379–386, sep 2007.

[125] F. M. Alfieri, C. d. S. Dias, A. C. A. dos Santos, and L. R. Battistella, "Acute Effect of Robotic Therapy (G-EO System™) on the Lower Limb Temperature Distribution of a Patient with Stroke Sequelae," *Case Reports in Neurological Medicine*, vol. 2019, pp. 1–5, may 2019.

[126] X. Zhang, Z. Yue, and J. Wang, "Robotics in Lower-Limb Rehabilitation after Stroke," *Behavioural Neurology*, vol. 2017, pp. 1–13, 2017.

[127] R. S. Calabrò, A. Cacciola, F. Bertè, A. Manuli, A. Leo, A. Bramanti, A. Naro, D. Milardi, and P. Bramanti, "Robotic gait rehabilitation and substitution devices in neurological disorders: where are we now?," *Neurological Sciences*, vol. 37, pp. 503–514, apr 2016.

[128] A. Wall, J. Borg, and S. Palmcrantz, "Clinical application of the Hybrid Assistive Limb (HAL) for gait training: a systematic review," *Frontiers in Systems Neuroscience*, vol. 9, mar 2015.

[129] A. E. Palermo, J. L. Maher, C. B. Baunsgaard, and M. S. Nash, "Clinician-Focused Overview of Bionic Exoskeleton Use After Spinal Cord Injury," *Topics in Spinal Cord Injury Rehabilitation*, vol. 23, pp. 234–244, jun 2017.

[130] K. Schmidt, J. E. Duarte, M. Grimmer, A. Sancho-Puchades, H. Wei, C. S. Easthope, and R. Riener, "The Myosuit: Bi-articular Anti-gravity Exosuit That Reduces Hip Extensor Activity in Sitting Transfers," *Frontiers in Neurorobotics*, vol. 11, oct 2017.

[131] Technaid, "Exoesqueleto Exo-H3," 2019.

[132] G. Zeilig, H. Weingarden, M. Zwecker, I. Dudkiewicz, A. Bloch, and A. Esquenazi, "Safety and tolerance of the ReWalk ™ exoskeleton suit for ambulation by people with complete spinal cord injury: A pilot study," *The Journal of Spinal Cord Medicine*, vol. 35, pp. 96–101, mar 2012.

[133] A. Chu, H. Kazerooni, and A. Zoss, "On the Biomimetic Design of the Berkeley Lower Extremity Exoskeleton (BLEEX)," in *Proceedings of the 2005 IEEE International Conference on Robotics and Automation*, pp. 4345–4352, IEEE, 2005.

[134] J. Pratt, B. Krupp, C. Morse, and S. Collins, "The RoboKnee: an exoskeleton for enhancing strength and endurance during walking," in *IEEE International Conference on Robotics and Automation, 2004. Proceedings. ICRA '04. 2004*, pp. 2430–2435 Vol.3, IEEE, 2004.

[135] M. Sanchez-Manchola, D. Gomez-Vargas, D. Casas-Bocanegra, M. Munera, and C. A. Cifuentes, "Development of a Robotic Lower-Limb Exoskeleton for Gait Rehabilitation: AGoRA Exoskeleton," in *2018 IEEE ANDESCON*, pp. 1–6, IEEE, aug 2018.

[136] M. Manchola, D. Serrano, D. Gómez, F. Ballen, D. Casas, M. Munera, and C. A. Cifuentes, "T-FLEX: Variable Stiffness Ankle-Foot Orthosis for Gait Assistance," in *Wearable Robotics: Challenges and Trends.*, pp. 160–164, Springer, Cham, 2019.

[137] M. Martins, C. Santos, E. Seabra, A. Frizera, and R. Ceres, "Design, implementation and testing of a new user interface for a smart walker," in *2014 IEEE International Conference on Autonomous Robot Systems and Competitions (ICARSC)*, pp. 217–222, IEEE, may 2014.

[138] G. J. Lacey and D. Rodriguez-Losada, "The evolution of guido," *IEEE Robotics and Automation Magazine*, vol. 15, no. 4, pp. 75–83, 2008.

[139] A. Morris, R. Donamukkala, A. Kapuria, A. Steinfeld, J. Matthews, J. Dunbar-Jacob, and S. Thrun, "A robotic walker that provides guidance," *2003 IEEE International Conference on Robotics and Automation (Cat. No.03CH37422)*, vol. 1, pp. 25–30, 2003.

[140] J. Alves, E. Seabra, I. Caetano, and C. P. Santos, "Overview of the ASBGo++ Smart Walker," in *2017 IEEE 5th Portuguese Meeting on Bioengineering (ENBENG)*, pp. 1–4, IEEE, 2017.

[141] I. Caetano, J. Alves, J. Goncalves, M. Martins, and C. P. Santos, "Development of a Biofeedback Approach Using Body Tracking with Active Depth Sensor in ASBGo Smart Walker," in *2016 International Conference on Autonomous Robot Systems and Competitions (ICARSC)*, pp. 241–246, IEEE, may 2016.

[142] G. Lee, T. Ohnuma, and N. Y. Chong, "Design and control of JAIST active robotic walker," *Intelligent Service Robotics*, vol. 3, no. 3, pp. 125–135, 2010.

[143] G. Lee, E. J. Jung, T. Ohnuma, N. Y. Chong, and B. J. Yi, "JAIST Robotic Walker control based on a two-layered Kalman filter," *Proceedings - IEEE International Conference on Robotics and Automation*, pp. 3682–3687, 2011.

[144] M. M. Martins, A. Frizera-Neto, E. Urendes, C. dos Santos, R. Ceres, and T. Bastos-Filho, "A novel human-machine interface for guiding: The NeoASAS smart walker," in *2012 ISSNIP Biosignals and Biorobotics Conference: Biosignals and Robotics for Better and Safer Living (BRC)*, pp. 1–7, IEEE, jan 2012.

[145] M. F. Jiménez, M. Monllor, A. Frizera, T. Bastos, F. Roberti, and R. Carelli, "Admittance Controller with Spatial Modulation for Assisted Locomotion using a Smart Walker," *Journal of Intelligent & Robotic Systems*, p. 1, jul 2018.

[146] M. Spenko, H. Yu, and S. Dubowsky, "Robotic personal aids for mobility and monitoring for the elderly," *IEEE Transactions on Neural Systems and Rehabilitation Engineering*, vol. 14, no. 3, pp. 344–351, 2006.

[147] E. Efthimiou, S.-E. Fotinea, T. Goulas, A.-L. Dimou, M. Koutsombogera, V. Pitsikalis, P. Maragos, and C. Tzafestas, "The MOBOT Platform – Showcasing Multimodality in Human-Assistive Robot Interaction," in *Universal Access in Human-Computer Interaction. Interaction Techniques and Environments*, pp. 382–391, Springer, 2016.

[148] E. Efthimiou, S. E. Fotinea, and T. Goulas, "The MOBOT rollator human-robot interaction model and user evaluation process," *2016 IEEE Symposium Series on Computational Intelligence, SSCI 2016*, 2017.

[149] X. S. Papageorgiou, G. Chalvatzaki, K. N. Lianos, C. Werner, K. Hauer, C. S. Tzafestas, and P. Maragos, "Experimental validation of human pathological gait analysis for an assisted living intelligent robotic walker," *Proceedings of the IEEE RAS and EMBS International Conference on Biomedical Robotics and Biomechatronics*, vol. 2016-July, pp. 1086–1091, 2016.

[150] W.-H. Mou, M.-F. Chang, C.-K. Liao, Y.-H. Hsu, S.-H. Tseng, and L.-C. Fu, "Context-aware assisted interactive robotic walker for Parkinson's disease patients," in *2012 IEEE/RSJ International Conference on Intelligent Robots and Systems*, pp. 329–334, IEEE, oct 2012.

[151] J. Paulo, P. Peixoto, and U. J. Nunes, "ISR-AIWALKER: Robotic Walker for Intuitive and Safe Mobility Assistance and Gait Analysis," *IEEE Transactions on Human-Machine Systems*, vol. 47, no. 6, pp. 1110–1122, 2017.

[152] L. Garrote, J. Paulo, J. Perdiz, P. Peixoto, and U. J. Nunes, "Robot-Assisted Navigation for a Robotic Walker with Aided User Intent," *RO-MAN 2018 - 27th IEEE International Symposium on Robot and Human Interactive Communication*, pp. 348–355, 2018.

[153] C. Huang, G. Wasson, M. Alwan, and P. Sheth, "Shared navigational control and user intent detection in an intelligent walker," *AAAI Fall 2005*, 2005.
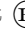
[154] A. Wachaja, P. Agarwal, M. Zink, M. R. Adame, K. Möller, and W. Burgard, "Navigating blind people with walking impairments using a smart walker," *Autonomous Robots*, vol. 41, pp. 555–573, 2017.

[155] G. Wasson, J. Gunderson, S. Graves, and R. Felder, "Effective Shared Control in Cooperative Mobility Aids," in *Proceedings of the Fourteenth international Florida Artificial intelligence Research Society Conference*, pp. 509 – 513, AAAI Press, 2001.

[156] G. Wasson, J. Gunderson, S. Graves, and R. Felder, "An assistive robotic agent for pedestrian mobility," in *Proceedings of the fifth international conference on Autonomous agents - AGENTS '01*, (New York, New York, USA), pp. 169–173, ACM Press, 2001.

[157] L. Palopoli, A. Argyros, and J. Birchbauer, "Navigation assistance and guidance of older adults across complex public spaces : the DALi approach," *Intel Serv Robotics*, pp. 77–92, 2015.

[158] W.-c. Cheng and Y.-Z. Wu, "A user's intention detection method for smart walker," in *2017 IEEE 8th International Conference on Awareness Science and Technology (iCAST)*, pp. 35–39, IEEE, nov 2017.

[159] J. Ye, J. Huang, J. He, C. Tao, and X. Wang, "Development of a width-changeable intelligent walking-aid robot," in *2012 International Symposium on Micro-NanoMechatronics and Human Science (MHS)*, pp. 358–363, IEEE, apr 2012.

[160] Y. Hirata, A. Hara, and K. Kosuge, "Passive-type intelligent walking support system "RT Walker"," in *2004 IEEE/RSJ International Conference on Intelligent Robots and Systems (IROS) (IEEE Cat. No.04CH37566)*, vol. 4, pp. 3871–3876, IEEE, 2004.

[161] A. Frizera-Neto, R. Ceres, E. Rocon, and J. L. Pons, "Empowering and assisting natural human mobility: The simbiosis walker," *International Journal of Advanced Robotic Systems*, vol. 8, no. 3, pp. 34–50, 2011.

[162] V. Kulyukin, A. Kutiyanawala, E. LoPresti, J. Matthews, and R. Simpson, "IWalker: Toward a rollator-mounted wayfinding system for the elderly," *2008 IEEE International Conference on RFID (Frequency Identification), IEEE RFID 2008*, pp. 303–311, 2008.

[163] C.-K. Lu, Y.-C. Huang, and C.-J. Lee, "Adaptive guidance system design for the assistive robotic walker," *Neurocomputing*, vol. 170, pp. 152–160, dec 2015.

[164] M. Reyes Adame, J. Yu, and K. Moeller, "Mobility Support System for Elderly Blind People with a Smart Walker and a Tactile Map," in *IFMBE Proceedings*, vol. 57, pp. 602–607, Springer, 2016.

[165] Adept Mobile Robots, "Pioneer LX: Mobile Research Platform," 2013.

[166] Adept Mobile Robots, "RosAria Node," 2017.

[167] HP Development Company, "OMEN by HP - 15-ce003la Product Especifications," 2019.

[168] A. THORSTENSSON, J. NILSSON, H. CARLSON, and M. R. ZOMLEFER, "Trunk movements in human locomotion," *Acta Physiologica Scandinavica*, vol. 121, pp. 9–22, may 1984.

[169] V. Bonnet, C. Mazzà, J. McCamley, and A. Cappozzo, "Use of weighted Fourier linear combiner filters to estimate lower trunk 3D orientation from gyroscope sensors data," *Journal of NeuroEngineering and Rehabilitation*, vol. 10, no. 1, p. 29, 2013.

[170] A. Frizera, J. Gallego, E. Rocon de Lima, A. Abellanas, J. Pons, and R. Ceres, "Online Cadence Estimation through Force Interaction in Walker Assisted Gait," in *ISSNIP Biosignals and Biorobotics Conference 2010*, (Vitória), pp. 1 – 5, 2010.

[171] A. Frizera Neto, J. A. Gallego, E. Rocon, J. L. Pons, and R. Ceres, "Extraction of user's navigation commands from upper body force interaction in walker assisted gait," *BioMedical Engineering Online*, vol. 9, pp. 1–16, 2010.

[172] U. Cortés, A. Martínez-Valesco, C. Barrué, T. Benedico, F. Campana, J. Fernandez, and R. Annichiarico, "A SHARE-it service to elders' mobility using the i-walker," *Gerontechnology*, vol. 7, apr 2008.

[173] M. Belas Dos Santos, C. Barros de Oliveira, A. Dos Santos, C. Garabello Pires, V. Dylewski, and R. M. Arida, "A Comparative Study of Conventional Physiotherapy versus Robot-Assisted Gait Training Associated to Physiotherapy in Individuals with Ataxia after Stroke.," *Behavioural neurology*, vol. 2018, p. 2892065, 2018.

[174] A. Dijkstra, "Care Dependency," in *Dementia in Nursing Homes*, pp. 229–248, Cham: Springer International Publishing, 2017.

[175] J. L. Pons, *Wearable Robots: Biomechatronic Exoskeletons*. Madrid: John Wiley & Sons Ltd, 2008.

[176] L. F. Aycardi, C. A. Cifuentes, M. Múnera, C. Bayón, O. Ramírez, S. Lerma, A. Frizera, and E. Rocon, "Evaluation of biomechanical gait parameters of patients with Cerebral Palsy at three different levels of gait assistance using the CPWalker," *Journal of NeuroEngineering and Rehabilitation*, vol. 16, p. 15, dec 2019.

[177] V. H. Andaluz, F. Roberti, J. M. Toibero, R. Carelli, and B. Wagner, "Adaptive Dynamic Path Following Control of an Unicycle Like Mobile Robot," in *Intelligent Robotics and Applications*, ch. 56, pp. 563–574, Springer Berlin Heidelberg, 2011.

[178] Venkatesh, Morris, Davis, and Davis, "User Acceptance of Information Technology: Toward a Unified View," *MIS Quarterly*, vol. 27, no. 3, p. 425, 2003.

[179] V. Venkatesh, J. Y. L. Thong, and X. Xu, "Consumer Acceptance and Use of Information Technology : Extending the Unified Theory," *MIS Quarterly*, vol. 36, no. 1, pp. 157–178, 2012.

[180] M. Heerink, B. Kröse, B. Wielinga, and V. Evers, "Measuring the influence of social abilities on acceptance of an interface robot and a screen agent by elderly users," in *Proceedings of the 23rd British HCI Group Annual Conference on People and Computers: Celebrating People and Technology*, BCS-HCI '09, (Swinton, UK, UK), pp. 430–439, British Computer Society, 2009.

[181] S. D. Sierra, J. F. Molina, D. A. Gómez, C. A. Cifuentes, and M. C. Múnera, "Development of an Interface for Human-Robot Interaction on a Robotic Platform for Gait Assistance : AGoRA Smart Walker," in *IEEE ANDESCON*, 2018.

[182] G. Grisetti, C. Stachniss, and W. Burgard, "Improved Techniques for Grid Mapping With Rao-Blackwellized Particle Filters," *IEEE Transactions on Robotics*, vol. 23, pp. 34–46, feb 2007.

[183] D. Fox, W. Burgard, F. Dellaert, and S. Thrun, "Monte Carlo Localization: Efficient Position Estimation for Mobile Robots," in *Proceedings of the Sixteenth National Conference on Artificial Intelligence (AAAI'99)*, pp. 343–349, 1999.

[184] D. V. Lu, D. Hershberger, and W. D. Smart, "Layered costmaps for context-sensitive navigation," in *2014 IEEE/RSJ International Conference on Intelligent Robots and Systems*, pp. 709–715, IEEE, sep 2014.

[185] D. Fox, W. Burgard, and S. Thrun, "The dynamic window approach to collision avoidance," *IEEE Robotics & Automation Magazine*, vol. 4, pp. 23–33, mar 1997.

[186] C. Rösmann, W. Feiten, T. Wösch, F. Hoffmann, and T. Bertram, "Trajectory modification considering dynamic constraints of autonomous robots," in *Proc. 7th German Conference on Robotics*, (Germany, Munich), pp. 74–79, 2012.

[187] E. P. Fotiadis, M. Garzón, and A. Barrientos, "Human detection from a mobile robot using fusion of laser and vision information.," *Sensors (Basel, Switzerland)*, vol. 13, no. 9, pp. 11603–11635, 2013.

[188] K. O. Arras, B. Lau, S. Grzonka, M. Luber, O. M. Mozos, D. Meyer-Delius, and W. Burgard, "Range-Based People Detection and Tracking for Socially Enabled Service Robots," in *Springer Tracts in Advanced Robotics*, vol. 76, pp. 235–280, Springer, 2012.

[189] L. Spinello, R. Triebel, and R. Siegwart, "Multimodal detection and tracking of pedestrians in urban environments with explicit ground plane extraction," *2008 IEEE/RSJ International Conference on Intelligent Robots and Systems, IROS*, pp. 1823–1829, 2008.

[190] M. A. Garzon Oviedo, A. Barrientos, J. Del Cerro, A. Alacid, E. Fotiadis, G. R. Rodríguez-Canosa, and B.-C. Wang, "Tracking and following pedestrian trajectories, an approach for autonomous surveillance of critical infrastructures," *Industrial Robot: An International Journal*, vol. 42, pp. 429–440, aug 2015.

[191] R. E. Schapire and R. E. Schapire, "Improved Boosting Algorithms Using Confidence-rated Predictions," *Computer*, vol. 336, no. 3, pp. 297–336, 1999.

[192] Q. Zhang and R. Pless, "Extrinsic Calibration of a Camera and Laser Range Finder (improves camera calibration)," *IROS*, vol. 3, pp. 2301–2306, 2004.

[193] N. Dalal and B. Triggs, "Histograms of oriented gradients for human detection," *Proceedings - 2005 IEEE Computer Society Conference on Computer Vision and Pattern Recognition, CVPR 2005*, vol. I, pp. 886–893, 2005.

[194] A. Niculescu-Mizil and R. Caruana, "Predicting good probabilities with supervised learning," in *Proceedings of the 22nd international conference on Machine learning - ICML '05*, (New York, New York, USA), pp. 625–632, ACM Press, 2005.

[195] P. Papadakis, P. Rives, and A. Spalanzani, "Adaptive spacing in human-robot interactions," in *2014 IEEE/RSJ International Conference on Intelligent Robots and Systems*, pp. 2627–2632, Sep. 2014.

[196] C. F. Joost and D. Dodou, "Five-Point Likert Items : t test versus Mann-Whitney-Wilcoxon," *Practical Assessment, Research & Evaluation*, vol. 15, no. 11, pp. 1–16, 2010.

[197] R. C. Blair and J. J. Higgins, "A Comparison of the Power of Wilcoxon's Rank-Sum Statistic to That of Student's t Statistic under Various Nonnormal Distributions," *Journal of Educational Statistics*, vol. 5, no. 4, p. 309, 1980.

[198] T. Alkjær, P. K. Larsen, G. Pedersen, L. H. Nielsen, and E. B. Simonsen, "Biomechanical analysis of rollator walking," *BioMedical Engineering Online*, vol. 5, pp. 1–7, 2006.

[199] T. Wang, C. Dune, J.-P. Merlet, P. Gorce, G. Sacco, P. Robert, J.-M. Turpin, B. Teboul, A. Marteu, and O. Guerin, "A new application of smart walker for quantitative analysis of human walking," in *The Second Workshop on Assistive Computer Vision and Robotics (ACVR'14)*, (zuric, Switzerland), Sept. 2014.

[200] R. Soubra, A. Chkeir, and J.-L. Novella, "A Systematic Review of Thirty-One Assessment Tests to Evaluate Mobility in Older Adults," *BioMed Research International*, vol. 2019, pp. 1–17, jun 2019.

[201] C. Vaughan, B. Davis, and J. O'Connor, *Dynamics of Human Gait.* Kiboho Publishers, 2nd ed., 1992.

[202] S. Delp, J. Loan, M. Hoy, F. Zajac, E. Topp, and J. Rosen, "An interactive graphics-based model of the lower extremity to study orthopaedic surgical procedures," *IEEE Transactions on Biomedical Engineering*, vol. 37, no. 8, pp. 757–767, 1990.

[203] S. L. Delp, F. C. Anderson, A. S. Arnold, P. Loan, A. Habib, C. T. John, E. Guendelman, and D. G. Thelen, "OpenSim: Open-Source Software to Create and Analyze Dynamic Simulations of Movement," *IEEE Transactions on Biomedical Engineering*, vol. 54, pp. 1940–1950, nov 2007.

[204] M. Bourgain, S. Hybois, P. Thoreux, O. Rouillon, P. Rouch, and C. Sauret, "Effect of shoulder model complexity in upper-body kinematics analysis of the golf swing," *Journal of Biomechanics*, vol. 75, pp. 154–158, jun 2018.

[205] S. Hybois, P. Puchaud, M. Bourgain, A. Lombart, J. Bascou, F. Lavaste, P. Fodé, H. Pillet, and C. Sauret, "Comparison of shoulder kinematic chain models and their influence on kinematics and kinetics in the study of manual wheelchair propulsion," *Medical Engineering & Physics*, vol. 69, pp. 153–160, jul 2019.

[206] J. E. Graham, S. R. Fisher, I.-M. Bergés, Y.-F. Kuo, and G. V. Ostir, "Walking Speed Threshold for Classifying Walking Independence in Hospitalized Older Adults," *Physical Therapy*, vol. 90, pp. 1591–1597, nov 2010.

[207] BTS Bioengineering, "G-WALK," 2019.

[208] HBM, "The Working Principle of a Compression Load Cell," 2019.

[209] B. G. Lipták, "Weight Sensors," in *Instrument Engineers' Handbook: Process Measurement and Analysis* (B. G. Lipták, ed.), ch. Safety and, p. 1101, Boca Ratón: CRC Press, 2003.

[210] National Instruments, "Measuring Strain with Strain Gages," 2019.

[211] FUTEK Advanced Sensor Technology, "Triaxial Load Cell: MTA400," 2019.

[212] FUTEK Advanced Sensor Technology, "Strain Gauge Analog Amplifier: IAA100," 2019.

[213] National Instruments, "USB-6008: Multifunction I/O Device," 2019.

[214] Acuity, "Principles Of Measurement Used By Laser Sensors And Scanners," 2016.

[215] SICK Sensor Intelligence, "Operating Instructions S300 Safety Laser Scanner," 2019.

[216] Hokuyo Automatic CO, "Scanning Rangefinder: URG-04LX-UG01," 2019.

[217] B. P. Gerkey, J. Leibs, and B. Gassend, "Hokuyo Node," 2014.

[218] P. Corke, *Robotics, Vision and Control*, vol. 118 of *Springer Tracts in Advanced Robotics*. Cham: Springer International Publishing, 2017.

[219] R. Szeliski, *Computer Vision : Algorithms and Applications*, vol. 5. Springer, dec 2010.

[220] G. C. Holst and T. S. Lomheim, *CMOS/CCD Sensors and Camera Systems*. SPIE–The International Society for Optical Engineering, 2 ed., 2011.

[221] Microsoft, "Microsoft ® LifeCam Studio™ Technical Specifications," 2016.

[222] B. Pitzer, "USB Cam Node," 2017.